



National Library  
of Canada

Bibliothèque nationale  
du Canada

Canadian Theses Service    Service des thèses canadiennes

Ottawa, Canada  
K1A 0N4

## NOTICE

The quality of this microform is heavily dependent upon the quality of the original thesis submitted for microfilming. Every effort has been made to ensure the highest quality of reproduction possible.

If pages are missing, contact the university which granted the degree.

Some pages may have indistinct print especially if the original pages were typed with a poor typewriter ribbon or if the university sent us an inferior photocopy.

Reproduction in full or in part of this microform is governed by the Canadian Copyright Act, R.S.C. 1970, c. C-30, and subsequent amendments.

## AVIS

La qualité de cette microforme dépend grandement de la qualité de la thèse soumise au microfilmage. Nous avons tout fait pour assurer une qualité supérieure de reproduction.

S'il manque des pages, veuillez communiquer avec l'université qui a conféré le grade.

La qualité d'impression de certaines pages peut laisser à désirer, surtout si les pages originales ont été dactylographiées à l'aide d'un ruban usé ou si l'université nous a fait parvenir une photocopie de qualité inférieure.

La reproduction, même partielle, de cette microforme est soumise à la Loi canadienne sur le droit d'auteur, SRC 1970, c. C-30, et ses amendements subséquents.

THE UNIVERSITY OF ALBERTA

GEOCHEMICAL & ISOTOPIC STUDY OF THE ROZA MEMBER  
FEEDER SYSTEM, COLUMBIA RIVER BASALT GROUP

BY  
SUZAN SARAH ATKINSON



A THESIS  
SUBMITTED TO THE FACULTY OF GRADUATE STUDIES AND RESEARCH IN  
PARTIAL FULFILLMENT OF THE REQUIREMENTS FOR THE DEGREE OF  
MASTER OF SCIENCE

DEPARTMENT OF GEOLOGY

EDMONTON, ALBERTA

FALL 1990



**National Library  
of Canada**

**Bibliothèque nationale  
du Canada**

**Canadian Theses Service    Service des thèses canadiennes**

**Ottawa, Canada  
K1A 0N4**

**The author has granted an irrevocable non-exclusive licence allowing the National Library of Canada to reproduce, loan, distribute or sell copies of his/her thesis by any means and in any form or format, making this thesis available to interested persons.**

**The author retains ownership of the copyright in his/her thesis. Neither the thesis nor substantial extracts from it may be printed or otherwise reproduced without his/her permission.**

**L'auteur a accordé une licence irrévocable et non exclusive permettant à la Bibliothèque nationale du Canada de reproduire, prêter, distribuer ou vendre des copies de sa thèse de quelque manière et sous quelque forme que ce soit pour mettre des exemplaires de cette thèse à la disposition des personnes intéressées.**

**L'auteur conserve la propriété du droit d'auteur qui protège sa thèse. Ni la thèse ni des extraits substantiels de celle-ci ne doivent être imprimés ou autrement reproduits sans son autorisation.**

**ISBN 0-315-65071-0**

THE UNIVERSITY OF ALBERTA

RELEASE FORM

NAME OF AUTHOR SUZAN SARAH ATKINSON  
TITLE OF THESIS GEOCHEMICAL & ISOTOPIC STUDY OF THE ROZA  
MEMBER FEEDER SYSTEM, COLUMBIA RIVER  
BASALT GROUP

DEGREE FOR WHICH THESIS WAS PRESENTED MASTER OF SCIENCE

YEAR THIS DEGREE GRANTED FALL 1990

Permission is hereby granted to THE UNIVERSITY OF ALBERTA LIBRARY to reproduce single copies of this thesis and to lend or sell such copies for private, scholarly or scientific research purposes only.

The author reserves other publication rights, and neither the thesis nor extensive extracts from it may be printed or otherwise reproduced without the author's written permission.

  
.....  
S. Atkinson

Permanent address:  
Route 1, Box 30  
Hondo, Texas 78861 U.S.A.  
(512) 426-2716

Date September 4, 1990

".....in taking my leave of the Basalt Rocks, I may safely say, that, although I have paid attention everywhere, to find some trace of an igneous origen, yet I have not found any, no ashes, no scoriae, and every spring of water cold. For my part I have no belief in its supposed origen, but believe that as the Deity has created all the other various rocks, he has likewise created the several hundred miles of Basalt Rocks of the Columbia River.."

Excerpt from the diary of  
David Thompson, August 9, 1911.

FACULTY OF GRADUATE STUDIES AND RESEARCH

The undersigned certify that they have read, and recommend to the FACULTY OF GRADUATE STUDIES AND RESEARCH for acceptance, a thesis entitled GEOCHEMICAL & ISOTOPIC STUDY OF THE ROZA MEMBER FEEDER SYSTEM, COLUMBIA RIVER BASALT GROUP submitted by SUZAN SARAH ATKINSON in partial fulfillment of the requirements for the degree of MASTER OF SCIENCE.

*R. St. J. Lambert*  
.....  
Dr R. St J. Lambert

*H. Baadsgaard*  
.....  
Dr H. Baadsgaard

*R. W. Luth*  
.....  
Dr R. W. Luth

*F. W. Jones*  
.....  
Dr F. W. Jones

Date September 4, 1990

dedicated to my family, Bill, Rosemary, Wendy,  
Tom and Jazz

## ABSTRACT

The Roza Member of the Columbia River Basalt Group (CRBG) erupted along a narrow 160 kilometer long, NNW trending zone of fissures and vents in eastern Washington and northeastern Oregon around 15 Ma ago. This line of eruptive centers cuts across the suture between the North American craton and accreted oceanic type Mesozoic terranes. The Roza flows have been divided into six chemical subtypes and four cooling units, also recognizable in the feeder system (Martin, 1989). Thus the nature of the magma source, the role of contamination and the mode of emplacement can be deduced.

Each chemical subtype erupted along overlapping segments of varying lengths. No systematic migration of activity with time can be seen. One of the oldest subtypes erupted along nearly the whole system, while the youngest eruption was restricted to the northern half. Subtypes of intermediate age, are similarly located along overlapping segments of varying lengths and geographic restriction.

The initial five subtypes are characterized by a gradual increase in Ca and Cr with time, and a steady decrease in Ti, P, Zr and Nb. High precision Sr isotope analysis, using a quintuple collector array, and internally consistent to  $\pm 0.00003$ , shows that  $^{87}/^{86}$  Sr varies from 0.7051 to 0.7053, apparently at random. In contrast, Subtype IV has  $^{87}/^{86}$  Sr = 0.7054 and high incompatible element abundances. Sr isotope



ratios for plagioclase phenocrysts from all subtypes are constant at 0.7051.  $^{143}/^{144}$  Nd varies from 0.51258 to 0.51264 +/- 0.00001. Lead isotopic variation is entirely within error of analysis. These small variations in isotopic properties put severe constraints on the nature of contaminants and thus their locations below the dike system. The contaminant is not likely to have been ancient crust as Nd and Pb in the nearest known crust to the north are very different from those in the Roza Member. Pb would reveal such contamination more readily than Sr. Random variations of K, Ba, and Rb reveal the irregular nature of possible mantle or crustal contamination. Multiple use of single fissures is also documented while no differences between sublithospheric mantle across the craton\terrane suture is found.

## ACKNOWLEDGEMENTS

I would like to extend my most grateful thanks to Dr R. St J. Lambert and also Dr H. Baadsgaard, who kindly supervised my work while Dr Lambert was on sabbatical. Their support and enthusiasm have been most appreciated.

Special thanks is also given to both Dr P. Hooper for guidance in the field and XRF analysis of my samples and B. Martin for providing both powders and analyses of twelve Roza powders.

Friendship and guidance into the mysteries of isotopic chemical separations and analysis by Dr Baadsgaard, Dr Pat Cavell, John Duke and Steve Prevec over many months are also greatly appreciated. In addition, Wayne Day and Alex Stelmac have been of great help in regards to the makings of a smooth and efficient lab environment.

I would also like to thank both Yves Beaudoin for computer advice and Frank Dimitrov for his drafting expertise. In addition, the continual support of the staff of the geology main office and University of Alberta libraries is appreciated.

Finally, I would like to give my thanks and love to my family and friends. I can say without a doubt that I have always been generously supported. It is through all of your kindness and patience that I have had a wonderful and rewarding experience in Canada.

## TABLE OF CONTENTS

	PAGE
<b>CHAPTER 1 INTRODUCTION</b>	
1.1. Problems and objectives.....	1
1.2. Regional setting of the CRBG.....	2
1.3. CRBG dike swarms and eruptive centers.....	6
1.4. Previous CRBG geochemical and isotopic studies.....	9
<b>CHAPTER 2 THE ROZA MEMBER</b>	
2.1. Roza flow characteristics.....	20
2.2. Roza eruptive centers characteristics.....	23
2.3. Sampling and methodology.....	25
<b>CHAPTER 3 ROZA GEOCHEMISTRY AND ISOTOPIC COMPOSITION</b>	
3.1. Geochemistry of the Roza Member.....	30
3.2. Isotope Geochemistry.....	32
<b>CHAPTER 4 GENERAL DISCUSSION AND CONCLUSIONS</b>	
4.1. Discussion	
4.1.1. Dike Emplacement.....	57
4.1.2. Geochemistry.....	60
4.1.3. Isotopes.....	61
4.2. Conclusions and Summary.....	64
<b>REFERENCES.....</b>	<b>85</b>
<b>APPENDIX A XRF ANALYSES.....</b>	<b>95</b>
<b>APPENDIX B ROZA CHEMICAL SUBTYPE CLASSIFICATION METHOD.....</b>	<b>102</b>
<b>APPENDIX C ISOTOPIC CHEMICAL SEPARATION METHODS.....</b>	<b>108</b>

LIST OF TABLES

	PAGE
TABLE 1. The CRBG stratigraphy modified after Reidel and others (1989).....	18
TABLE 2. Selected geochemical compositions of various proposed sources for the CRBG. Sr and Nd isotopic values are reported relative to $87/86 \text{ Sr} = 0.71014$ for NBS 987, $143/144 \text{ Nd} = 0.511929$ respectively. Modified after Carlson (1984) and Carlson and Hart (1988).....	19
TABLE 3. Locations and descriptions of the Roza Member samples in this study. Descriptions: dikes (d); near vent flows (v); dikelets (dl); scoria (s); plateau proper flows (p).....	29
TABLE 4. Average composition of Roza Member subtypes.....	36
TABLE 5. Average Chemical Compositions for Roza flows and feeder Rocks.....	37
TABLE 6. Strontium and neodymium isotopic analyses of Roza samples from this study.....	38
TABLE 7. Lead isotopic data for Roza samples in this study..	40
TABLE 8. $\delta^{18}\text{O}$ values of selected Roza Member whole rock powders.....	41

## LIST OF FIGURES

PAGE

- FIGURE 1.** Generalized map of the CRBG stressing the Roza Member and feeder dike system, the cratonic margin, and key features discussed in the text. Modified after Anderson and others (1987), Hooper (1988b) and Reidel and others (1989)..16
- FIGURE 2.** Sr and Nd isotopic variation in the CRBG. Fields for MORB and selected OIB's are shown along with the compositions of proposed CRBG sources (C1,C2,C3). Modified after Carlson (1984).....17
- FIGURE 3.** Generalized sample location map of the Roza feeder system. Locus of each Roza chemical subtype found along the feeder system is also depicted. ....28
- FIGURE 4.** AFM variation diagram for Roza Member feeder and flow rocks. A = K<sub>2</sub>O + MgO; F = FeO; M = MgO. All in weight percent. Modified after Irvine and Barager (1971).....42
- FIGURE 5.** Alkali-silica diagram, modified after Irvine and Barager (1971). Subtypes identified as follows: circles (IA); squares (IB); triangles (IIA); diamonds (IIB); stars (III); filled triangles (IV).....43
- FIGURE 6.** Zr variation diagrams. Symbols as presented in Figure 5.....44
- FIGURE 7.** Zr variation diagrams. Symbols as presented in Figure 5.....45
- FIGURE 8.** Zr variation diagrams. Symbols as presented in Figure 5.....46
- FIGURE 9.** Strontium versus silica plot of all Roza samples. Symbols refer to the chemical subtypes of these rocks.....47
- FIGURE 10.** <sup>87</sup>/<sub>86</sub> Strontium versus strontium (ppm) plot of Roza samples. Symbols depict the chemical subtypes for whole rock samples, while open squares mark plagioclase separates.....48
- FIGURE 11.** <sup>87</sup>/<sub>86</sub> Strontium versus silica (ppm) plot of Roza samples. Symbols depict the chemical subtypes for whole rock samples, while open squares mark plagioclase separates.....49
- FIGURE 12.** <sup>87</sup>/<sub>86</sub> Strontium versus chromium (ppm) plot of Roza samples. Symbols depict the chemical subtypes for whole rock samples, while open squares mark plagioclase separates.....50

**FIGURE 13.** 87/86 Strontium versus rubidium/strontium ratio plot of Roza samples. Symbols depict the chemical subtypes for whole rock samples, while open squares mark plagioclase separates.....51

**FIGURE 14.** 143/144 neodymium versus 87/86 strontium plot of Roza samples. Symbols depict the chemical subtype of each sample.....52

**FIGURE 15.** 207/204 lead versus 206/204 lead plot of Roza whole rock powders. Symbols depict the chemical subtype of each sample.....53

**FIGURE 16.** 208/204 lead versus 206/204 lead plot of Roza whole rock powders. Symbols depict the chemical subtype of each sample.....54

**FIGURE 17.**  $\delta^{18}\text{O}$  versus silica plot of Roza samples. Symbols depict the chemical subtype of each sample.....55

**FIGURE 18.**  $\delta^{18}\text{O}$  versus 87/86 strontium plot of Roza samples. Symbols depict the chemical subtype of each sample.....56

**FIGURE 19.** Schematic diagram of the three main phases of fissure-type lava eruptions. Modified after Bruce and Huppert (1989).....66

**FIGURE 20.** Distribution map of Roza chemical subtype IA flow and feeder samples. Flow distribution modified after Martin (1989).....67

**FIGURE 21.** Distribution map of Roza chemical subtype IB flow and feeder samples. Flow distribution modified after Martin (1989).....68

**FIGURE 22.** Distribution map of Roza chemical subtype IIA flow and feeder samples. Flow distribution modified after Martin (1989).....69

**FIGURE 23.** Distribution map of Roza chemical subtype IIB flow and feeder samples. Flow distribution modified after Martin (1989).....70

**FIGURE 24.** Distribution map of Roza chemical subtype III flow and feeder samples. Flow distribution modified after Martin (1989).....71

**FIGURE 25.** Distribution map of Roza chemical subtype IV flow and feeder samples. Flow distribution modified after Martin (1989).....72

**FIGURE 26.** Discrimination diagram using Ti, Zr and Y. Within plate basalts (WPB) i.e. OIB's or CFB's plot in field D, ocean-floor basalts (OFB) in field B, low-potassium tholeiites (LKT) in fields A and B, calc-alkali basalts (CAB) in fields C and B. Modified after Pearce and Cann (1973).....73

**FIGURE 27.** Zr-Ti/100-Sr/2 discrimination diagram. Ocean-floor basalts (OFB) plot in field C, low-potassium tholeiites (LKT) in field A, and calc-alkali basalts (CAB) in field B. Modified after Pearce and Cann (1973).....74

**FIGURE 28.** MgO-FeO\*-Al<sub>2</sub>O<sub>3</sub> tectonic discrimination diagram. Categories are ocean island (OI); ocean-ridge and floor (ORF); continental (C); orogenic (O); and spreading-center island (SCI). Modified after Pearce and others (1977).....75

**FIGURE 29.** K<sub>2</sub>O-TiO<sub>2</sub>-P<sub>2</sub>O<sub>5</sub> plot of Roza flow and feeder system rocks, showing the position of the dividing line between the oceanic field (upper portion) and the non-oceanic field (lower portion). Modified after Pearce and others (1974).....76

**FIGURE 30.** N-type MORB normalized multi-element plot of averaged Roza subtypes and the Guaymas Basin, Gulf of California. Symbols as presented in Figure 5. Normalizing factors and figure modified from Saunders and Tarney (1984).....77

**FIGURE 31.** 87/86 Strontium versus strontium (ppm) plot of Roza samples. Filled circles indicate proposed CRBG contaminant compositions.....78

**FIGURE 32.** 143/144 neodymium versus 87/86 strontium plot of Roza samples. Filled circles indicate proposed CRBG contaminant compositions.....79

**FIGURE 33.** 207/204 lead versus 206/204 lead plot of Roza whole rock powders. Filled circles indicate proposed CRBG contaminant compositions.....80

**FIGURE 34.** 208/204 lead versus 206/204 lead plot of Roza whole rock powders. Filled circles indicate proposed CRBG contaminant compositions.....81

**FIGURE 35.** 206/204 lead versus 87/86 strontium plot of Roza samples. Filled circles indicate proposed CRBG contaminant compositions.....82

**FIGURE 36.** 206/204 lead versus 143/144 neodymium plot of Roza samples. Filled circles indicate proposed CRBG contaminant compositions.....83

FIGURE 37.  $\delta^{18}\text{O}$  versus 87/86 strontium plot of Roza samples (circles), CRBG main series flows (triangles), Saddle Mountains Basalt (square) and proposed CRBG contaminants (hexagons). Curves calculated using combined fractional crystallization-assimilation model of Carlson and others (1981), show effects of assimilation of two distinct crustal endmembers, one with  $\delta^{18}\text{O}=9.4$  and another with  $\delta^{18}\text{O}=13.4$ . See text for further discussion.....84

FIGURE 38. Cr normalization diagram. Equation is that of the line.....104

FIGURE 39. P2O5 normalization diagram. Equation is that of the line.....105

FIGURE 40. TiO2 normalization diagram. Equation is that of the line.....106

FIGURE 41. Ca normalization diagram. Equation is that of the line.....107



## LIST OF SYMBOLS, NOMENCLATURE AND ABBREVIATIONS

- C1, C2, C3, C4 Distinct CRBG source components as defined in Carlson and Hart (1988).
- C Continental
- CAB Calc-alkali Basalts
- CFB Continental Flood Basalt
- CRBG Columbia River Basalt Group
- HFS High Field Strength
- LKT Low Potassium Tholeiite
- LIL Large Ion Lithophile
- O Orogenic
- OFB Ocean-Floor Basalt
- OI Oceanic Island
- ORF Ocean-ridge and Floor
- SCI Spreading-Center Island
- WPB Within plate Basalts
- XRF X-ray Fluorescence
- 87/86 strontium (or Sr)  $^{87}\text{Sr}/^{86}\text{Sr}$  isotopic ratio
- 143/144 neodymium (or Nd)  $^{143}\text{Nd}/^{144}\text{Nd}$  isotopic ratio
- 206/204 lead (or Pb)  $^{206}\text{Pb}/^{204}\text{Pb}$  isotopic ratio
- 207/204 lead (or Pb)  $^{207}\text{Pb}/^{204}\text{Pb}$  isotopic ratio
- 208/204 lead (or Pb)  $^{208}\text{Pb}/^{204}\text{Pb}$  isotopic ratio

# CHAPTER 1

## INTRODUCTION

### 1.1. PROBLEMS AND OBJECTIVES

The reasons for the substantial chemical and isotopic differences between continental flood basalts (CFB) and similarly effusive mid-ocean ridge basalts (MORB) are the subject of considerable investigation. Compared to MORB's and oceanic island basalts (OIB), CFB's are enriched in K, Rb, Ba and light rare earth elements (LREE) relative to Nb, Sr and P contents. Possible explanations for these differences include either the assimilation of crustal material by a "typical" primary mantle material (i.e., the proverbial parental source for all basaltic magmas) or a long lived, incompatible element enriched subcontinental lithospheric source (Norry and Fitton, 1983).

The Columbia River Basalt Group's (CRBG) role in model development is significant because it is relatively younger, less altered, more accessible and better exposed than other flood basalt provinces. Preserved by a semiarid climate, these near horizontal Miocene flows, deeply incised by rivers, afford a multitude of natural cross sections (Hooper, 1988b). However, the CRBG is significantly smaller than other CFB provinces and unique in that it lies behind an active

convergent plate margin (Carlson and Hart, 1988; Hooper & Reidel, 1989).

## 1.2. REGIONAL SETTING OF THE CRBG

The CRBG Province lies south of the Okanogan Highlands, west of the Idaho Batholith, east of the Cascades and north of the Basin and Range Province. The CRBG flows cover large areas of Washington State and also smaller portions of western Idaho and northern Oregon (see Figure 1). The Miocene CRBG lavas erupted between 17.5 and 6 m.y. ago. The greatest volume, 97 percent, vented during the first 3.5 million years and includes the Roza Member, the subject of this study, which erupted towards the end of that time (Baksi and Watkins 1973; McKee et al 1977). In total 174,300 km<sup>3</sup> of primarily tholeiitic basalt flows (47-56 wt. % SiO<sub>2</sub>) covered an area of approximately 163,700 km<sup>2</sup> (Tolan and others, 1989). Of the nearly 300 individual flows, the average thickness is 15 to 30 meters, while that for the entire group is over 1 kilometer (Hooper, 1982; Hooper and Reidel, 1989). The thickest flow accumulation, 5 to 12 kilometers, fills the Pasco basin west of the main eruptive centers (Catchings and Mooney, 1988).

Four main stratigraphic Formations are now defined for the CRBG. These Formations plus Members and informal subdivisions are presented in Table 1. From oldest to

youngest these Formations are the Imnaha Basalt, the Grande Ronde Basalt (including the Picture Gorge Basalt), the Wanapum Basalt and the Saddle Mountains Basalt. The Wanapum Basalt is composed of these Members from oldest to youngest: Eckler Mountain, Frenchman Springs, Roza and Priest Rapids. Anderson and others (1987) have compiled distribution maps of the CRBG stratigraphic units including the Roza Member which is illustrated in Figure 1.

The Columbia Plateau can be subdivided into three principle Subprovinces, each of which has its own unique structural style that reflects the complex crustal and tectonic history of the Pacific Northwest. These three regions are known as the Yakima Foldbelt Subprovince, the Palouse Subprovince and the Blue Mountains Subprovince (See Figure 1) (Hooper, 1988b; Reidel and others, 1989).

The Yakima foldbelt overlies the relatively slender wedge of subducted crust beneath the Pasco Basin and its overlying CRBG flows has endured the most intense deformation forming east-west trending anticlines with associated reversed faults (Campbell, 1989; Price and Watkinson, 1989; Reidel and others, 1989; Shaffer and West, 1989; Watters, 1989; West and Shaffer, 1989).

The Palouse Subprovince is characterized by the virtually undeformed CRBG flows overlying the stable North American craton. The lack of tectonic deformation in these flows reflects the relatively stable nature of the underlying North

American craton which also extends north and east of this CFB province.

The Blue Mountains Subprovince is composed of "a complex of ocean-derived rock suites dominated by island arcs, ophiolites, and sediments derived from these" (Hooper, 1988b). CRBG flows in this region have endured significant deformation as a result of the relatively thin and dynamic nature of the underlying crust. Conjugate near vertical northwest-southeast (right-lateral) and northeast-southwest (left-lateral) strike-slip faults predominate in this Subprovince (Hooper and Conrey, 1989). The majority of known CRBG feeder systems appear to be confined to this region.

One might expect chemical and isotopic variations if crustal contamination and/or varying lithospheric types are present for a feeder system that crosses a craton/oceanic terrane boundary. The Roza Member is examined here because it crosses a proposed craton/terrane suture between the Palouse and Blue Mountains Subprovinces. The Roza is unique in that the majority of other CRBG feeder systems are restricted to the Blue Mountains Subprovince (Hooper, 1988b). The Roza feeder system is also one of the best constrained systems in terms of the location of eruptive centers, flow stratigraphy, areal extent, and eruptive and flow rates.

The delineation of the suture zone between the North American craton and the accreted terrane has been the subject of many studies. Field relations, isotopic (Nd, Sr, Pb and O)

(Bennett and DePaulo, 1987; Bennett and others, 1988; Farmer, 1989; Farmer and DePaulo, 1983; Fleck and Kistler, 1989; Kistler and Peterman, 1978; and Solomon and Taylor, 1988) sedimentary facies (Kistler, 1989), and gravity and magnetic studies (Johnson, Thiessen and Parodi, 1989) have all contributed to the delineation of this suture.

Oriented north-south along the western edge of the Idaho Batholith, the craton-terrane suture as defined by the 0.706 strontium isopleth is believed to curve 90 degrees to the west just north of Lewiston. Its trace then strikes north-south along the eastern edge of the Pasco Basin, becoming obscure north of the Columbia Plateau (Hooper, 1988b). This boundary crosscuts the Roza feeder system at right angles between Almota and Pomeroy, Washington (see Figure 3, Chapter 2). Comparing the strontium isopleth to the boundaries defined by the Palouse and Blue Mountains Subprovinces, they are roughly coincident only in the Almota-Pomeroy area. While the "Subprovince" boundary skims the eastern edge of the feeder system along its central section and then again cuts southwest at the Washington-Oregon border, the 0.706 isopleth swings far east into Idaho.

The ill-defined craton margin has functioned as a hingeline for the southeast to northwest tilting of the eastern half of the Plateau. This process has been augmented by the continuous rise of the Idaho Batholith to the east and the downwarping of the Pasco Basin to the west. Progressive

offlap of each successive CRBG eruption attests to the development of this hinge mechanism during the Miocene (Camp and Hooper, 1981).

### 1.3. CRBG DIKE SWARMS AND ERUPTIVE CENTERS

Many studies have examined the nature of the Roza Member, within the last 30 years. Bingham and Grolier (1966) first identified spatter cones cut by small dikes near Winona, Washington to be Roza source vents. Swanson and others (1975, 1980), during field studies and reconnaissance mapping of southeastern Washington recognized additional Roza feeder dikes and vents. The Roza feeder system is now perceived to be a discrete linear array of spatter cones, exhumed dikes and relatively large shield cones of flow ramparts and spatter. This NNW trending line of echelon segments is at least 160 km long and less than 20 km wide. It is identified from Winona, Washington to just north of Enterprise, Oregon (Atkinson and Lambert, 1990). Lefebvre (1970) also studied and mapped the Roza flows in the Grande Coulee area of central Washington.

Shaw and Swanson (1970) and Swanson and others (1975) studied the magma production and eruptive rates of the CRBG stressing the Roza Member. Using observed dike widths, they proposed that magma erupted from a supply in the upper mantle. Flow rates down even a shallow slope of 1:1000 were estimated

to be in the range of 5 to 15 km per hour. This speed would have allowed thick sheet flows to travel great distances with little cooling. Maximum daily eruption volumes of 1 km<sup>3</sup>/day/km for the Roza flows are estimated. However, uncertainties in area and volume estimates lead Tolán and others (1989) to revise some of this work. Average volume eruption rates have increased to 3 km<sup>3</sup>/day/km of fissure for some of the great flows (>102 km<sup>3</sup>).

The CRBG dike swarms are arrays of eruptive centers recognized today as dikes, and more rarely, as remnant spatter cones and flow ramparts. The Monument dike swarm fed the Picture Gorge basalts in the John Day Basin of northcentral Oregon, while the Grande Ronde and Cornucopia dike swarms fed flows in southeastern Washington and northeastern Oregon respectively (Camp and Hooper, 1981; Hooper and Reidel, 1989). The Grande Ronde and Cornucopia dike swarms together have been designated the Chief Joseph dike swarm (Taubeneck, 1970).

The CRBG flows erupted from linear vent systems each relatively restricted in width compared to that of the dike swarms that encompass them (Swanson and others, 1975). Most CRBG vent systems trend N20°W +/- 20°. Hooper (1988b) suggests this pattern is controlled by a pre-existing structural fabric in the underlying basement rocks and the regional north-south compression, east-west extension.

The majority of known CRBG eruptive centers are restricted to the more mafic Blue Mountains Subprovince. Some



exceptions include a few dikes of the Frenchman Springs Member and Ice Harbour Member situated within the Yakima Foldbelt Subprovince and the Weippe dike which is restricted to the Palouse Subprovince (Hooper, 1988b). The Roza is also exceptional in that it extends northward from the Blue Mountains Subprovince into the probable position of the craton. The relatively thinner and weaker nature of the Blue Mountains Subprovince compared to the craton to the north and east may have focused most eruptive centers in this area (Hooper and Reidel, 1989). However, Swanson and Wright (1979) note that the extreme topography and resulting good exposure in this region may also account for this concentration bias. Moreover, others (eg., Swanson and others, 1975; Camp and others, 1982; Tolan and others, 1989) have concluded from the distribution pattern of various flows, that feeder dikes, either undiscovered or still overlain by subsequent flows, must also be present in the central and northern parts of the plateau.

Wright and others (1989) note that there is no apparent migration of the locations of active feeder systems with time. Most notably, the Grande Ronde and Saddle Mountains linear vent systems are scattered throughout the Chief Joseph dike swarm. However, the locus of eruptive centers for the upper Members of the Wanapum Basalt do migrate eastward with time. The Frenchman Springs feeder system is located near the western margin of the dike swarm, the Roza in the central

portion and the Priest Rapids is found far to the east in the Clearwater Embayment (see Figure 3, Wright and others, 1989).

#### 1.4. PREVIOUS CRBG GEOCHEMICAL AND ISOTOPIC STUDIES

The present comprehensive CRBG stratigraphy results from the use of advanced rapid major and trace elemental analysis and portable fluxgate magnetometers in conjunction with field mapping and petrography (Hooper, 1982) (Table 1). Hooper (1980) and Tolzn (1989) both present reviews of the development of the CRBG's regional stratigraphy, and the role that developing technology has had on its evolution. Once the regional stratigraphy was adequately worked out, study of the CRBG's physical and chemical evolution could be better addressed.

Multiple explanations for the chemical variation in the CRBG have been generated. Early theories unsuccessfully invoked crystal fractionation of a magma derived from a peridotite source. More recently, works include multiple sources and crustal contaminants in addition to crystal fractionation. Physical and geochemical constraints on this CRBG province provide a framework for this work.

Constraints on the petrogenesis of the CRBG have been outlined by Hooper (1984, 1988b), Hooper and Swanson (1987) and Carlson (1984). Many of these physical and chemical

limitations are outlined below.

1. Consistent NNW-SSE orientation of fissure systems indicate control by a regional stress field.

2. The great length of some fissures (> 70km) and absence of magma chamber collapse features indicate that fissures probably extended to the base of the crust, 25-35 kilometers.

3. Fissures tapped large reservoirs of well-mixed magma since virtually identical contemporaneous lavas erupted from points tens of kilometers apart.

4. Homogeneous flows also imply a well-mixed source and no significant change in bulk composition of magmas as they ascended the crust.

5. The range of silica compositions is between 47 and 57 weight percent, indicating little if any upper crustal assimilation.

6. Incompatible elements are relatively abundant and have a greater variation than silica especially within small apparently comagmatic groups. Likewise,  $Mg/(Mg + Fe^2)$  exhibit considerable variation without significant changes in silica content.

7. Xenoliths of country rock are of local affinity and little reaction with host rocks.

8.  $^{87}Sr/^{86}Sr$  strontium isotopic ratios for the Innaha, Grande Ronde and Wanapum Basalts (the "main Series") increase with time.

9. In the Saddle Mountains, the youngest and most chemically diverse CRBG Formation,  $87/86$  strontium ratios show no correlation with time.

10.  $87/86$  strontium and silica contents of the CRBG are not correlatable.

Using a data base of several thousand chemical analyses and physical and chemical constraints, multiple explanations for the compositional variation in the CRBG have been developed (see Carlson and Hart, 1988, Table 1 for the average CRBG chemical compositions). Compared to MORB, the CRBG is depleted in compatible elements (Mg, Ni and Cr) and enriched in incompatible elements. If a normal peridotitic source for these flood basalts is assumed, then the basalts must be products of extreme crystal fractionation and are in effect quite highly evolved (Carlson and Hart, 1988). The Mg' ranges between 64 and 30; thus the highest numbers are still too low for the magma to have been in equilibrium with a source unless it is an unusually Fe-rich pyroxenite (Hooper, 1988b; Helz, 1978; Swanson and Wright, 1981; Prestvik and Goles, 1985).

Wright (1961) and Wright and others (1973) first unsuccessfully tried to both qualitatively and quantitatively model the entire CRBG variation by crystal fractionation alone. The incompatible element ratios vary too significantly to allow either partial melting of a common source and/or crystal fractionation of similar parental magmas as the only

processes involved (Hooper, 1988a). Later work concentrated on individual flow sequences to use crystal fractionation plus other processes to explain observed chemical variations. Fractionation of plagioclase is widely used in these theories.

Less emphasis on crystal fractionation and more on the proposal that many flows are separate partial melts of a heterogeneous relatively iron and pyroxene-rich mantle source rather than a peridotite source has been presented. Wilkinson and Binns (1977) first proposed that iron-rich lherzolites of the chrome-diopside suite are the mantle source of the CRBG. In addition, others have suggested that these magmas may have been derived from partial melting of an iron-rich and olivine-poor clinopyroxene mantle source (Helz, 1978; Wright and Helz, 1981; Helz and Wright, 1982, and Wright and others, in press). However, no evidence for either of these sources has been found in the form of mantle xenoliths.

In addition to the unusual pyroxenite sources, eclogite from the adjacent subducted slab has been put forward as the source for the CRBG by both Lambert and Chamberlain (1988) and Takahashi (1988).

Silicic wallrock contamination of magmas either by wallrock assimilation or subducted sediments added to the source region may explain some of the major element trends not resolved by crystal fractionation alone. For instance,  $TiO_2$  and  $K_2O$  versus  $P_2O_5$  ratios tend to remain constant until either magnetite or apatite begin to crystallize. However, the CRBG

displays a wide range of both  $\text{TiO}_2/\text{P}_2\text{O}_5$  and  $\text{K}_2\text{O}/\text{P}_2\text{O}_5$  (see Carlson and Hart, 1988, Figures 2a and 2b). The elevated  $\text{K}_2\text{O}/\text{P}_2\text{O}_5$  ratios found in the majority of the CRBG can not be reached by fractional crystallization alone (Carlson and Hart, 1988).

In addition, crustal contamination alone can not explain the wide range of  $\text{TiO}_2/\text{P}_2\text{O}_5$  ratios of the CRBG. Multiple sources have been invoked, higher  $\text{TiO}_2/\text{P}_2\text{O}_5$  ratios are associated with sources similar to those of many intraplate oceanic island basalts, while low  $\text{TiO}_2/\text{P}_2\text{O}_5$  types are compatible with kimberlite sources. The Wanapum Basalt (including the Roza Member) has low  $\text{TiO}_2/\text{P}_2\text{O}_5$  ratios, which may imply that lavas have been metasomatically enriched by incompatible enriched melts or fluids possibly prior to melt generation (Carlson and Hart, 1988).

Besides sudden changes in incompatible element ratios, variations in strontium, neodymium, lead and oxygen isotope ratios invoke the need for multiple sources in the evolution of the CRBG (Waters, 1961; Wright and others, 1973; Carlson, 1981, 1984; Carlson and others, 1981; Carlson and Hart, 1988).

Several explanations for the gradual increase in  $87/86$  strontium isotopic values coupled with the steady decrease in  $143/144$  neodymium isotopic ratios have been proposed (see Figure 2). Progressive assimilation of crust has been ruled out as an explanation since there is no correlation of isotopes with silica content (constraint # 10). Similarly

repudiated is the proposal that there has been a NW migration of eruptive activity with time through a laterally heterogeneous source since isotopic changes are not entirely smooth with time and there are no obvious changes in overall chemical compositions with these isotopic steps (Hooper, 1984).

The strontium and neodymium isotopic trends may suggest two component mixing between a primary magma (C1) and another more evolved source (C4) (see Table 2 and Figure 2). However, trace and major elements as well as lead and oxygen isotopes are not correlated with the strontium-neodymium trend, therefore conflicting with this simple two component fractional crystallization and assimilation model (Carlson, 1984). Additional sources have been proposed (C2 and C3) (Carlson, 1984; Hooper, 1988b; Carlson and Hart, 1988). The natures of these four possible sources, three mantle derived, one a crustal component are presented in Table 2.

C1 is believed to be a depleted mantle source for the Picture Gorge and lowest Imnaha Basalt flow, while C2 represents a mantle source contaminated by a subducted crustal component. The C2 mantle source serves as the primary source for the typical Imnaha flows and primitive Wanapum Formation flows such as the Robinette Mountain. It is best identified as a kink in the trends of the main CRBG series on plots of  $^{206}/^{204}$  Pb versus  $^{87}/^{86}$  Sr or  $^{143}/^{144}$  Nd. C3 is defined as an enriched mantle source that evolved around 2.5 billion years

ago, best illustrated in oxygen versus a radiogenic isotope diagrams, due to its low  $\delta^{18}O$  ( $< +6$ ) and epsilon neodymium ( $-5$ ) but relatively high  $^{87}Sr/^{86}Sr$  (0.7075) values. C3 is the primary source for the Saddle Mountains Formation. C4 is believed to be a crustal contaminant with very high  $^{87}Sr/^{86}Sr$  and  $\delta^{18}O$  and nonradiogenic Nd and Pb composition. It is best defined as an old sialic lower crustal rock type with low Rb/Sr and U/Pb due to granulite facies metamorphism (Carlson, 1984).



FIGURE 1. Generalized map of the study area emphasizing key features discussed in the text. Modified after Anderson and others (1987), Hooper (1988b) and Reidel and others (1989).

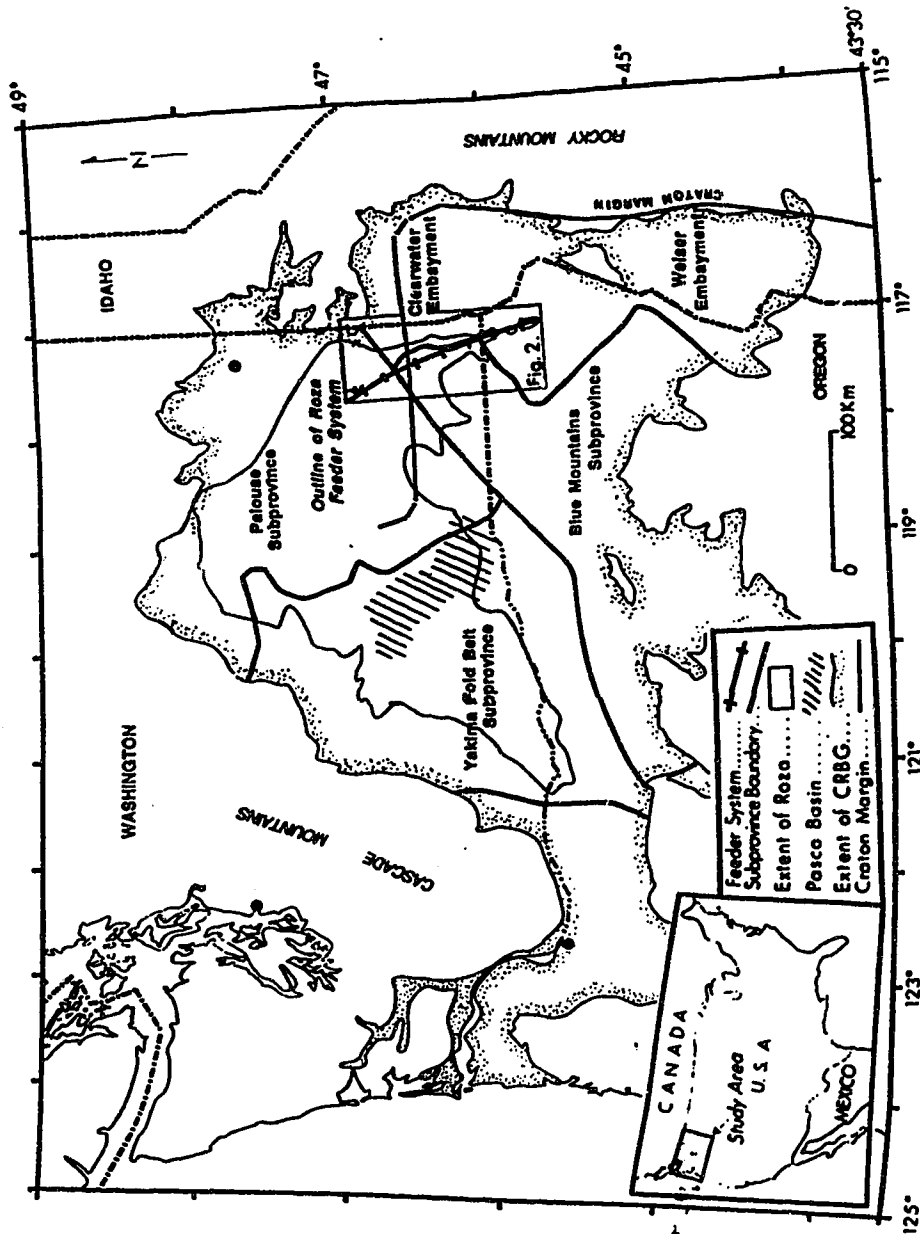


FIGURE 2. Sr and Nd isotopic variation in the CRBG. Fields for MORB and selected OIB's are shown along with the compositions of proposed CRBG sources (C1,C2,C3). Modified after Carlson (1984).

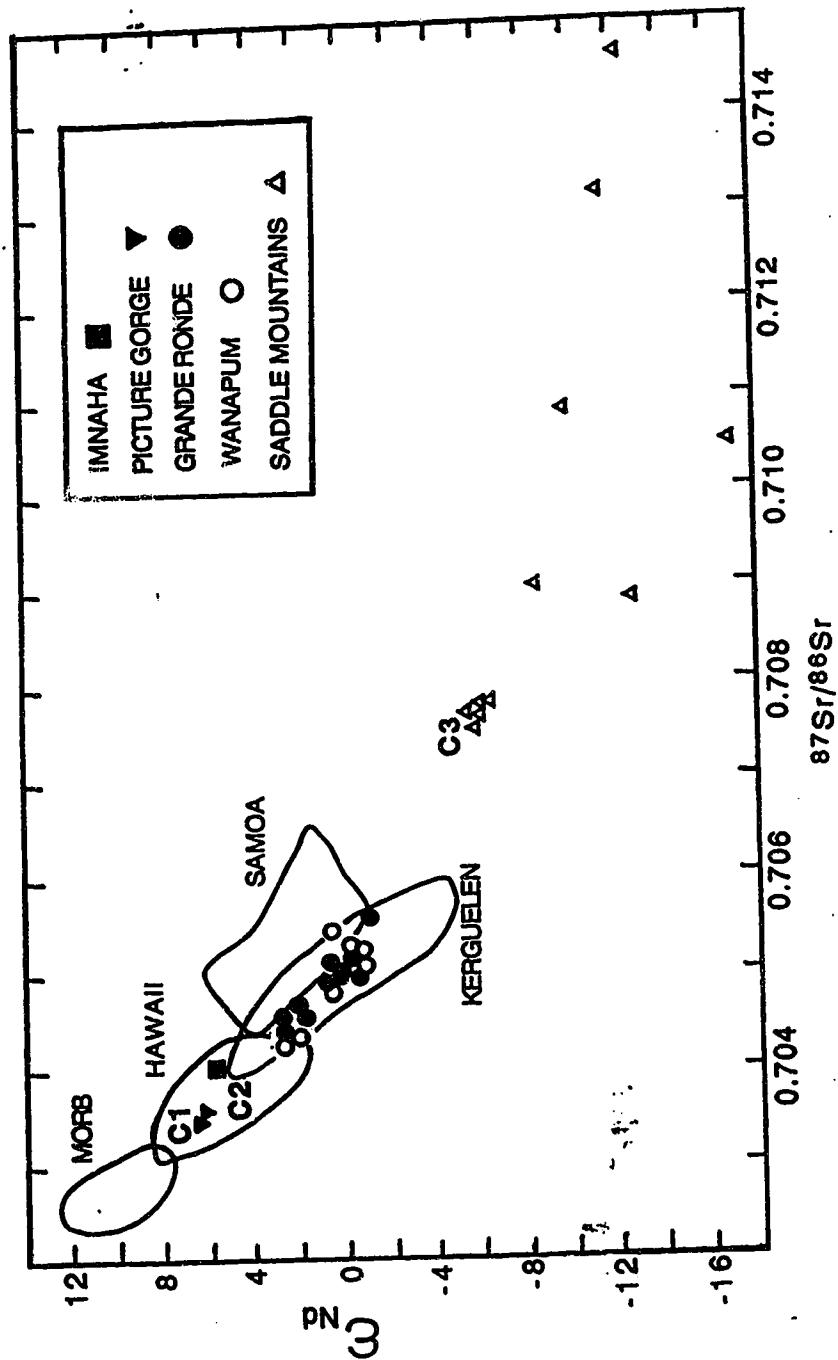


TABLE 2. Selected geochemical compositions of various proposed sources for the CRBG. Sr and Nd isotopic values are reported relative to  $^{87}/^{86}\text{Sr} = 0.71014$  for NBS 987,  $^{143}/^{144}\text{Nd} = 0.511929$  respectively. Modified after Carlson (1984) and Carlson and Hart (1988).

	C1	C2	C3	C4
$^{87}/^{86}\text{Sr}$	0.7025	0.7038	0.7076	0.715
epsilon Nd	+6.5	+4.5	-6.0	-30.0
$^{143}/^{144}\text{Nd}$	0.51315	0.5128	0.5124	
$^{206}/^{204}\text{Pb}$	18.77	19.09	18.66	17.0
$^{207}/^{204}\text{Pb}$	15.51	15.65	15.65	15.52
$^{208}/^{204}\text{Pb}$	38.28	38.73	39.44	38.5
$\delta^{18}\text{O}$	+5.6	+6.1	+5.8	+14.0
Sr (ppm)	400	300	250	350
Nd (ppm)	12	23	20	26
Pb (ppm)	1	10	5	15

## CHAPTER 2

### THE ROZA FLOW AND FEEDER SYSTEM

#### 2.1. ROZA FLOW CHARACTERISTICS

There are at least four Roza Member cooling units covering an area of 40,352 km<sup>2</sup> and having a total volume of 1,294 km<sup>3</sup> (Martin, 1989; Anderson and others, 1989). All are easily distinguished from other CRBG Members by field appearance, magnetic polarity and most importantly, chemistry.

The Roza Member has unusual, individual, clear to honey-colored plagioclase phenocrysts. These abundant, large phenocrysts, often greater than 5 mm in length, are regularly distributed in a fine-grained groundmass, comprising 5-8 volume percent. Phenocryst abundances increase from the oldest to youngest flow units (Swanson and others, 1979; Martin, 1989). The underlying Frenchman Springs Basalt Member contains roughly one third as many phenocrysts, while the overlying Priest Rapids Basalt Member is aphanitic (Lefevbre, 1970; Swanson and others, 1975; Hooper, 1982). Plagioclase phenocrysts are typically convolutedly zoned, simply twinned and often have resorbed cores. Occasionally, they contain inclusion rings of minute pyroxene or isolated brown spinel grains. Rare resorbed augite and olivine phenocrysts, less than 2 mm in diameter, are also found in the Roza Member.

The Roza Member ground mass is composed predominantly of microlaths of plagioclase ( $An_{58}$ ) and lesser amounts of resorbed augite. These two minerals are typically intergrown but occasionally larger grains are found in syneusis. Plagioclase microlaths exhibit both Carlsbad and albite twinning. Minor amounts of intergranular resorbed olivine and dendritic to lath shaped oxides are also commonly found with interstitial brown and clear glass, apatite and immiscible yellow sulfide droplets. Resorption features in olivine, augite, and plagioclase phenocrysts, plus zoning and inclusion rings indicate that magma mixing and/or crystallization at different pressures may have occurred (Atkinson and Lambert, 1990).

The Roza Member is magnetically either of transitional or reversed nature, while the Priest Rapids and the Frenchman Springs Members are respectively solely reversed or normal in polarity. This widespread transitional magnetic polarity of the Roza Member is additional evidence for its rapid accumulation. Furthermore, the finding of a Roza dike and flow extruded during the ensuing reversed polarity indicate that the final eruptions in the Roza feeder system were confined to its southern portion (Choiniere and Swanson, 1979).

Between Roza flow units there is no sediment accumulation, tuff layering, weathered zones or accompanying plant remains. Lack of these features reflects the extremely brief interludes between individual eruptions. In contrast,

cts between the Roza and other CRBG flows are often marked by erosional surfaces and/or regolith soils. White diatomaceous mudstones also form localized interbeds, particularly in the Grande Coulee-Vantage area. These features represent periods of CRBG volcanic inactivity.

The Roza Member and other Members of the Wanapum Formation are all ferrobasalts with relatively low Si and high Fe, and P, Ti, Zr and other incompatible elements compared to most older CRBG flows. Trace elements are the best discriminators between Wanapum and the younger, more chemically diverse Saddle Mountains Basalt. Incompatible elements (except Cs) are all highly enriched, while a few (ex. Sc and Sr) are depleted in the Saddle Mountains Basalt relative to the older units (Wright and others, 1989). The Roza can be distinguished chemically from the underlying Frenchman Springs Member by its phyric nature and higher Mg, Ca, and P contents. The overlying Priest Rapids Member is aphyric and also has lower silica, higher P, and quite different trace-element abundances than the Roza (Martin, 1989).

The Roza has been subdivided into four major cooling units and at least six chemical subtypes. These divisions are based on lithologic and chemical variations. The areal distribution of each subtype has also been constrained, controls being "the interaction" of vent location, constructional topography of older CRBG flows, regional

structure and paleodrainage" (Martin, 1989).

Cooling units (designated in stratigraphic order by roman numerals) may be composed of multiple flows and chemical subtypes, but are distinguished as one cooling event. Cooling units, I and II are each composed of two chemical subtypes, denoted by appending "A's" and "B's" to their subtype designations. Both cooling units III and IV are single cooling units and chemical subtypes. Unlike cooling units I and II, III and IV consist of multiple flows. Vesicular horizons with ropy texture in conjunction with the reversal of fracture propagation directions on cooling joint surfaces mark the interface between flows of one cooling event. Chemical subtypes are designated by systematic variations in the abundances of compatible elements (Ca and Cr) and incompatible elements (P<sub>2</sub>O<sub>5</sub>, Nb, Zr, TiO<sub>2</sub>).

## 2.2. ROZA ERUPTIVE CENTER CHARACTERISTICS

Spatter cones and feeder dikes are easily identified in the field. Close to vent areas, distinctive red oxidized, scoriaceous material is common. In some cases, the location of an eruptive center has been based solely on the presence of this scoria (Swanson and others, 1975). Also common near vent areas are flowlets. These relatively thin (2 mm to 10 cm) glassy flows typically comprise ramparts or flow packages

that define the shapes of spatter cones. These spatter cones vary greatly in areal extent. Some are subdued (like the vents near Winona), while others (such as Big and Little Butte in southeastern Washington) form major topographic highs on the plateau surface (see figure 3). Flows forming these larger cones tend to be thicker, up to several meters thick. Relatively small irregular dikelets (<10 cm in width), commonly crosscut vent areas. The much larger and more obvious dikes (5 to 40 meters wide) are not commonly associated with a subaerial vent area, but have been exposed in road cuts, hillsides and gorges. Except for the very fine-grained chill margins, typically only several centimeters wide, no significant compositional or textural zonation was noted across dike widths. Joint surfaces and thin, planar zones of vesicles parallel to and within dikes are occasionally observed. Feeder dikes and spatter cones are easily correlated with their flows through major oxide and trace-element chemistry, few exceptions exist (Wright and others, 1989).



### 2.3. SAMPLING AND METHODOLOGY

In total, forty-four samples were collected from along the Roza feeder system and its four cooling units, including twelve (SA1 through SA12) which were kindly provided by B. Martin. In all cases, the freshest possible outcrops were sampled. Suitability of samples for this geochemical study is based on the degree of fracturing, infilling of vesicles, weathering of phenocrysts, iron oxide staining, patinas, etc.

Due to the susceptibility of glass shards to weathering, pristine scoriaceous material is rare. Marginal (m) and core (c) specimens of the dikes were gathered whenever possible, to establish the degree of intradike variation. Marginal does not imply a chilled margin, but rather a sample in close proximity (6-10 cm) to the actual dike margin. Cores are samples from the measured center of the dike width.

All sample locations are easily accessed by car and light hiking. All specimens were analyzed for both major and trace elements using x-ray fluorescence (XRF) on fused glass disks at Washington State University, Pullman, Washington. Normalization was done on a volatile-free basis. All major elements are expressed in weight percent, trace elements in ppm. Table 1 presents averaged analyses of units discussed. Appendix A is a tabulation of all these XRF analyses.

Systematic differences between analyses made for this study and those done by Martin (1989) necessitate

normalization of those elements used to designate Roza chemical subtypes. Biases between Cr, P<sub>2</sub>O<sub>5</sub>, TiO<sub>2</sub>, and CaO contents of twelve samples analyzed by both laboratories have been calculated. Correction factors have only been applied to the other Roza samples in this study for purposes of subtype classification. XRF data quoted in the following sections and in Appendix A are "uncorrected". See Appendix B for details of this classification system.

The detection of the small geochemical variations within the Roza Member is limited by the degree to which these differences range beyond analytical error. Zr variation diagrams have been scaled such that roughly equal degrees of data reliability are presented. Zr is chosen because it is almost completely incompatible within a series of magmas such as that studied in the Roza system. Mg, which is often substituted for Si in this type of diagram, is inappropriate in that its abundance may reflect the end-product of several different processes.

All isotopic analyses were made at the University of Alberta between December 1988 and January 1990. All strontium and neodymium isotopic ratios were measured using a VG354 solid source mass spectrometer, housed in the Physics department. Strontium is measured using a quintuple collector array. Strontium isotopic ratios for each sample are reported relative to the product of the <sup>87</sup>/<sub>86</sub> Strontium ratio of the concurrently run 987 Sr Standard against the long running

average for that standard ( $0.710242 \pm 0.000006(2\text{-sigma})$ ). Similarly, Nd values for each sample are reported relative to the product of the  $^{143}/^{144}$  Nd ratio of the concurrently run La Jolla Nd Standard against the long running average for that standard. Lead isotopic ratios were measured on both the VG354 and MM30 solid source mass spectrometers. Lead isotopic ratios have been normalized using the following correction factors based on NBS 981 Pb Standard:  $^{206}/^{204}$  Pb = 1.002061,  $^{207}/^{204}$  Pb = 1.003006 and  $^{208}/^{204}$  Pb = 1.004530. The mean 2-sigma error on each of these ratios is plus or minus 0.04.

See Appendix C for details of the wet chemical separation process of these long lived radioactive isotopes.

$^{180}$  values for 12 dried whole rock samples were analyzed by Dr. K. Muehlenbachs also at the University of Alberta. Oxygen was extracted with the use of  $\text{BrF}_3$ . Errors listed for measurements indicate the ranges for double and triplicate analyses of each sample (Chapter 3, Table 8).

**FIGURE 3. Generalized sample location map of the Roza feeder system. Locus of each Roza chemical subtype found along the feeder system is also depicted.**

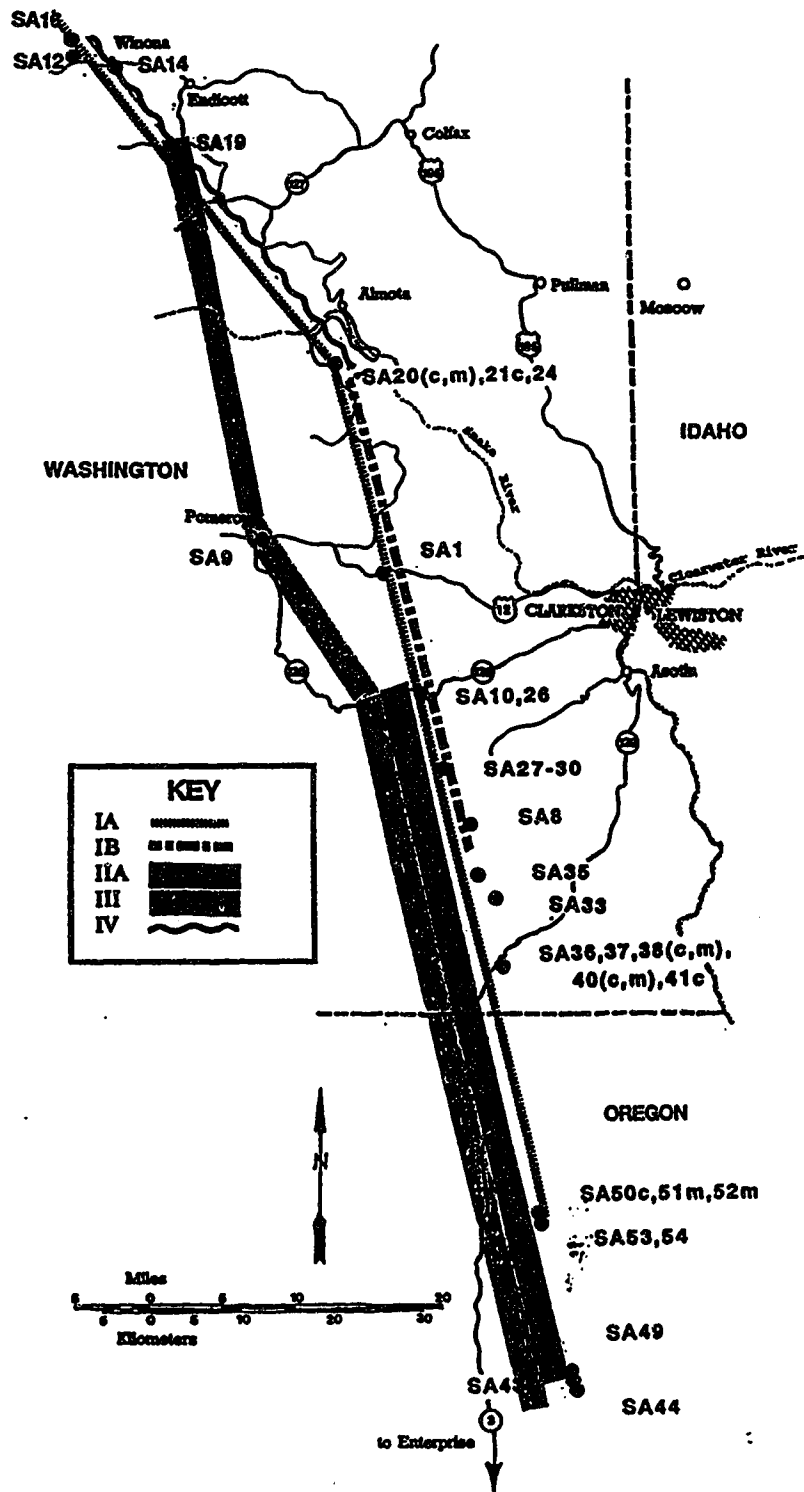


**TABLE 3. Locations and descriptions of the Roza Member samples in this study. Descriptions: dikes (d); near vent flows (v); dikelets (dl); scoria (s); plateau proper flows (p).**

Sample	state/county	Quadrangle	Township/Range/Sec
SA1 (d)	Wa./Garfield	Pullman	11N/43E/13NW
SA2 (p)	Grant	Ritzville	22N/28E/8NWSE
SA3 (p)	Grant	Ritzville	22N/28E/8NWSE
SA4 (p)	Or./Wasco	The Dalles	2N/15E/15NWNE
SA5 (p)	Wa./Grant	Walla Walla	17N/28E/15SSW
SA6 (p)	Wa./Franklin	Walla Walla	14N/36E/28SWNE
SA7 (p)	Wa./Lincoln	Ritzville	27N/32E/1NWSE
SA8 (v)	Wa./Asotin	Pullman	
SA9 (v)	Wa./Garfield	Pullman	12N/42E/32SNE
SA10 (v)	Wa./Asotin	Pullman	10N/44E/19SSW
SA11 (p)	Wa./Grant	Ritzville	23N/28E/15NWNE
SA12 (v)	Wa./Whitman	Winona	17N/39E/23SESE
SA14 (dl)	Wa./Whitman	Winona	17N/40E/20SE
SA16 (s)	Wa./Whitman	Winona	17N/39E/10NE
SA19 (v)	Wa./Whitman	Dusty	16N/41E/21
SA20c (d)	Wa./Garfield	Almota	13N/42E/1N
SA20m (d)	Wa./Garfield	Almota	13N/42E/1N
SA21c (d)	Wa./Garfield	Almota	13N/42E/1N
SA24 (d)	Wa./Garfield	Almota	13n/42E/1N
SA26 (v)	Wa./Asotin	Saddle Butte	10N/44E/30NNW
SA27 (d)	Wa./Asotin	Saddle Butte	9n/44E/20SWNE
SA28 (d)	Wa./Asotin	Saddle Butte	9N/44E/20SWNE
SA29 (d)	Wa./Asotin	Saddle Butte	9N/44E/20SWNE
SA30a (d)	Wa./Asotin	Saddle Butte	9N/44E/20SWNE
SA33 (p)	Wa./Asotin	Anatone	8N/44E/26W
SA35 (v)	Wa./Asotin	Anatone	7N/44E/1
SA36 (d)	Wa./Asotin	Anatone	7N/44E/25SE
SA37 (d)	Wa./Asotin	Anatone	7N/44E/25SE
SA38c (d)	Wa./Asotin	Anatone	7N/44E/25SE
SA38m (d)	Wa./Asotin	Anatone	7N/44E/25SE
SA40c (d)	Wa./Asotin	Anatone	7N/44E/25SE
SA40m (d)	Wa./Asotin	Anatone	7N/44E/25SE
SA41c (d)	Wa./Asotin	Anatone	7N/44E/25SE
SA43 (v)	Or./Wallowa	Elk Mountain	2N/45E/25SW
SA44 (v)	Or./Wallowa	Elk Mountain	2N/45E/25SW
SA49 (v)	Or./Wallowa	Elk Mountain	2N/45E/25SW
SA50m (d)	Or./Wallowa	Elk Mountain	4N/45E/34ENW
SA51c (d)	Or./Wallowa	Elk Mountain	4N/45E/34ENW
SA52c (d)	Or./Wallowa	Elk Mountain	4N/45E/34ENW
SA53 (d)	Or./Wallowa	Elk Mountain	4N/45E/34ESW
SA54 (d)	Or./Wallowa	Elk Mountain	4N/45E/34ESW
SA75 (p)	Wa./Yakima	Yakima	14N/19E/9W
SA77 (p)	Wa./Grant	Walla Walla	16N/23E/4NESW
SA78 (p)	Wa./Grant	Walla Walla	16N/23E/9NWNE

## CHAPTER 3

### ROZA GEOCHEMISTRY AND ISOTOPIC COMPOSITION

#### 3.1. GEOCHEMISTRY OF THE ROZA MEMBER

The Roza flow and feeder system rocks are classified as quartz-normative subalkaline tholeiites according to the scheme proposed by Irvine and Barager (1971) (see Figures 4 and 5). In addition, the Roza Member rocks, in this study, have been subdivided into the six chemical subtypes proposed by Martin (1989). For details of this classification scheme, please refer to Appendix B.

In general, the initial five chemical subtypes from oldest to youngest, IA, IB, IIA, IIB and III, define regular patterns of enrichment and depletion for various elements. In contrast, the youngest subtype, IV, has a distinct composition, yet still has definite Roza composition (Atkinson and Lambert, 1990). Refer to Table 4 (average compositions of Roza chemical subtypes), Figures 6 through 8 (zirconium variation diagrams) and Figure 9 (Sr (ppm) versus silica (weight %)) for the following discussion of these trends. Appendix A gives all XRF data for samples in this study.

The pattern of variation between the initial five subtypes is one of small overlapping groups. These groups define progressive enrichment in Ca, Ni, Cr, Cu, Al and Mg,

plus systematic depletion of Zr, Ti, P, and Zn. These five are also constant in Fe, Mn, and Na. Small, rather irregular decreases in Si and Sr may also be argued. Subtype IV behaves incongruently by defying to continue many of these patterns delineated by the earlier erupted Roza flows. Exceptions to this are Cr, Cu, Mn and Na. Subtype IV departs from other patterns by either reversing or enhancing enrichment factors. Subtype IV is enhanced in Si, Ti, Zr, P, Zn, Al, Ca, Ni, and Sr. Well defined depletions in Fe and Mg are also shown. All six Roza subtypes define diffuse variation patterns for Rb, Ba, K and Pb contents.

Figure 9 plots strontium against silica, for the Roza Member rocks in this study. While subtype IV's are relatively enriched in both species, there is no definite pattern of enrichment for the five older subtypes.

Samples SA38c and SA38m, both from one dike at one location, define one end member of the IA to III chemical trends. These samples are the most enriched in P, Ti and Zr, and similarly depleted in Ni and Mg. They also have the highest Si and Sr contents for a IA subtype. Sample SA7, defines the subtype III endmember of these Roza "main series" trends. It is characteristically high in Cr, Ca, Al, Mg, Ni, and Cu, and low in Si, Ti, P, Zr, and Zn.

At two separate locations, core and margin samples have been classified into different chemical subtypes from the same dike, possibly indicating that compound dikes, dikes of

contrasting compositions, do exist within the CRBG. SA40m and SA40c, both were sampled from a three meter wide dike in southern Washington. They classify respectively as III and IA subtypes. A planar zone of vesicles several centimeters wide, running parallel to and about thirty centimeters from the dike edge, separates these samples in outcrop. Another compound dike is found in northeastern Oregon. SA51c and SA52c are both subtype IA's, while a vesicular marginal sample from the same six meter wide dike outcrop, SA50m is a subtype IIA. No single dikes of contrasting Roza and other CRBG composition have been found. However, in one extremely brecciated vent area, one glassy flow (SA49, subtype IIA), entrained angular blocks of low Mg Grande Ronde Basalt. Glassy margins of SA49, about one centimeter wide, surround these flow supported clasts.

Besides the few exceptions mentioned above, intradike variation within the Roza Member is insignificant. In addition, variation between Roza dikes and flows is lacking. Table 5 compares the average XRF analyses of all the flow rocks studied to those of the feeder system.

### 3.2. ISOTOPE GEOCHEMISTRY

Strontium, neodymium, lead and oxygen isotopic ratios have been measured on whole rock powders of samples collected



along the Roza feeder system and on the plateau. In addition, plagioclase phenocrysts from along the feeder system have also been analyzed for 87/86 strontium. Tables 6 and 7 summarize all strontium, neodymium and lead isotopic analyses, while Table 8 gives  $\delta^{18}\text{O}$  data. Appendix C gives complete details of radiogenic isotopic chemical separations.

Sr isotopic values for each sample are reported relative to the product of the 87/86 Sr ratio of the concurrently run 987 Sr Standard against the long running average for that standard. Reproducibility of strontium isotopic data has been checked on many samples and averages better than 1 in the 4th decimal place (see table 6). Precision of this strontium isotopic data is less than 2 in the 5th place. Similarly, Nd values for each sample are reported relative to the product of the 143/144 Nd ratio of the concurrently run La Jolla Nd Standard against the long running average for that standard. Reproducibility for neodymium isotopic ratios average less than 8 in the 5th decimal place. Likewise, precision of these ratios are less than 10 in the 5th place. Lead isotopic ratios have been normalized using the following correction factors based on NBS 981 Pb Standard: 206/204 Pb = 1.002061, 207/206 Pb = 1.003006 and 208/204 Pb = 1.004530. The mean 2-sigma error on each of these lead-lead ratios is plus or minus 0.04.

The initial five subtypes that erupted along the feeder system have 87/86 strontium ratios that range from 0.7051 to

0.7053. The last subtype to erupt, IV, has ratios equal to 0.7054.  $^{143}/^{144}$  neodymium data for all subtypes ranges between 0.512575 and 0.512630.

$^{206}/^{204}$  lead values range from 18.77 and 18.86,  $^{208}/^{204}$  lead between 38.780 and 39.162, and  $^{207}/^{204}$  lead between 15.59 and 15.64. The line drawn through the data on the standard  $^{207}/^{204}$  Pb versus  $^{206}/^{204}$  Pb plot is defined by the following equation:  $Y = 1.06X - 4.23$ . Fractionation of lead data during mass spectrometric measurement is common and can be created through unsuitable filament temperatures, amounts of lead and silica gel loaded onto the filament and contaminants (Godwin and others, 1988). Fractionation can produce linear trends almost proportional to mass differences between isotopes used to calculate ratios. The slope for the  $^{207}/^{204}$  Pb versus  $^{206}/^{204}$  Pb plot is  $M = 3Y/2X$ . The average fractionation line slope for the Roza Member data points is approximately 1.25. Since this fractionation line does not run parallel to the data line, one concludes that the Roza Pb isotopic variation is not due to fractionation in the mass spectrometer. Further, "204" error (due to inexact measurement of the small  $^{204}\text{Pb}$  peak), has the equation  $Y = X$ : this form of error does not appear to be present in these data, because of the intercept of -4.23.

Figures 10 through 13 illustrate respectively the compositional variation of  $^{87}/^{86}$  strontium versus Sr (ppm),  $\text{SiO}_2$  (weight %), Cr (ppm) and Rb/Sr. Strontium, silica and

Rb/Sr have been chosen for their importance in determining crustal contamination. Chromium has been plotted because of its large compositional range and importance in chemical subtype classification. Where indicated by open squares the isotopic compositions of plagioclase separates have been plotted versus the elemental compositions of their whole rock powders. These diagrams show the elevated 87/86 strontium, silica and chromium contents of Subtype IV and except for chromium the relatively restricted overlap of the earlier erupted chemical subtypes. The 87/86 strontium isotopic compositions of the plagioclase separates range within that of their respective chemical subtypes.

Figure 14 depicts the slight, albeit poor, negative correlation between strontium and neodymium isotopic compositions within the Roza. Figures 15 and 16 are respectively plots of 207/204 lead and 208/204 lead versus 206/204 lead compositions of the Roza Member.

Twelve Roza whole rock samples (SA1 through SA12) have also been analyzed by Dr K. Muehlenbachs at the University of Alberta for  $\delta^{18}\text{O}$ . These values range between 5.28 and 7.11 and display an overall slightly positive correlation with SiO<sub>2</sub> and 87/86 Sr values (see Figures 17 and 18). While the youngest subtype (IV) does have the highest  $\delta^{18}\text{O}$ , there is no systematic trend defined for the earlier erupted I, II or III subtypes.

**TABLE 4. Average compositions of Roza chemical subtypes.**

Subtype	IA (n=18)	IB (n=3)	IIA (n=8)	IIB (n=1)	III (n=7)	IV (n=4)
<b>MAJOR OXIDES</b>						
SiO <sub>2</sub>	51.70	51.38	51.47	51.15	51.51	52.74
Al <sub>2</sub> O <sub>3</sub>	13.34	13.35	13.36	13.55	13.68	14.67
TiO <sub>2</sub>	3.171	3.182	3.10	3.126	3.08	3.21
FeO*	14.07	14.11	14.02	13.96	13.94	11.53
MnO	0.224	0.224	0.23	0.221	0.218	0.306
CaO	8.47	8.46	8.56	8.62	8.65	9.40
MgO	4.21	4.39	4.46	4.55	4.20	3.28
K <sub>2</sub> O	1.41	1.39	1.34	1.41	1.28	1.25
Na <sub>2</sub> O	2.70	2.82	2.79	2.75	2.79	2.91
P <sub>2</sub> O <sub>5</sub>	0.702	0.702	0.68	0.654	0.650	0.684
Total	100.0	100.0	100.0	100.0	100.0	100.0
<b>TRACE ELEMENTS</b>						
Ni	12	12	13	15	17	22
Cr	29	28	36	42	49	54
Sc	41	41	40	40	41	41
V	417	425	411	428	422	435
Ba	541	521	522	485	501	749
Rb	37	30	34	30	32	34
Sr	305	304	304	300	305	346
Zr	187	186	184	181	182	190
Y	46	46	45	45	45	46
Nb	17.50	17.57	17.46	16.50	17.46	17.20
Ga	22	23	21	18	21	23
Cu	23	23	24	26	29	33
Zn	135	135	132	133	133	139
Pb	9	7	9	7	7	9
La	24	14	18	24	24	21
Ce	60	60	52	53	46	54
Th	4	4	5	5	4	5

**TABLE 5. Average Chemical Compositions for Roza Flows and Feeder Rocks.**

	Flows n = 11	Feeder n = 33
<b>Normalized Results (weight %)</b>		
SiO <sub>2</sub>	51.24	51.82
Al <sub>2</sub> O <sub>3</sub>	13.40	13.57
TiO <sub>2</sub>	3.116	3.153
FeO	14.10	13.71
MnO	0.226	0.232
CaO	8.54	8.63
MgO	4.52	4.10
K <sub>2</sub> O	1.34	1.36
Na <sub>2</sub> O	2.83	2.74
P <sub>2</sub> O <sub>5</sub>	0.677	0.688
Total	100.0	100.0

<b>Trace Elements (ppm)</b>		
Ni	14	14
Cr	37	36
Sc	41	40
V	421	418
Ba	506	559
Rb	30	36
Sr	301	311
Zr	183	186
Y	45	46
Nb	17.4	17.5
Ga	20	22
Cu	26	25
Zn	133	134
Pb	8	9
La	20	22
Ce	58	54
Th	4	4

TABLE 6. Strontium and neodymium isotopic analyses of Roza samples from this study.

Sample (SA"X")	Subtype	87/86 Strontium (2 sigma error)	143/144 Neodymium (2 sigma error)
1	IA	0.705269 (21)	0.512620 (6)
1	IA	0.705250 (8)	
2	IA	0.705293 (14)	
3	IIA	0.705243 (21)	
3	IIA	0.705270 (14)	
4	IIA	0.705268 (16)	
4	IIA	0.705243 (16)	
5	III	0.705233 (21)	
5	III	0.705215 (18)	
6	IB	0.705261 (14)	
6	IB	0.705218 (14)	
6	IB	0.705289 (16)	
7	IB	0.705558 (21)	
8	IB	0.705219 (14)	0.512610 (8)
9	III		0.512622 (5)
10	IIA	0.705273 (16)	0.512604 (7)
10	IIA	0.705230 (25)	
10	IIA	0.705149 (25)	
12	IV	0.705423 (21)	
14	IV	0.705511 (34)	0.512581 (10)
16	IA	0.705271 (21)	0.512604 (9)
19	IA		0.512554 (10)
			0.512605 (18)
20C	IV	0.705358 (6)	0.512633 (27)
20C	IV	0.705389 (17)	
20M	IV		0.512607 (10)
21C	IB	0.705226 (28)	0.512556 (9)
24	IA		0.512608 (15)
26	IA	0.705282 (17)	0.512607 (9)
			0.512545 (6)
27	IA	0.705410 (39)	0.512608 (4)
27	IA	0.705218 (16)	0.512651 (6)
28	IA	0.705315 (17)	0.512600 (4)
			0.512676 (3)
			0.512524 (7)
29	IIA	0.705164 (18)	0.512613 (3)
29	IA	0.705279 (32)	0.512561 (6)
30	IA	0.705181 (32)	0.512619 (3)
33	IA		0.512854 (63)
35	IA	0.705226 (6)	0.512615 (10)
			0.512575 (11)
36	IA	0.705228 (16)	0.512684 (199)
37	IA	0.705306 (18)	0.512584 (14)
38C	IA	0.705260 (11)	0.512606 (4)
38C	IA	0.705163 (17)	0.512628 (6)

TABLE 6 - continued. Strontium and neodymium isotopic analyses of Roza samples from this study.

Sample (SA <sup>n</sup> X <sup>n</sup> )	Subtype	87/86 Strontium (2 sigma error)	143/144 Neodymium (2 sigma error)
38M	IA	0.705254 (8)	0.512610 (35)
40C	IA	0.705189 (20)	0.512603 (8)
			0.512580 (11)
40M	III	0.705213 (8)	0.512545 (25)
			0.512631 (75)
41C	IA	0.705218 (10)	0.512632 (6)
			0.512562 (8)
43	IIA	0.705089 (10)	
44	III	0.705241 (11)	0.512604 (5)
			0.512636 (5)
			0.512633 (4)
49	IIA	0.705236 (13)	0.512635 (7)
			0.512617 (11)
50	IIA	0.705225 (25)	0.512603 (4)
			0.512435 (8)
51C	IA	0.705186 (14)	0.512635 (16)
52C	IA	0.705156 (13)	
53	IIA	0.705145 (10)	
54	III	0.705186 (10)	0.512624 (10)
75	IIA		0.512569 (11)
77	IIA		0.512652 (12)
78	IIA		0.512631 (11)
Plagioclase separates			
P16	IA	0.705360 (101)	
P19	IA	0.705206 (34)	
P20C	IV	0.705106 (111)	
P24	IA	0.705252 (76)	
P26	IA	0.705124 (45)	
P30	IA	0.705108 (25)	
P35	IA	0.705102 (73)	

TABLE 7. Lead isotopic data for Roza samples in this study.

Sample (SA"X")	208/204	207/204	206/204
1	38.857	15.62	18.81
8	38.828	15.61	18.80
9	38.803	15.60	18.79
10	38.824	15.61	18.79
12	38.806	15.60	18.79
14	38.805	15.60	18.78
16	38.825	15.60	18.78
19	38.868	15.62	18.81
20m	38.790	15.60	18.79
24	38.793	15.60	18.79
26	38.790	15.60	18.79
27	38.781	15.60	18.77
28	38.787	15.59	18.77
30	39.162	15.69	18.86
35	38.796	15.59	18.77
38c	38.803	15.59	18.78
41c	38.917	15.64	18.80
44	38.795	15.60	18.79
50	38.892	15.62	18.80



TABLE 8.  $\delta^{18}\text{O}$  values of selected Roza Member whole rock powders.

Sample	Subtype	$\delta^{18}\text{O}$	(2 sigma error)
SA1	IA	5.28	0.02
SA2	IA	6.60	0.04
SA3	IIA	6.96	0.02
SA4	IIA	6.63	0.07
SA5	III	5.42	0.02
SA6	IB	6.35	0.07
SA7	IB	6.30	0.04
SA8	IB	6.09	0.02
SA9	III	6.54	0.02
SA10	IIA	6.16	0.06
SA11	IIB	6.42	0.02
SA12	IV	7.11	0.05

FIGURE 4. AFM variation diagram for all Roza samples included in this study. A =  $K_2O + MgO$ ; F = FeO; M = MgO. All in weight percent. Modified after Irvine and Barager, (1971).

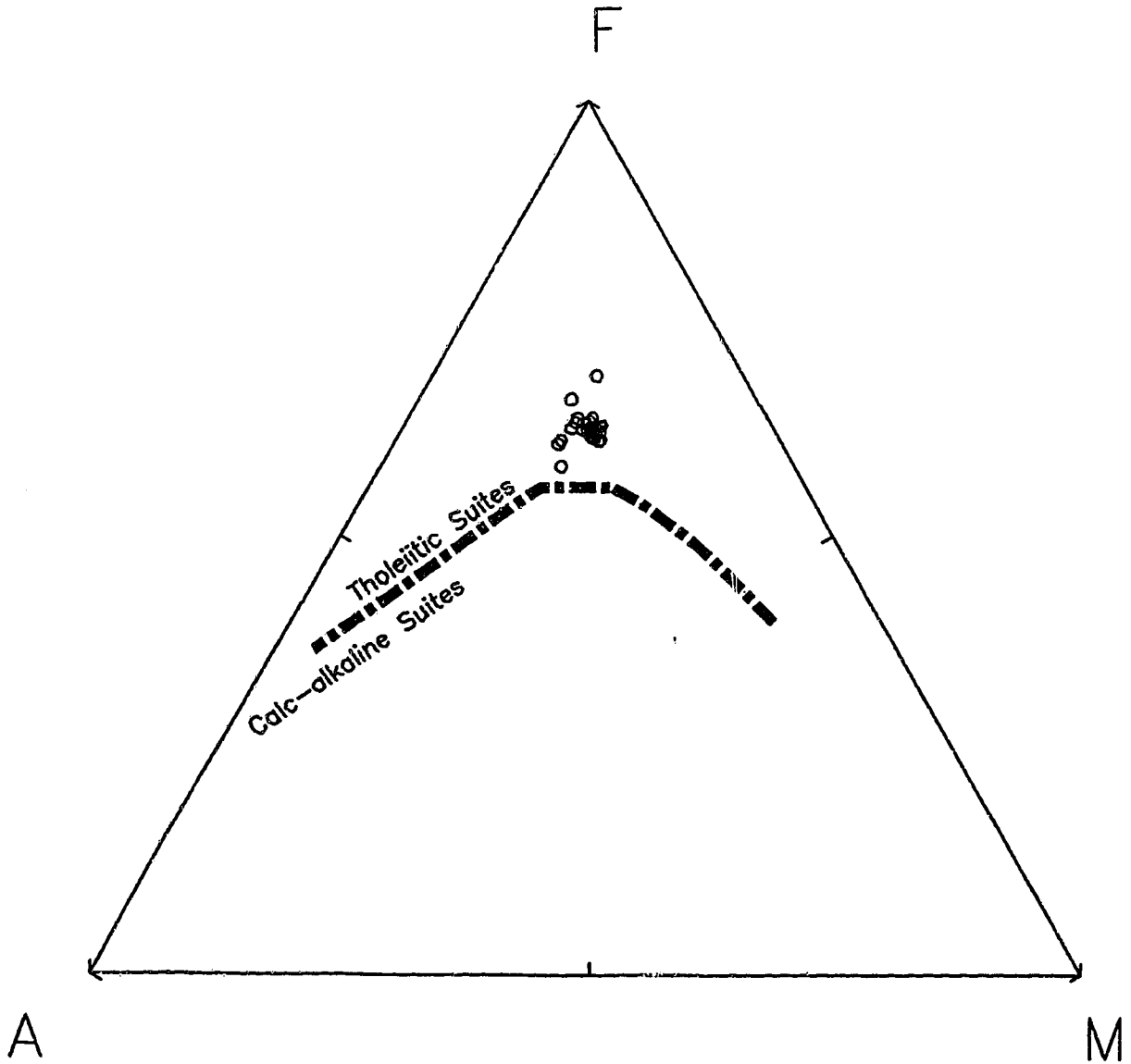
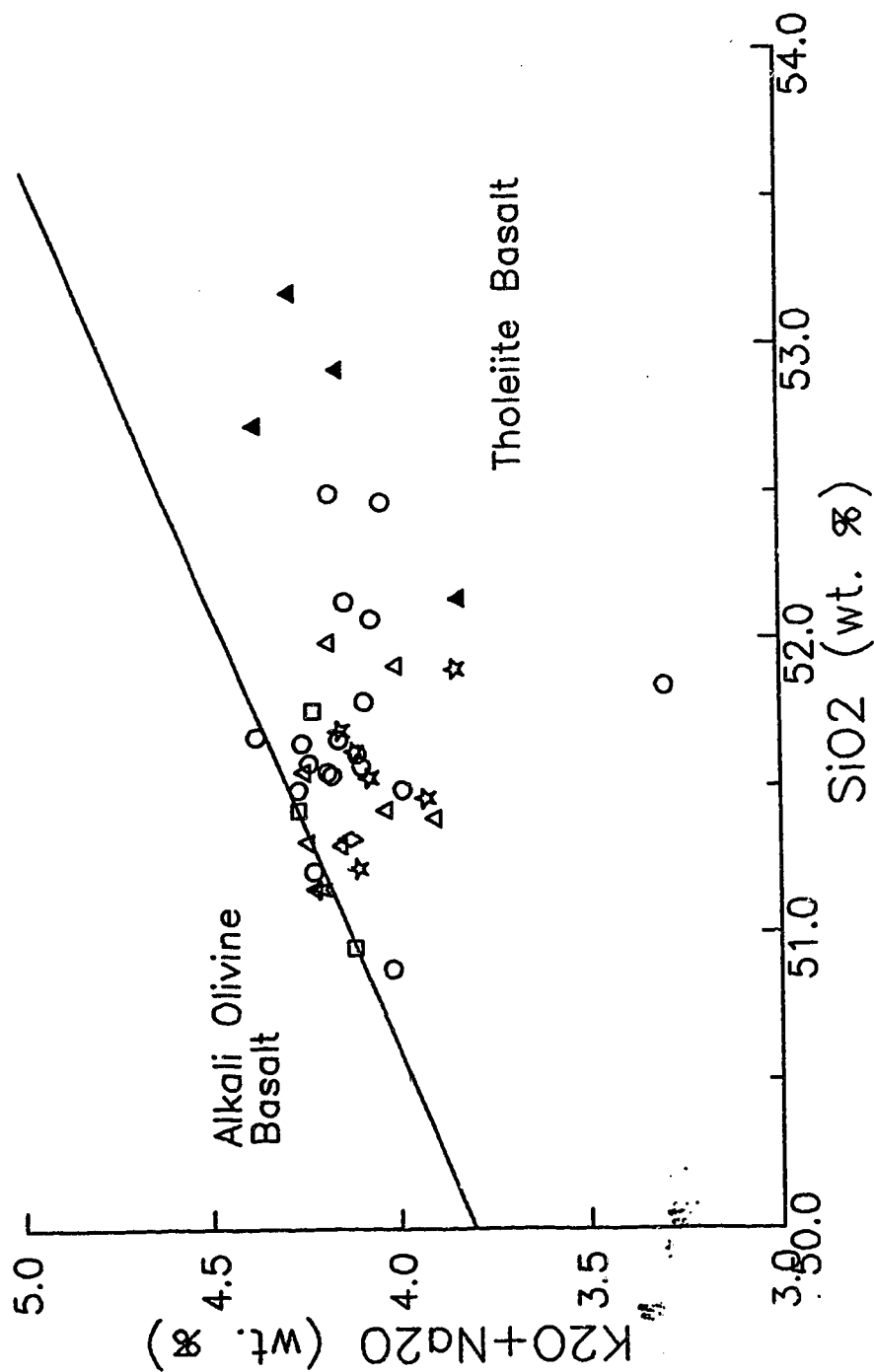


FIGURE 5. Alkali versus silica diagram of Roza Member Samples. Modified after Irvine and Barager (1971). Subtypes identified as follows: circles (IA); squares (IB); triangles (IIA); diamonds (IIB); stars (III); filled triangles (IV).



**FIGURE 6.** Zr variation diagrams. Symbols as presented in Figure 5.

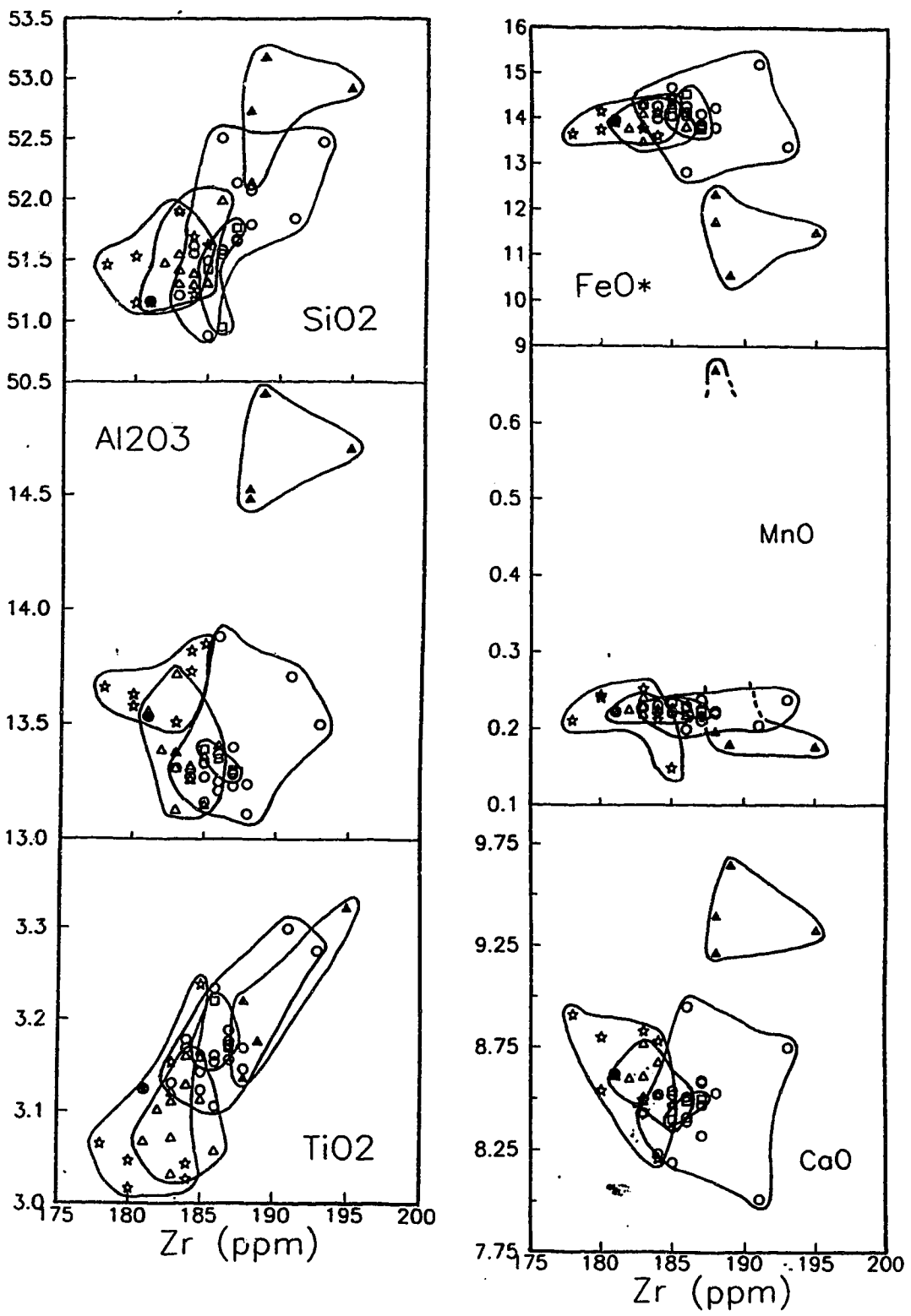
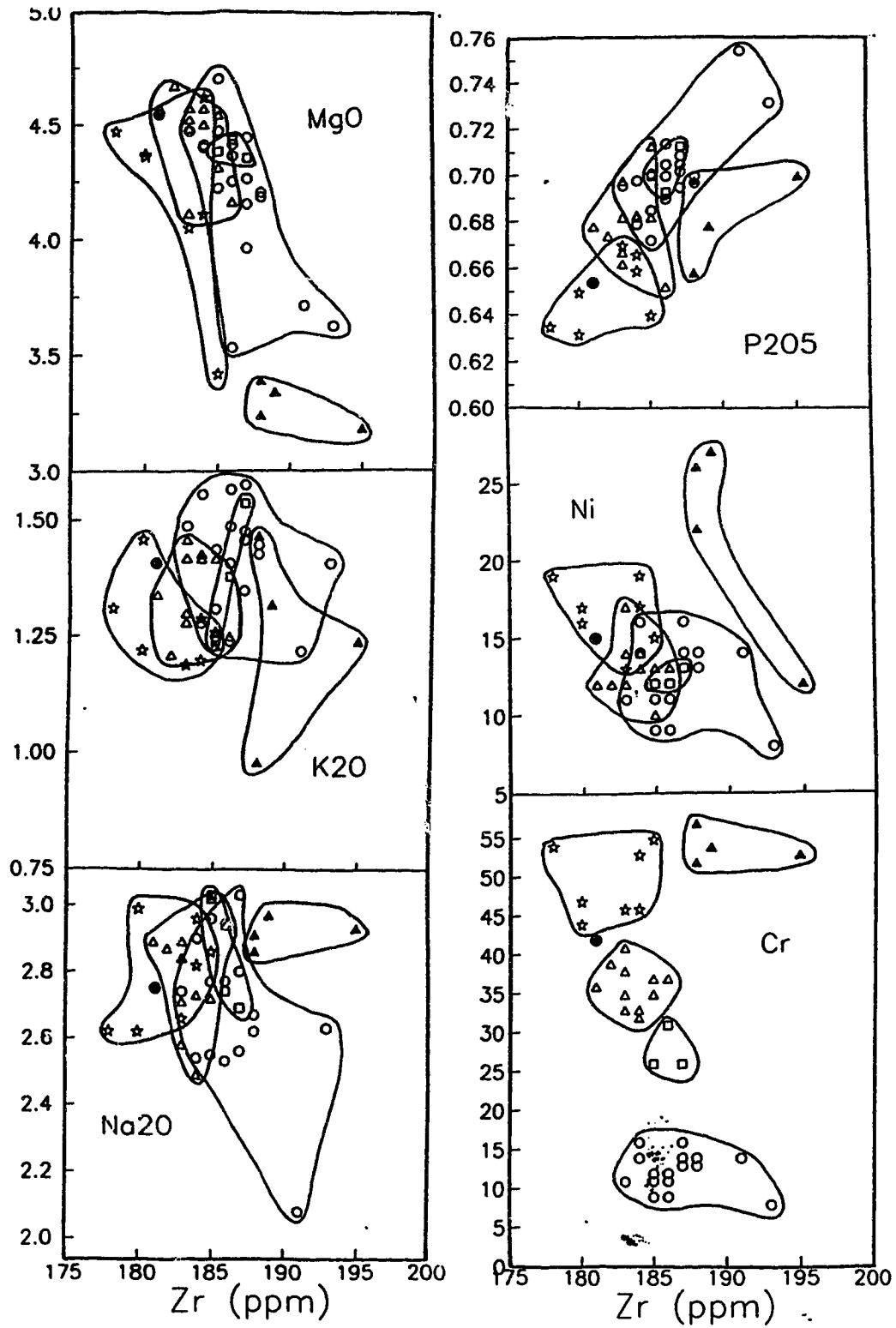


FIGURE 7. Zr variation diagrams. Symbols as presented in Figure 5.



**FIGURE 8.** Zr variation diagrams. Symbols as presented in Figure 5.

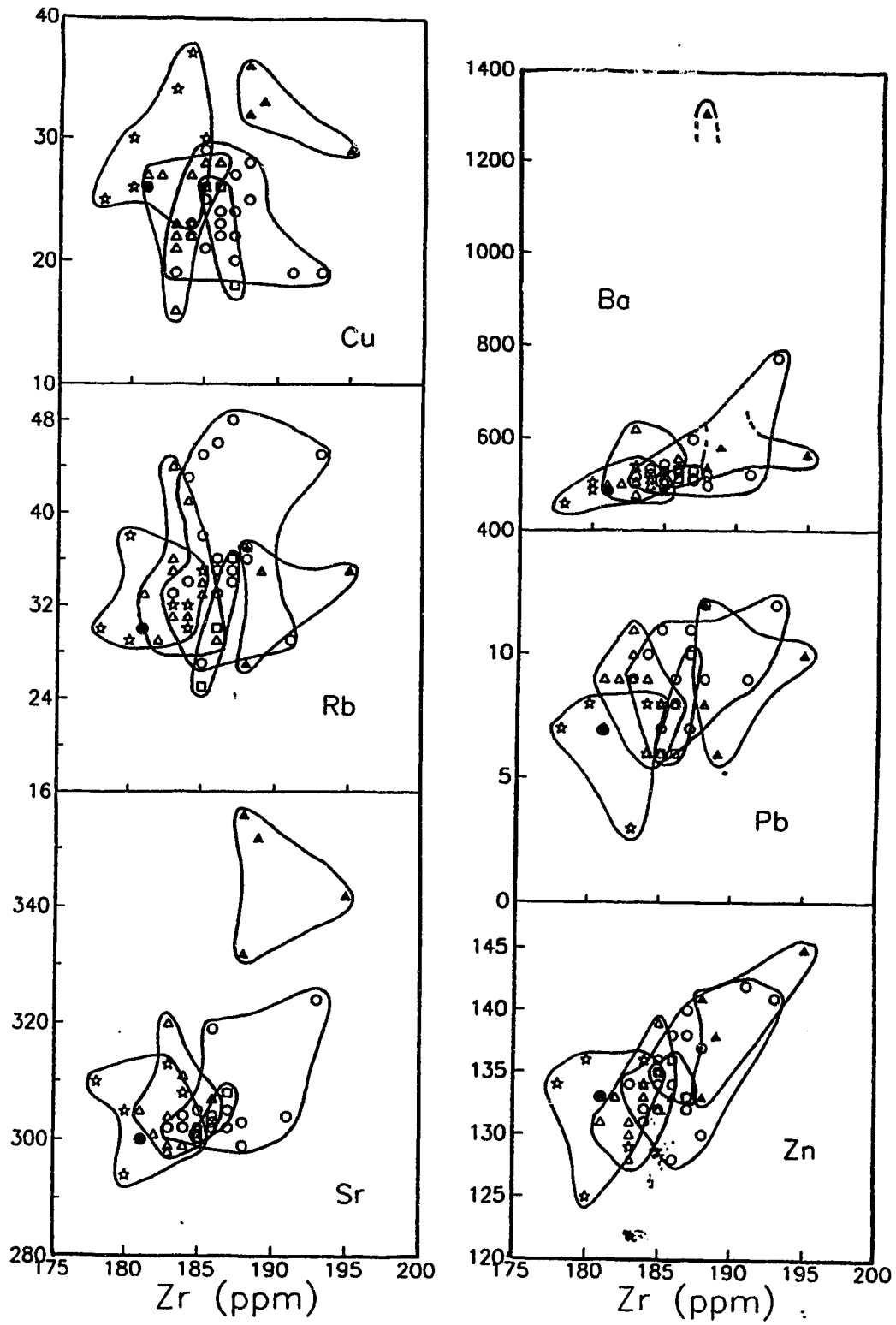


FIGURE 9. Strontium versus silica plot of all Roza samples. Symbols refer to the chemical subtypes of these rocks.

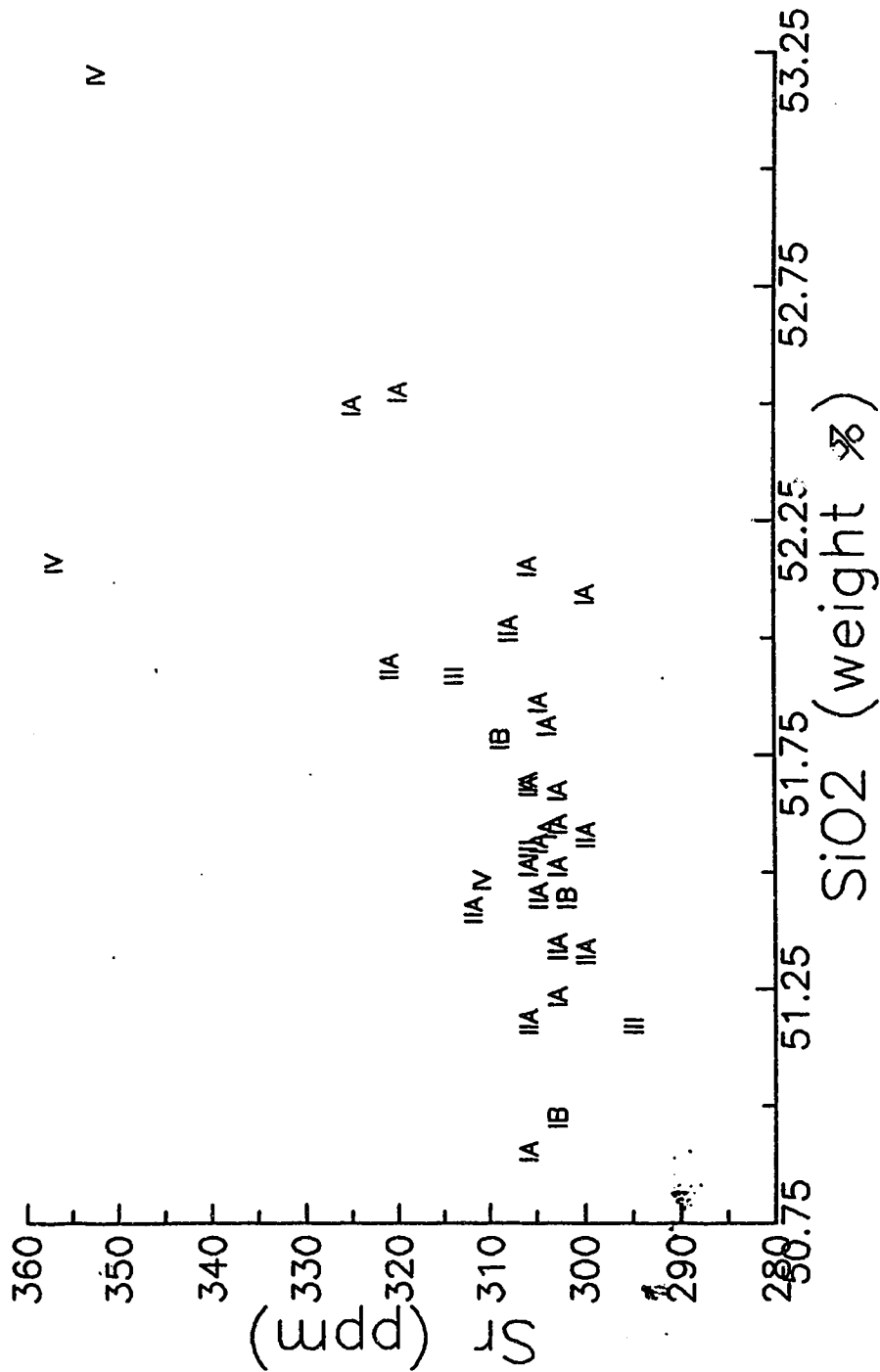


FIGURE 10.  $^{87}/^{86}$  Strontium versus strontium (ppm) plot of Roza samples. Symbols depict the chemical subtypes for whole rock samples, while open squares mark plagioclase separates.

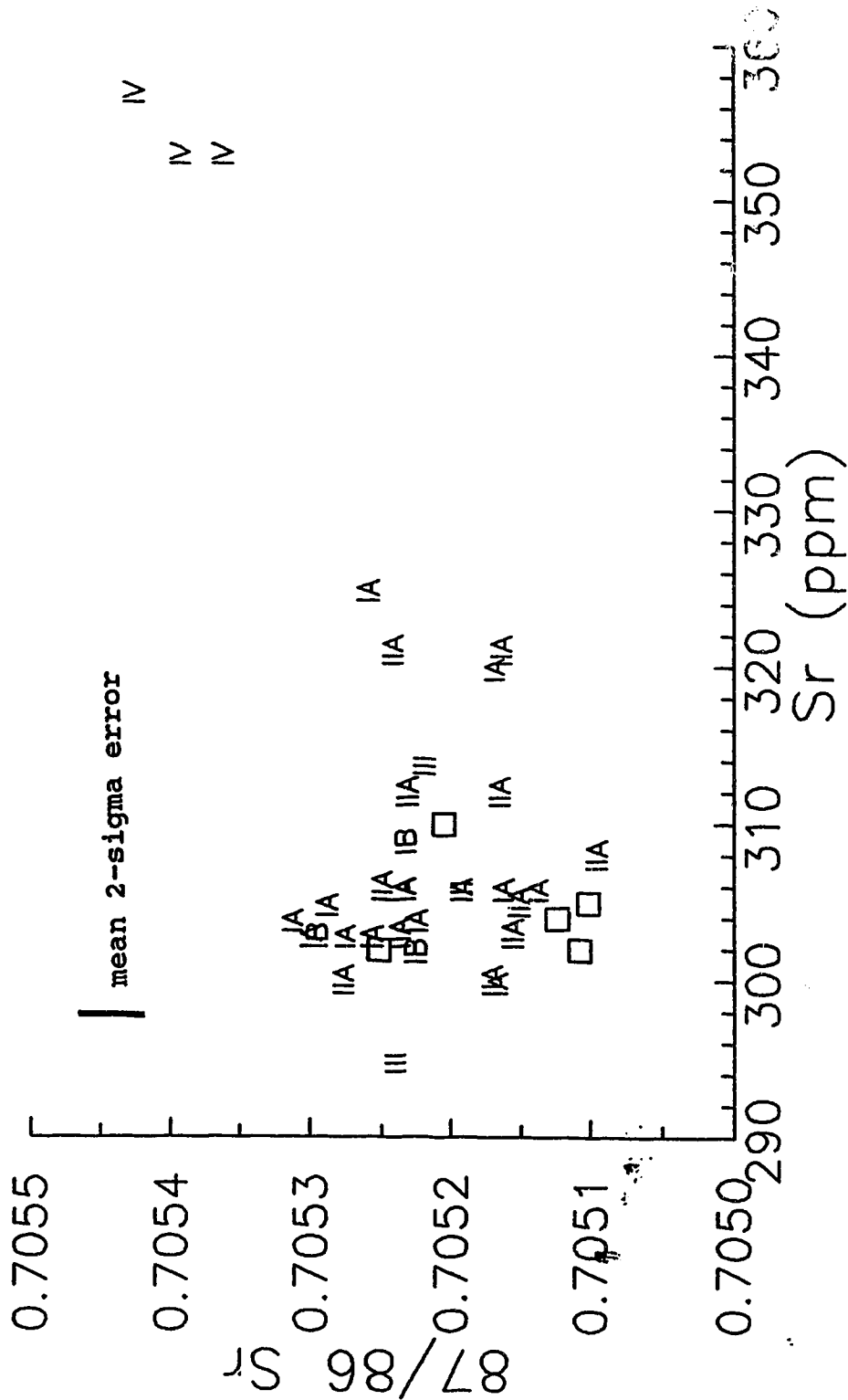




FIGURE 11. 87/86 Strontium versus silica (ppm) plot of Roza samples. Symbols depict the chemical subtypes for whole rock samples, while open squares mark plagioclase separates.

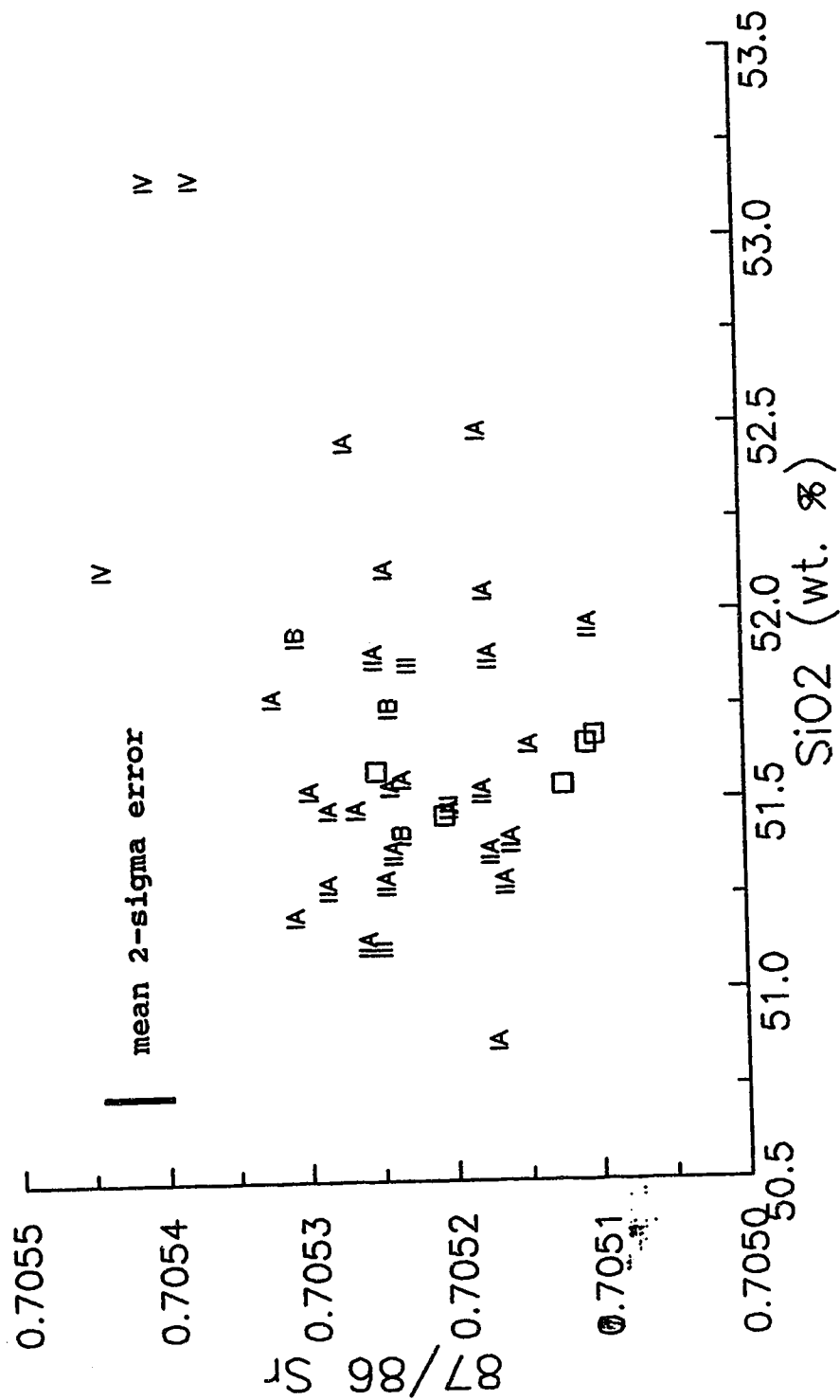




FIGURE 13.  $^{87}/^{86}$  Strontium versus rubidium/strontium ratio plot of Roza samples. Symbols depict the chemical subtypes for whole rock samples, while open squares mark plagioclase separates.

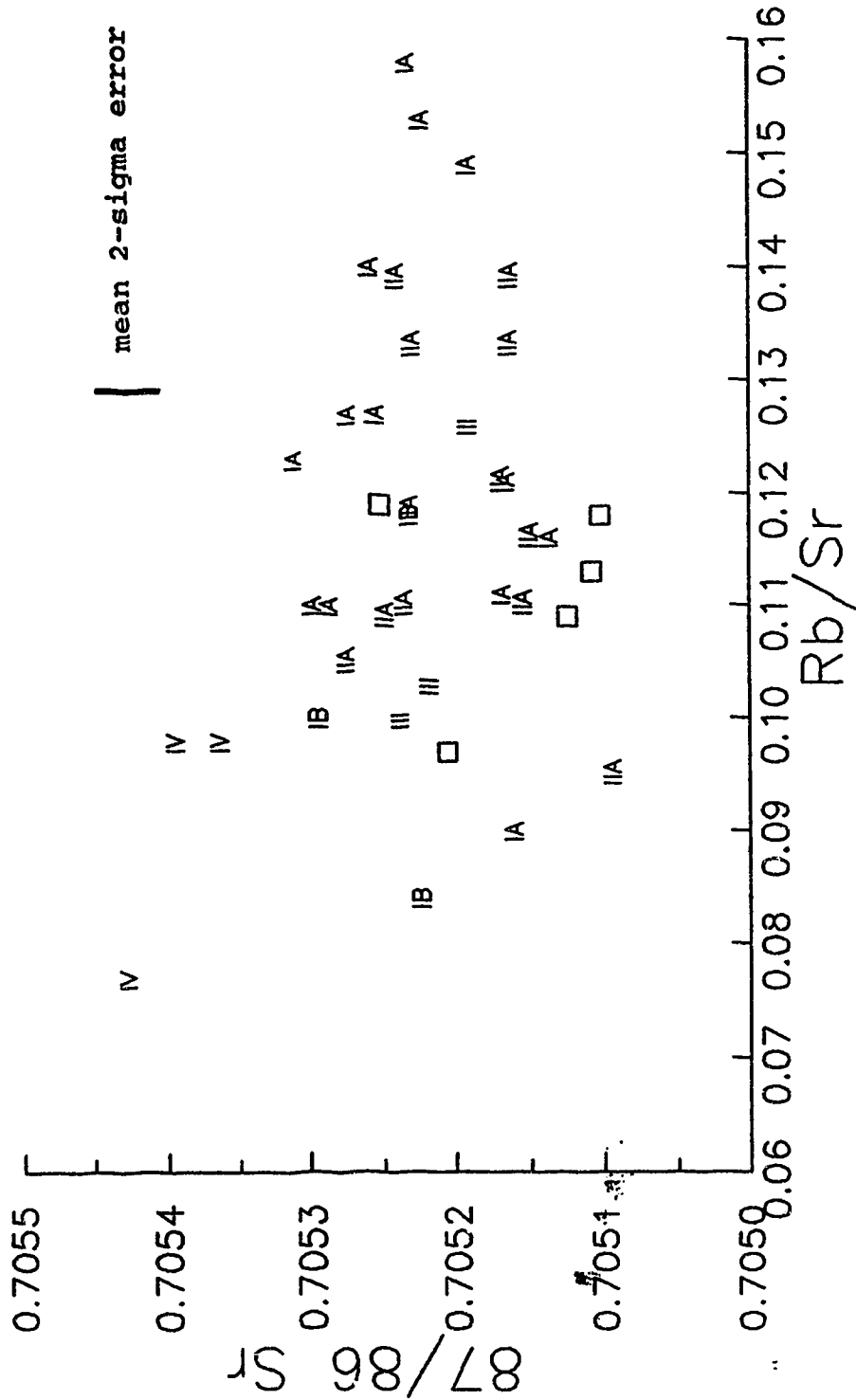


FIGURE 14.  $^{143}/^{144}$  neodymium versus  $^{87}/^{86}$  strontium plot of Roza samples. Symbols depict the chemical subtype of each sample.

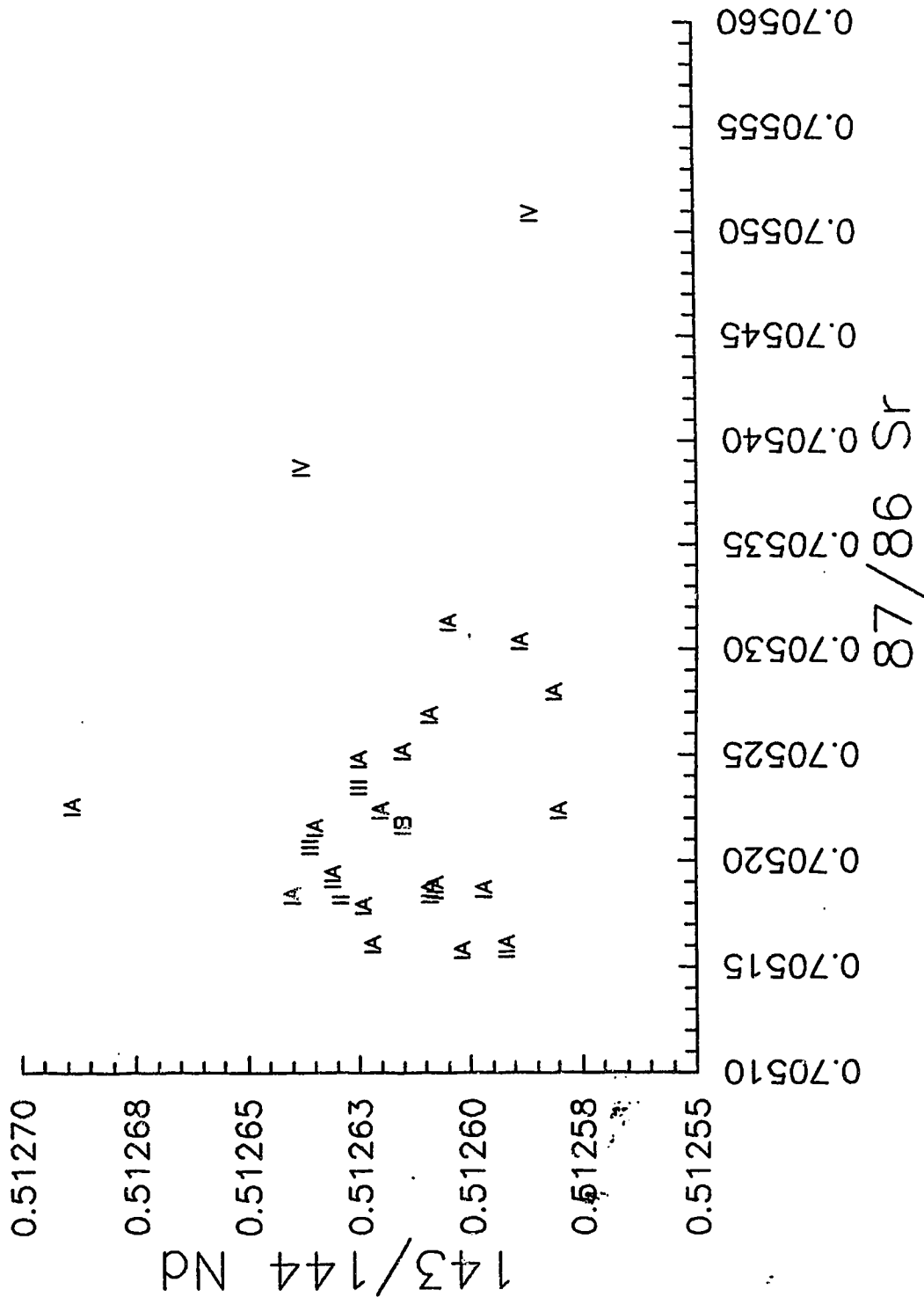






FIGURE 17.  $\delta^{18}\text{O}$  versus silica plot of Roza samples. Symbols depict the chemical subtype of each sample.

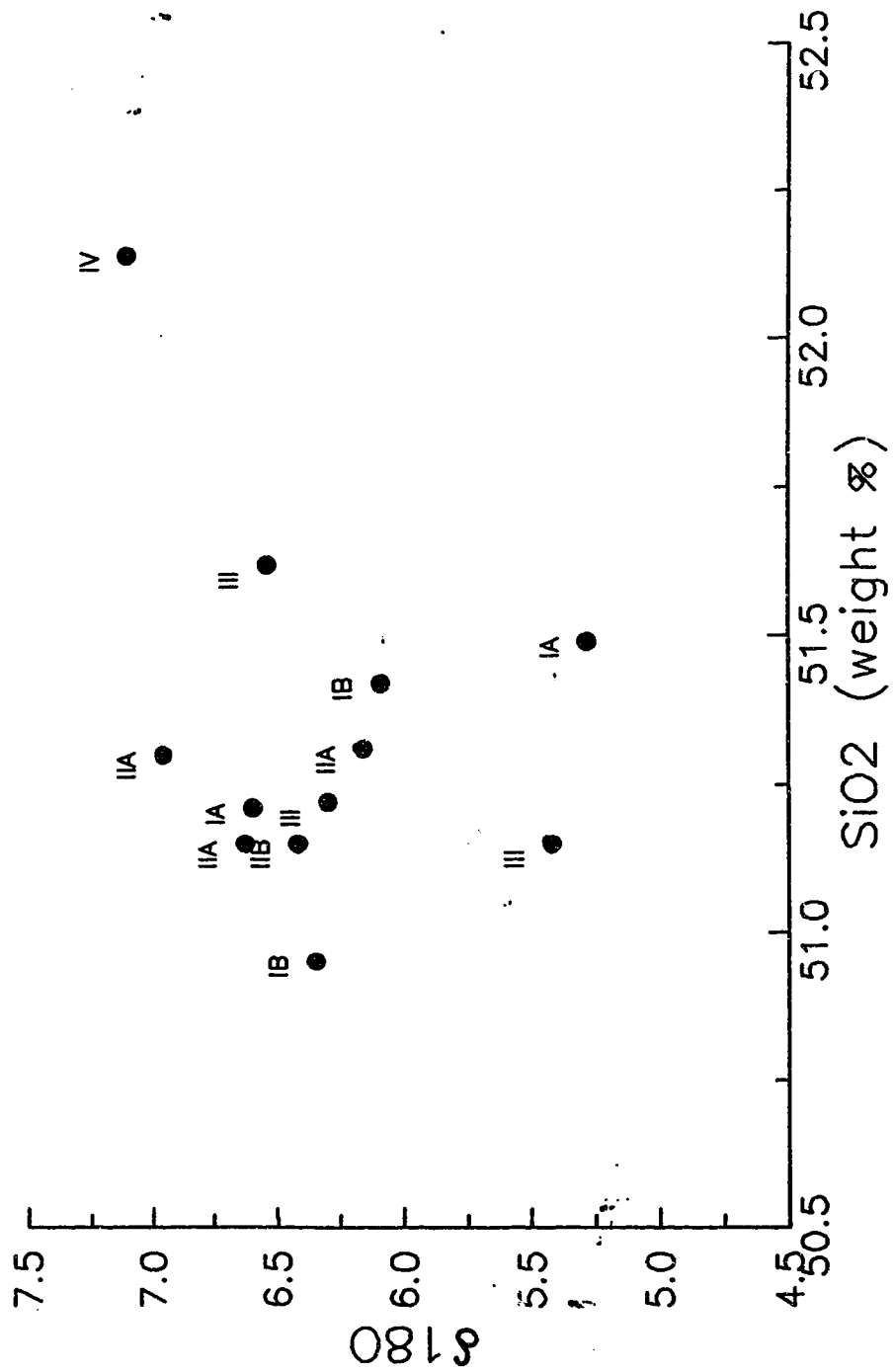
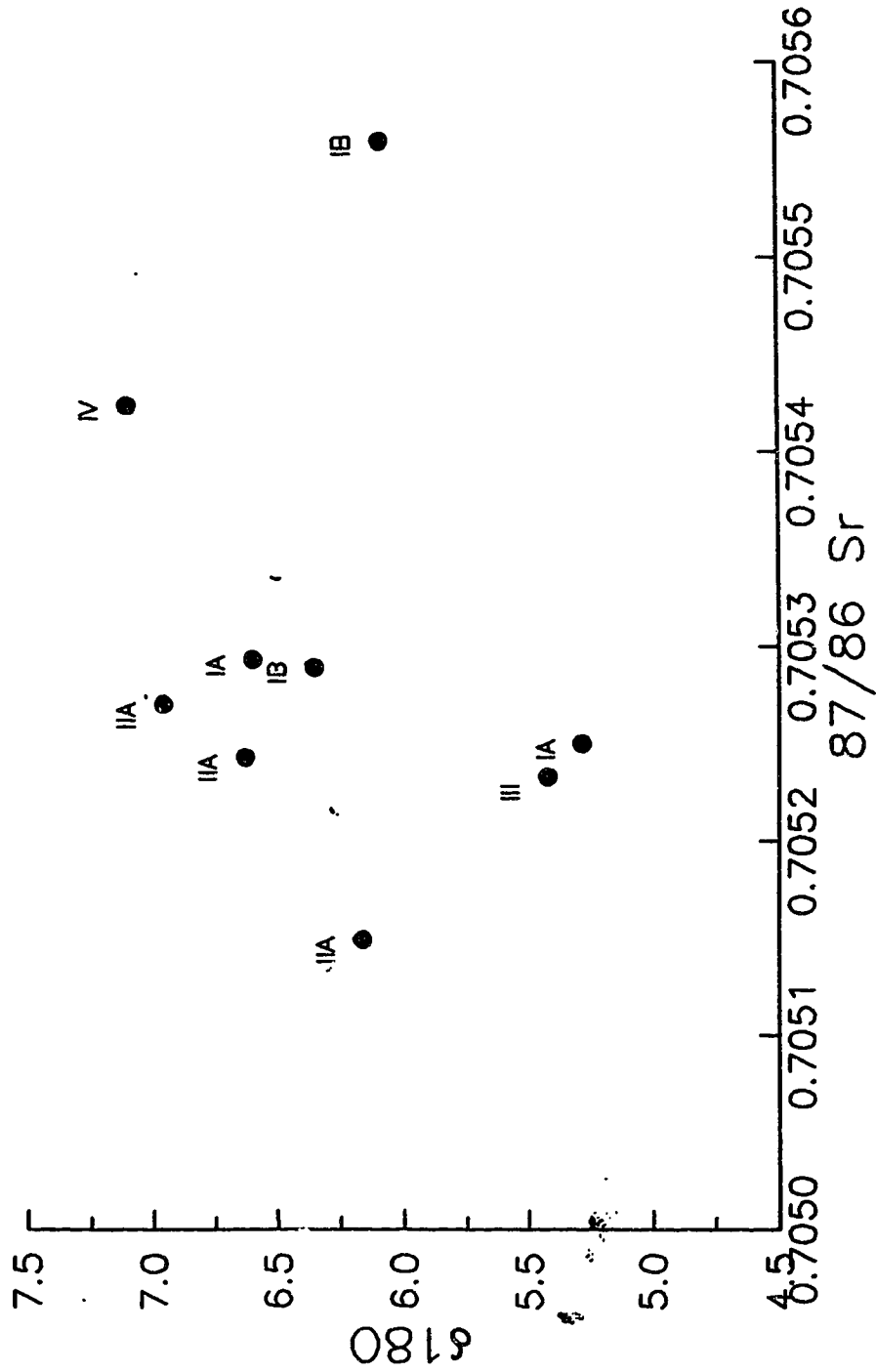


FIGURE 18.  $\delta^{18}\text{O}$  versus  $87/86$  strontium plot of Rozz samples. Symbols depict the chemical subtype of each sample.





**CHAPTER 4**  
**DISCUSSION, CONCLUSIONS, AND SUMMARY**

**4.1. DISCUSSION**

**4.1.1. Dike Emplacement**

The manner of Roza feeder emplacement can be recognized using observations of modern fissure eruptions, and field and chemical data. Modern fissure eruptions like those of Iceland and Hawaii are of similar magnitude and form as the CRBG. At least three main stages of fissure eruption have been documented from inception to final eruptions (see Figure 19). Stage one begins with the rapid propagation of eruptive fissures and the fountaining of lava all along it. This fountaining is also known as a "curtain of fire" type eruption. Small spatter ramparts may also develop at this time. Stage two is characterized by a general decrease in fountaining height and shortening of active fissure lengths as surface portions solidify. Localized growth of spatter cones is common. The final stage is typified by the continued growth of these cones and further reduction in fissure segment lengths and fountaining heights (Delaney and Pollard, 1982).

Although remnants of all these features exist along the system, details of the eruptive sequence at the scale described above is unresolved. However, each episode of Roza

flow eruption can be distinguished using chemical data (Atkinson and Lambert, 1990). See Figures 20 through 25 for the distribution of these subtypes along the feeder system and on the plateau. Figure 3 (chapter 2) also depicts the generalized locus of eruption along the feeder system for each of the different subtypes.

The oldest Roza flow (IA) issued from nearly the entire length of the known feeder system, while the next flow (IB) appears to be restricted to a 55 kilometer segment centered west of Clarkston, Washington. Data from this study, combined with those of Martin (1989,) indicate that the IIA chemical subtype erupted along the entire length of the known system. No vents have been found for the IIB subtype. However, the flow distribution of the IIB indicates that centers are located in the proximity of the systems northern end (Martin, 1989). Subtype III erupted along nearly the entire feeder system, while the subtype IV was restricted to the northern half.

Swanson and Wright (1978) and Wright and others (1989), note that CRBG dikes including those in the Roza feeder system are often compound or multiple dikes. Until now, composite dikes, those with two or more contrasting compositions have not been found. This new evidence suggests that separate magma pulses from the same intrusive event may follow the same path, and fissures may be used more than once.

Huppert and Sparks (1985) have studied the cooling and contamination of mafic to ultramafic magmas as they erupt through continental crust. They conclude that basalts would selectively be contaminated by rocks with lower fusion temperatures. In contrast, higher temperature komatiites would be less selective in what they assimilated. It was also concluded from flood basalt flow rates that turbulent flow must also have been reached and crustal contamination is inevitable. The fractal geometry of the feeder system would seem to oppose this statement. It is conceivable to have laminar flow within a very constricted planar conduit paired with turbulent flow at the surface as the confining pressure of the liquid is released.

Fusible incompatible element enriched veins in the ancient subcontinental lithospheric mantle are also possible candidates for basalt contamination. These veins in the metasomatized mantle may be comprised of phlogopite, amphibole or sodic amphibole (Harte, 1983; Menzies, 1983). These minerals would provide the unique enrichments in K, Ba and Rb while not changing the other major and trace elements by detectible amounts.

No apparent difference is observed in the composition of the same subtype across the craton\terrane suture. Therefore if the source of contamination for these magmas was in the metasomatized sublithosphere, no apparent difference exists between underlying the North American craton, and that

underlying the Mesozoic oceanic-type Blue Mountains terrane.

#### 4.1.2. Geochemistry

Geochemical tectonic discrimination diagrams for basalts lack consistency in establishing the setting for the Roza Member. The Roza Member appears to be either a within-plate basalt, an ocean ridge and floor basalt, or a continental basalt using the following diagrams respectively: Figure 26,  $Zr-Ti/100-Y*3$ ; Figure 27,  $Zr-Ti/100-Sr/2$ ; and both Figure 28,  $MgO-FeO^*-Al_2O_3$  and Figure 29,  $K_2O-TiO_2-P_2O_5$ . Wright and others (1989) report similar discrepancies for all the main series CRBG Members. Explanations for this include either the inability of chosen elements to discriminate accurately, the complex mixed nature of the source, or most likely the highly fractionated nature of these rocks (Goles, pers. comm., 1990; Wright and others, 1989).

The N-type MORB normalized multi-element plot of the Roza defines a trend similar to that of the Guaymas Basin, Gulf of California (see Figure 30). This basin "superficially resembles most 'conventional' back-arc basins, even though its extension has resulted from transform-style tectonics, and it is probably not presently underlain by a subducted slab" (Saunders and Tarney, 1984). Relative to N-MORB, the Roza and the Guaymas Basin are enriched in both LIL (large ion

lithophile) elements and HFS (high field strength) elements. Conventional back-arc basins are enriched in LIL, but depleted in HFS, relative to N-MORB. The Roza, like most of the CRBG, is still significantly enriched in both LIL and HFS elements and depleted in Ni and Cr, relative to both the Guaymas Basin and N-MORB. No significant difference is noted between those subtypes that erupted through the craton versus those that moved through the Blue Mountains Subprovince.

#### 4.1.3. Isotopes

##### Strontium, Neodymium and Lead

As outlined in 1.4. (Previous CRBG geochemical and isotopic studies), mixing between four possible CRBG sources, based on isotopic data, has been proposed to explain the variation in these flood basalts. The following discussion aided by diagrams attempts to decipher the means of isotopic variation within the Roza in light of these four sources (C1, C2, C3, C4). Although illustrated and defined as having precise compositions, these four sources should be regarded as having an unresolved range in isotopic ratios about their proposed values.

In Figure 31 ( $^{143}/^{144}$  Nd versus  $^{87}/^{86}$  Sr), the Roza appears to lie along a broad mixing line between C1, C2 and C3 mantle sources. However, the  $^{87}/^{86}$  strontium versus strontium (ppm) variation diagram, Figure 32, and all Pb-Pb diagrams,

Figures 33 and 34, show the Roza trend as a line between C1 and a composition intermediate to C2 and C3.

Figures 35 and 36 show the variation trends of 206/204 lead compositions against respectively 87/86 strontium and 143/144 neodymium ratios. In the last diagram in particular, the Roza Member lies between C2 and C3. These last diagrams compared to the Pb-Pb plots show the inability of 87/86 strontium and 143/144 neodymium data to show the C1 component in the Roza Member.

### Oxygen

Figure 37 displays the same Roza Member data as shown in Figure 18 (Chapter 3), along with the CRBG isotopic data of Carlson (1983) and Nelson (1983). The Roza data from this thesis are within range of the other main series CRBG flows shown, except for two (subtypes IA and III) with  $\delta_{18}O$  values less than 5.5. Carlson and others (1981) have calculated the curves, shown in figure 37, using a combined fractional crystallization-assimilation model. These curves demonstrate the effects of assimilation of two distinct crustal endmembers, one with  $\delta^{18}O = 9.4$  and another with  $\delta^{18}O = 13.4$ , and source components C1 and C2. In addition, the elevated 87/86 strontium composition of C3, the primary source for many Saddle Mountain Flows (shown in squares), is highlighted in this diagram.

As noted in the Chapter 3 (Figures 17 and 18), the silica and 87/86 strontium compositions versus  $\delta^{18}\text{O}$  content of the Roza samples analyzed display a slight positive correlation. This correlation is noted throughout the entire CRBG sequence, in whole rock and secondary mineral samples. It is thought that this correlation reflects the contamination and alteration of the basalts by groundwater (Harris, 1989; Hearn and others, 1989). CFB's that have undergone combined assimilation-fractional crystallization with a granitic crust contaminant will show a positive correlation between silica content and  $\delta^{18}\text{O}$ . However, the same trend can also be produced since volcanic rocks tend to concentrate  $\delta^{18}\text{O}$ , in part, on silica content (Harris, 1989). Therefore, using this correlation to model the degree of crustal contamination in the Roza may prove to be erroneous.

These very small variations in all isotopic properties put severe constraints on the nature of mantle sources and/or contaminants and thus their locations below the dike system. Ignoring the somewhat ambiguous oxygen isotopic data, the Roza Member can be modelled as a mixture of C2 and C3 mantle sources with variable yet small amounts of C1. The enrichments in K, Ba and Rb could also be explained by a K, Ba, Rb and Sr rich crustal contaminant with an 87/86 strontium > 0.7051 and either very low lead contents or by chance 206/204 lead = 18.80. The contaminant is not likely to have been ancient crust as neodymium and lead in the nearest known

crust to the north are very different isotopically and compositionally from those in the Roza Member.

#### 4.2. CONCLUSIONS AND SUMMARY

(1) The Roza flows erupted along discrete segments of various lengths. No apparent migration of activity with time is observed.

(2) It is possible for separate intrusions of the same eruptive series to use the same fissure paths, without significant disruption of the previously injected magma. Lack of internal chill margins in these composite dikes indicates near thermal equilibrium.

(3) The planar nature of the dikes and the interfaces between subtypes of the same dike, indicates that laminar rather than turbulent flow existed at these high crustal levels.

(4) Variable contamination where contamination may occur is evidenced by the random variation pattern of K, Ba and Rb compositions.

(5) Nearly identical lavas erupted concurrently along the entire length of the feeder system, thus magmas of each Roza



subtype must have been homogenized extensively prior to eruption.

(6) No apparent difference is observed in the composition of feeder rocks of the same subtype across the craton\terrane suture. Therefore if contamination of these magmas occurred in the sublithosphere, there is no apparent difference between this source underlying the North American craton and that underlying the Blue Mountains Subprovince.

(7) The gross similarity of the Roza Member to that of the Guaymas Basin indicates that the composition of the Roza need not explained by the effects of the subducted slab underlying the Columbia Plateau.

(8) The Roza Member can be modelled as a mixture of C2 and C3 mantle sources with variable yet small amounts of C1.

(9) The small-scale variations in K, Ba and Rb can be explained by a K, Ba, Rb and Sr rich crustal contaminant with an  $87/86$  strontium  $> 0.7051$  and either very low lead contents or by chance  $206/204$  lead = 18.80.

**FIGURE 19.** Schematic diagram of the three main phases of fissure-type lava eruptions. Modified after Bruce and Huppert (1989).

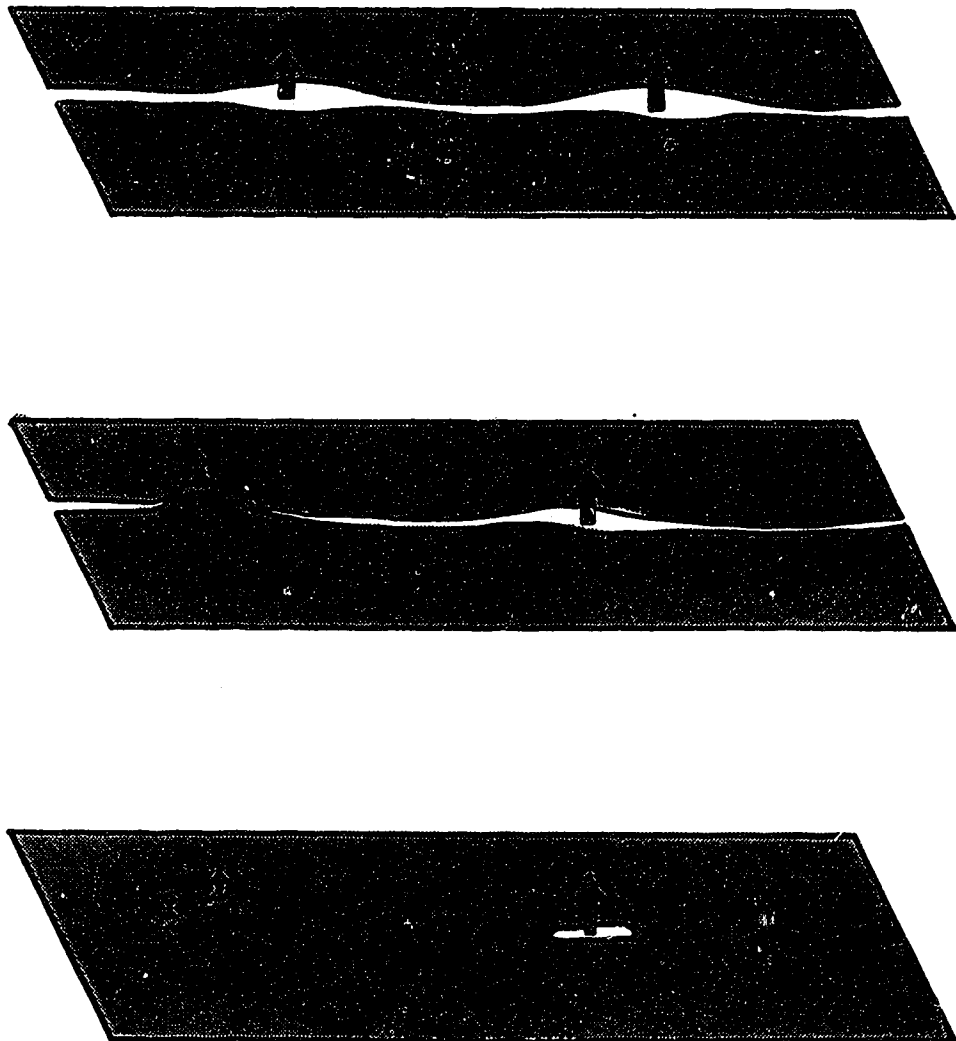


**FIGURE 20.** Distribution map of Roza chemical subtype IA flow and feeder samples. Flow distribution modified after Martin (1989).

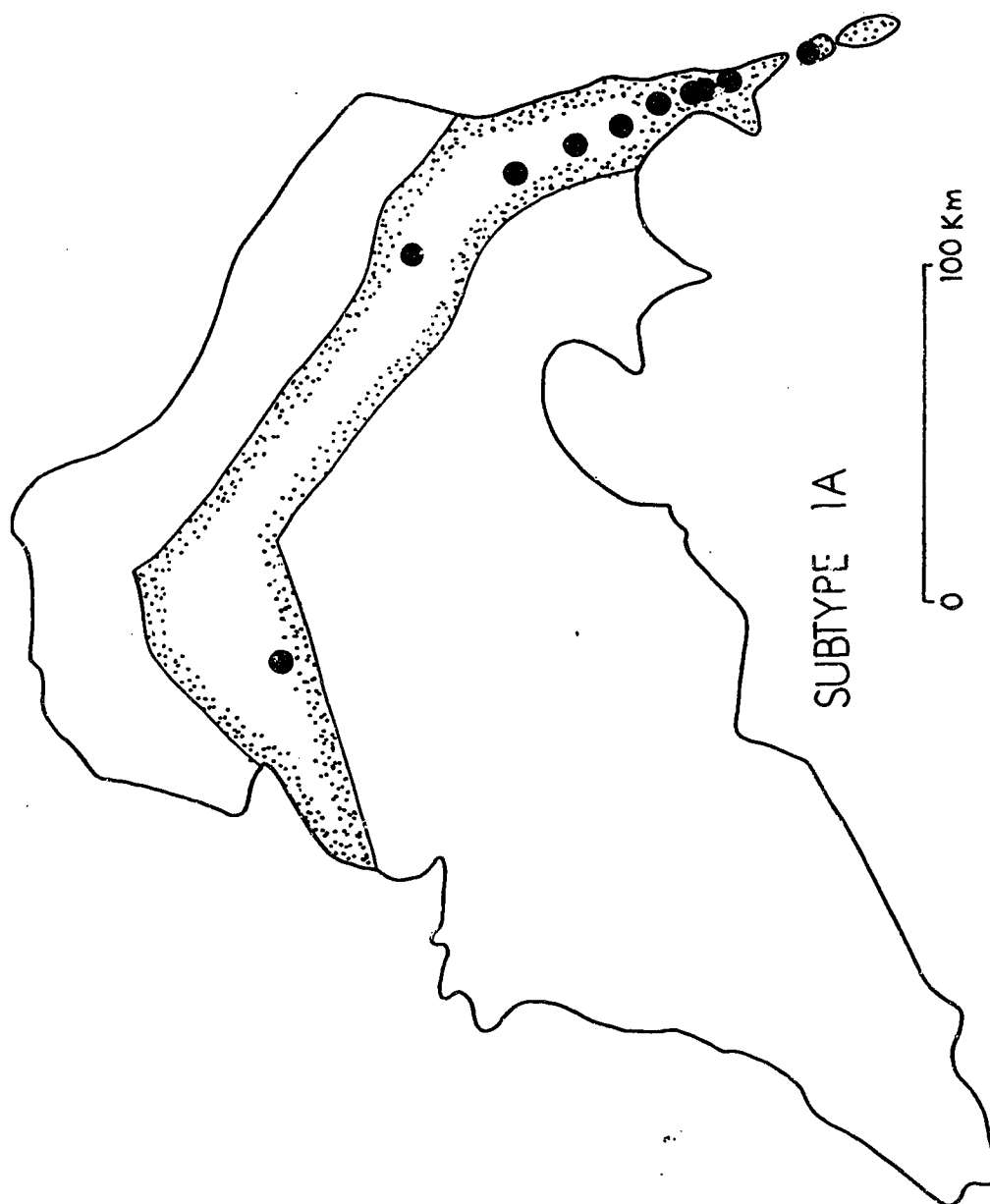


**FIGURE 21. Distribution map of Roza chemical subtype IB flow and feeder samples. Flow distribution modified after Martin (1989).**

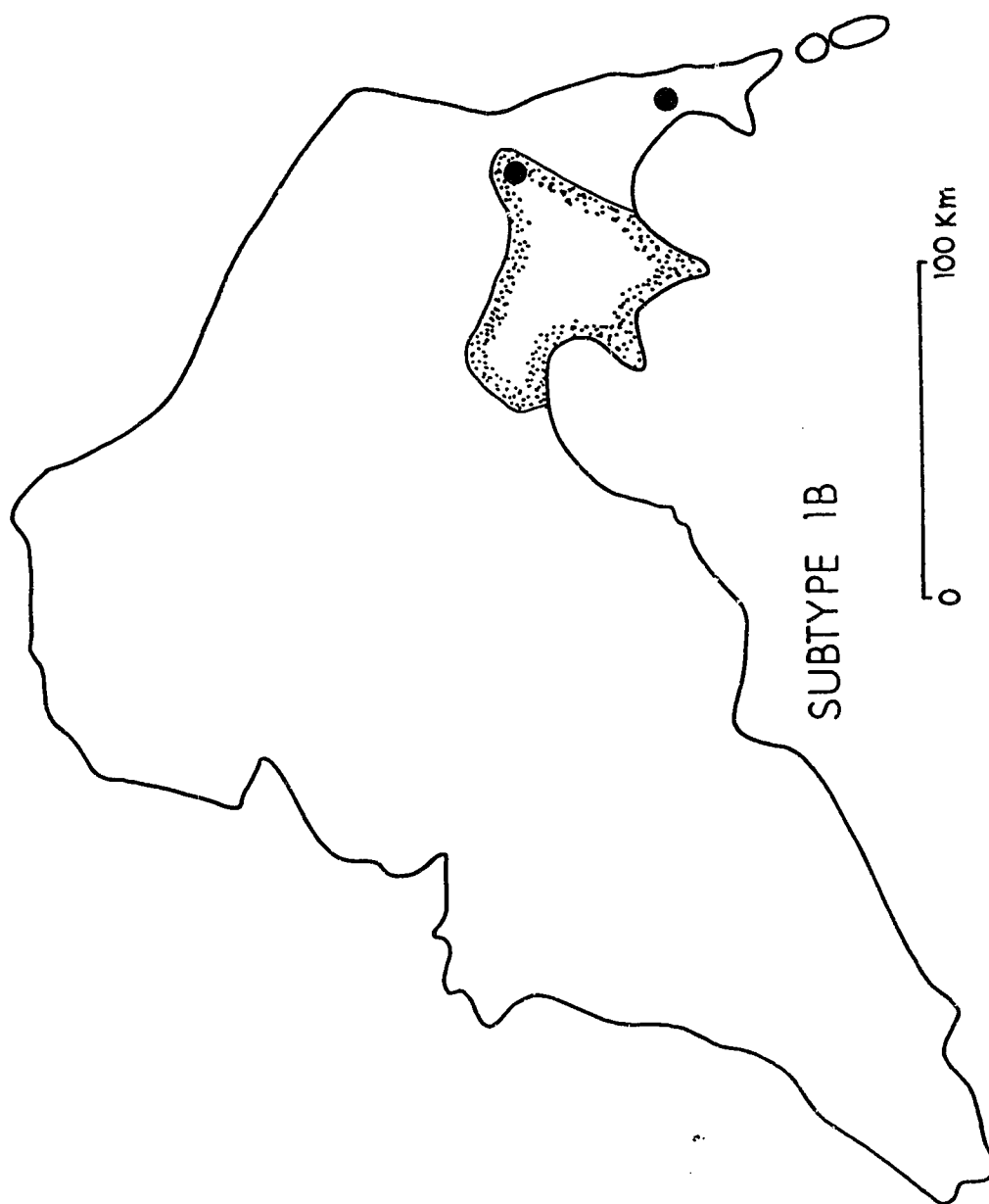


**FIGURE 22.** Distribution map of Roza chemical subtype IIA flow and feeder samples. Flow distribution modified after Martin (1989).

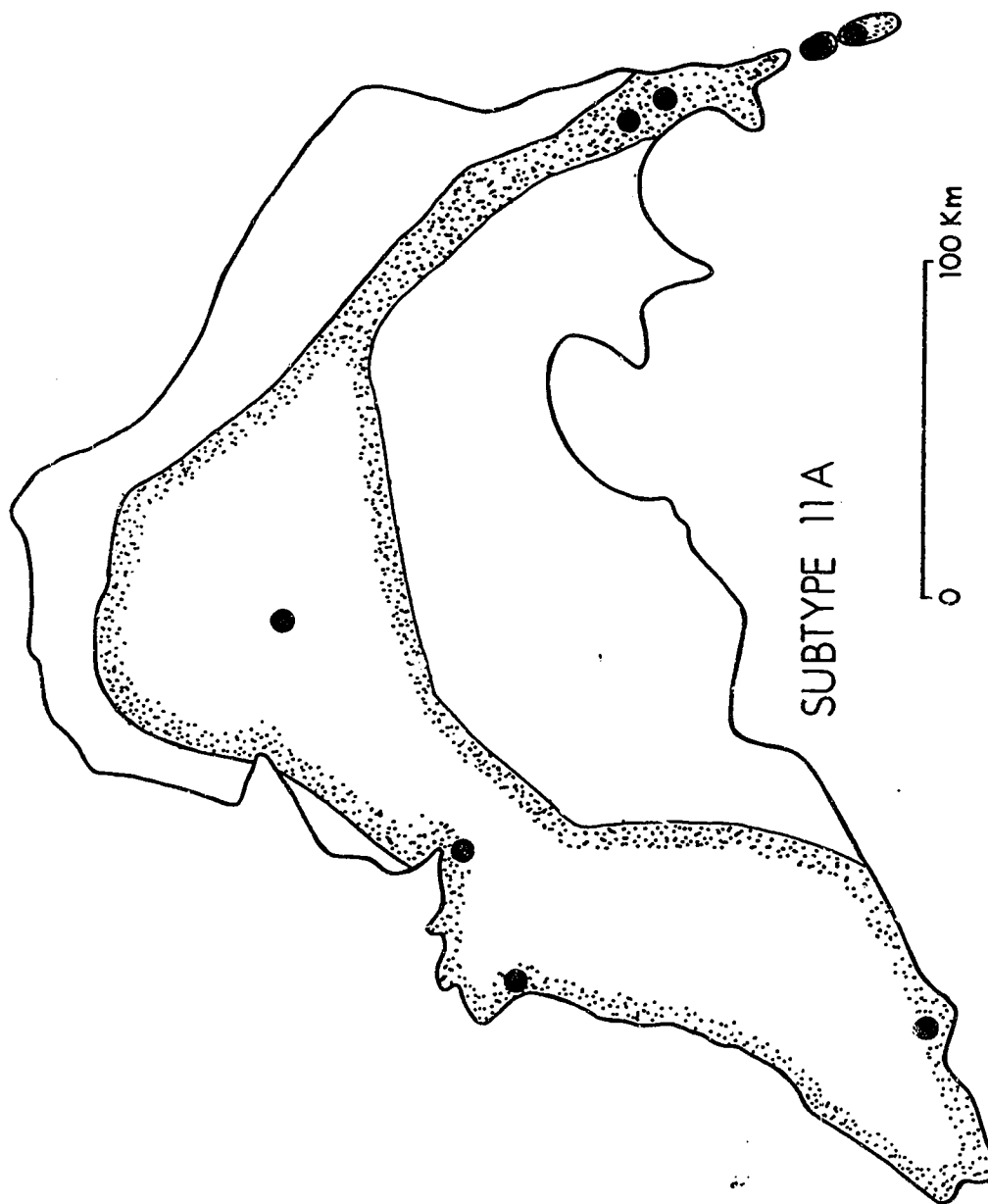


**FIGURE 23. Distribution map of Roza chemical subtype IIB flow and feeder samples. Flow distribution modified after Martin (1989).**

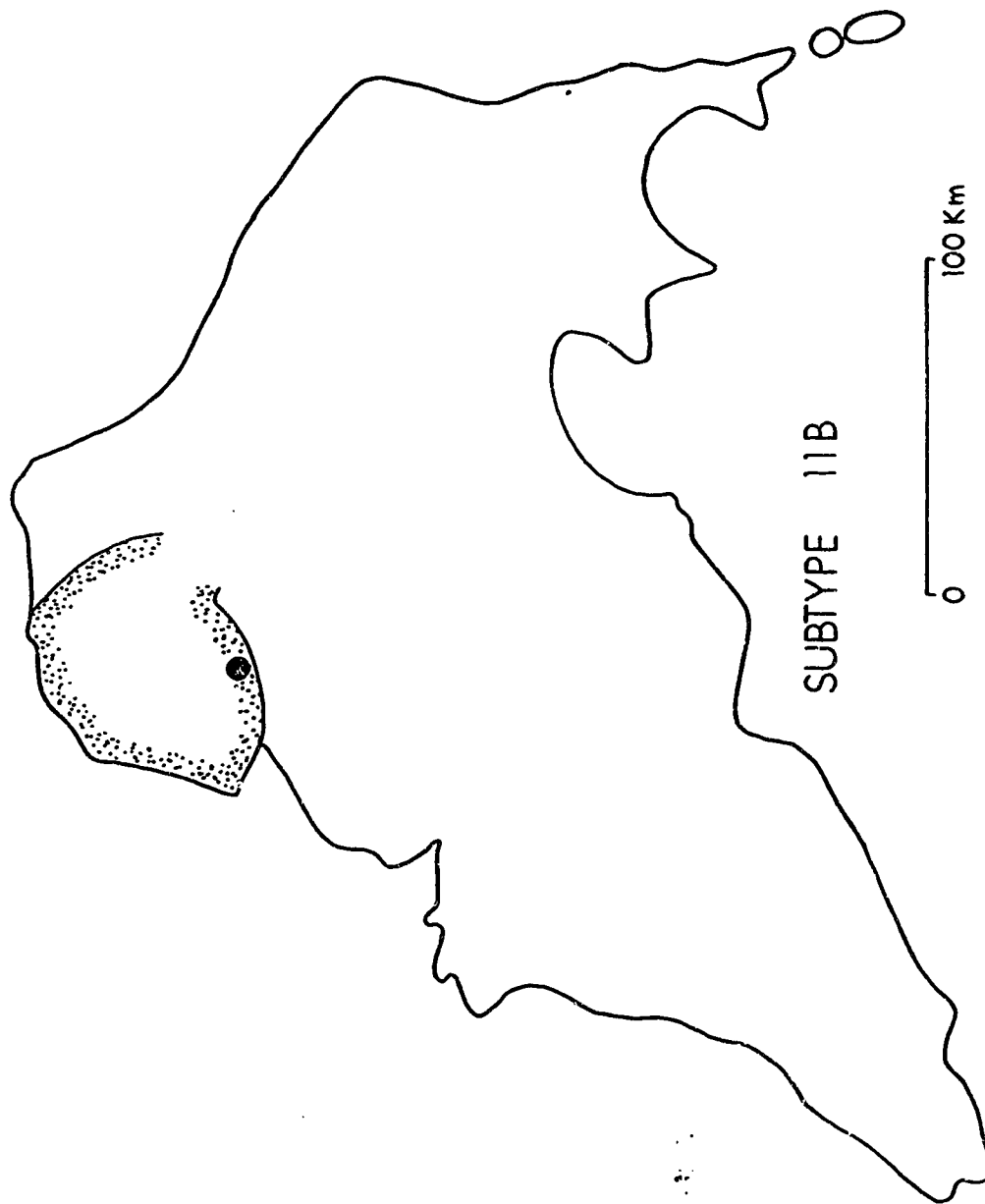


**FIGURE 24. Distribution map of Roza chemical subtype III flow and feeder samples. Flow distribution modified after Martin (1989).**

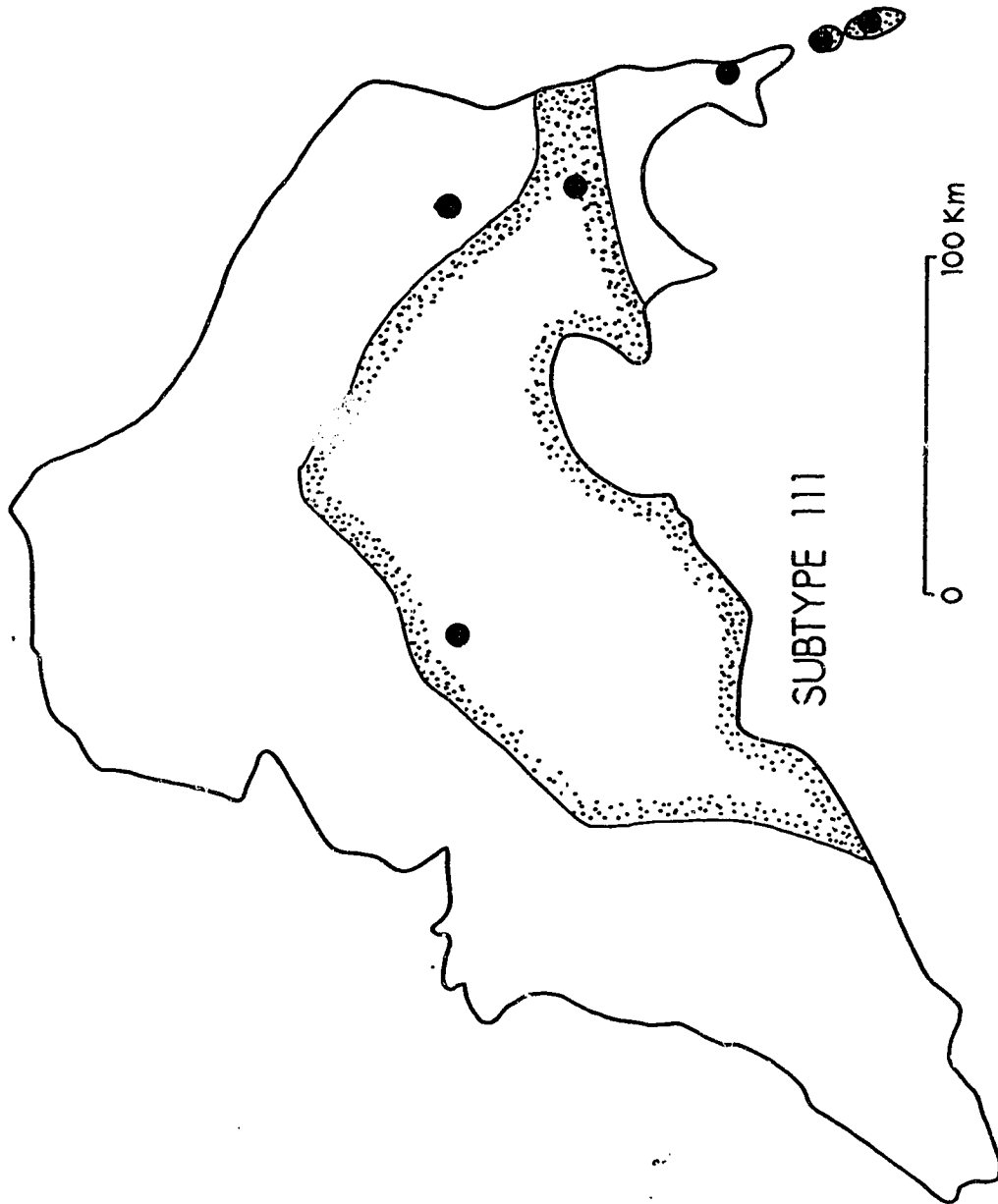


**FIGURE 25.** Distribution map of Roza chemical subtype IV flow and feeder samples. Flow distribution modified after Martin (1989).

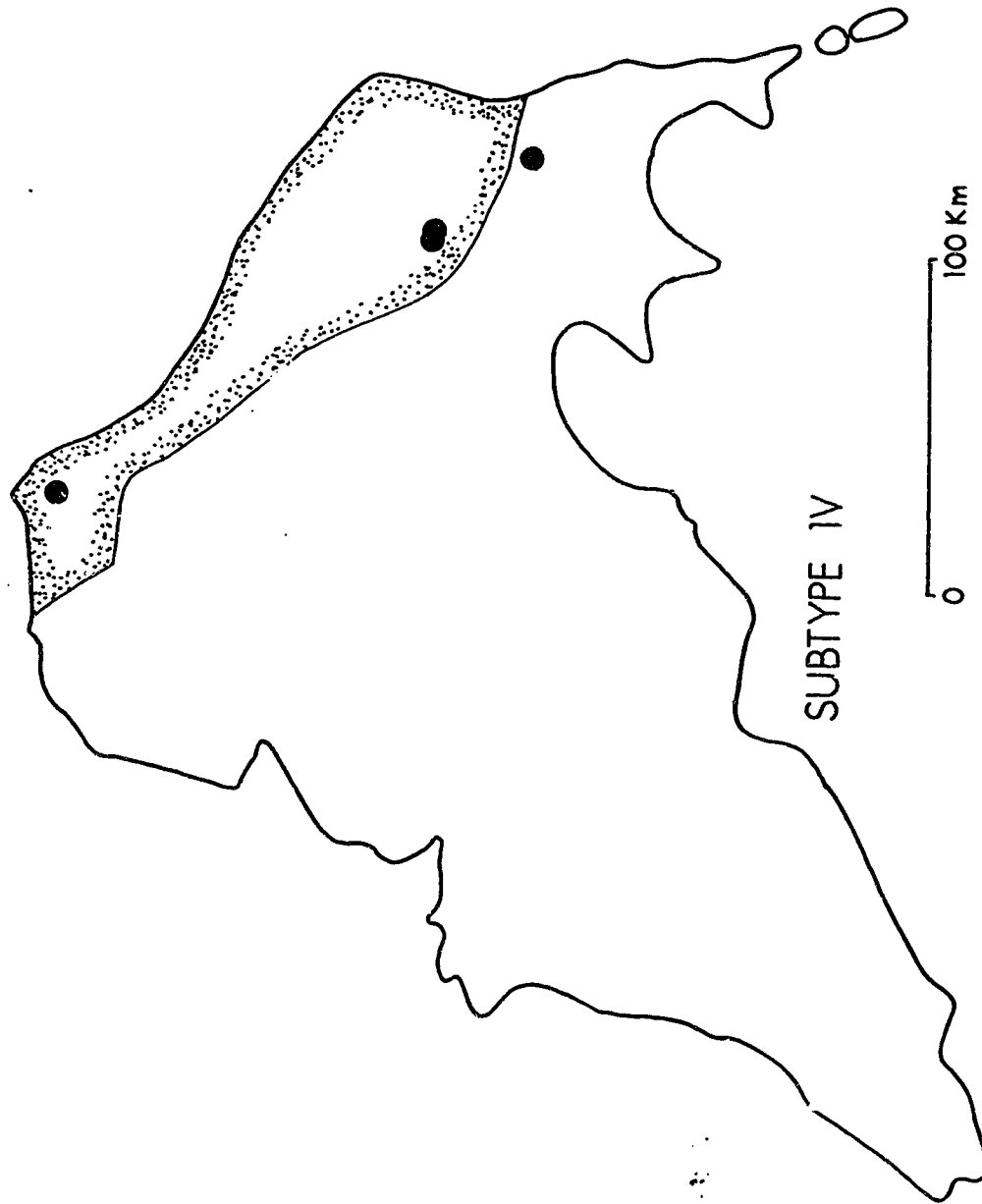
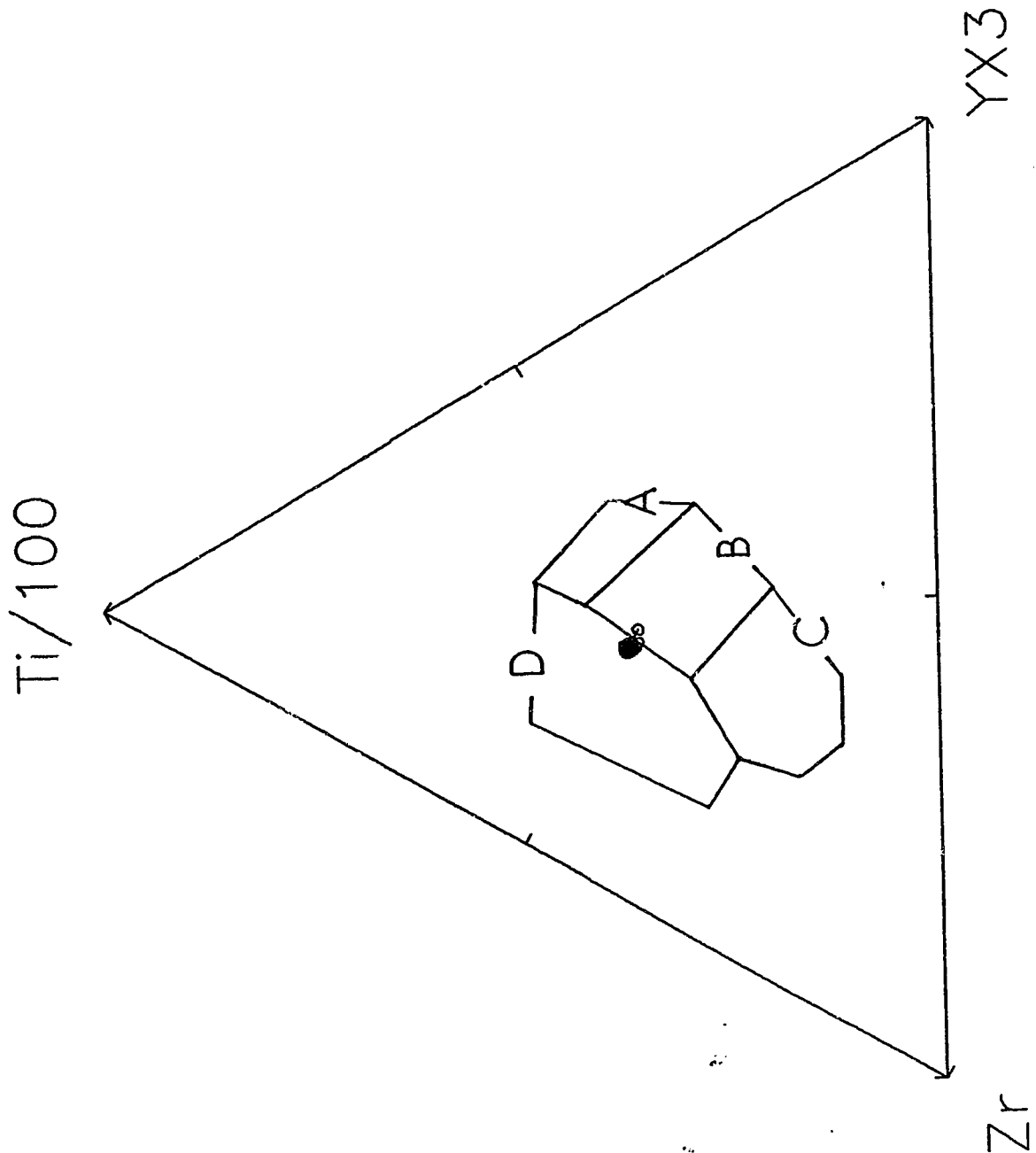




FIGURE 26. Discrimination diagram using Ti, Zr and Y. Within plate basalts (WPB) i.e. OIB's or CFB's plot in field D, ocean-floor basalts (OFB) in field B, low-potassium tholeiites (LKT) in fields A and B, calc-alkali basalts (CAB) in fields C and B. Modified after Pearce and Cann (1973).



**FIGURE 27. Zr-Ti/100-Sr/2 discrimination diagram. Ocean-floor basalts (OFB) plot in field C, low-potassium tholeiites (LKT) in field A, and calc-alkali basalts (CAB) in field B. Modified after Pearce and Cann (1973).**

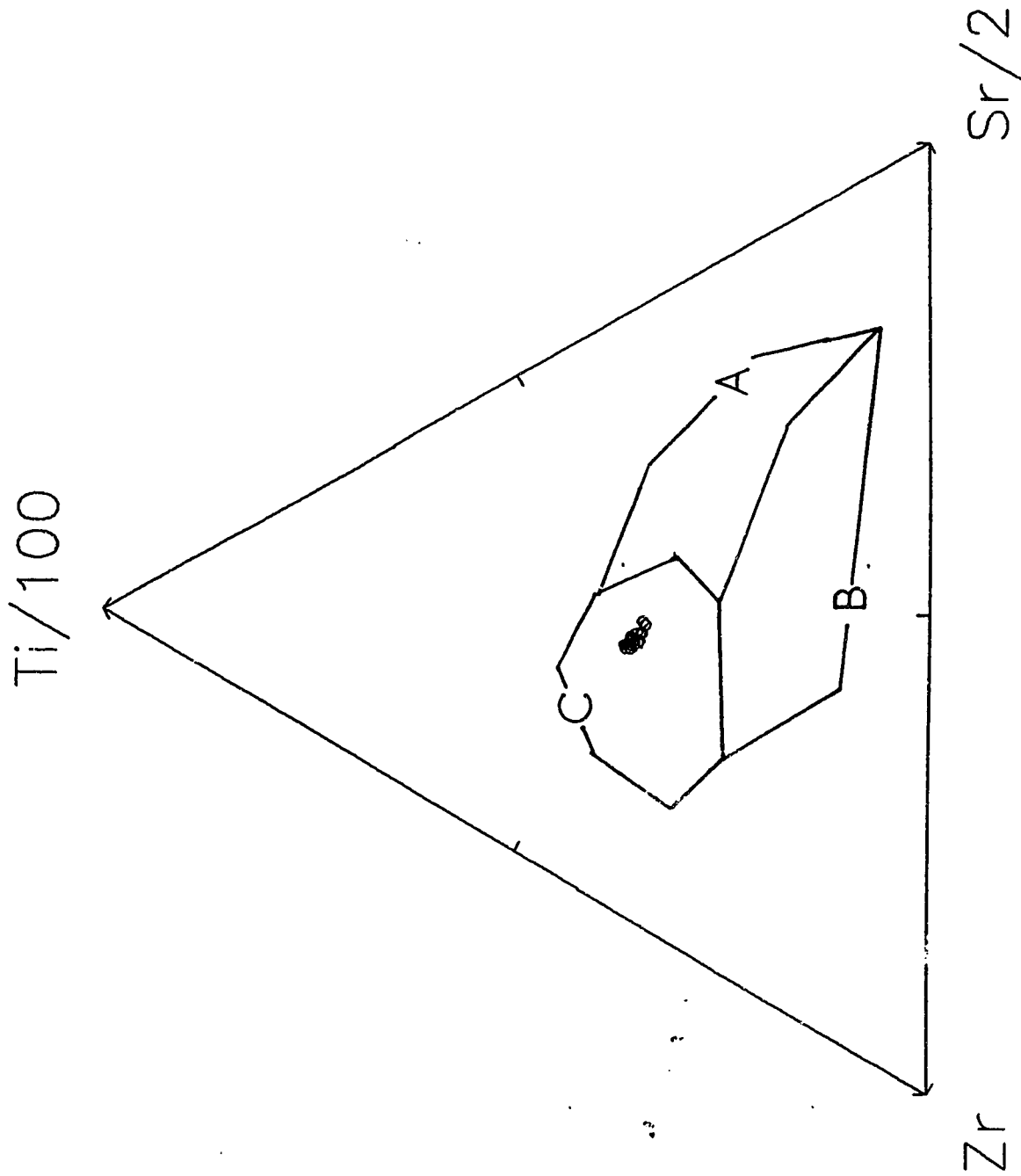


FIGURE 28. MgO-FeO\*-Al<sub>2</sub>O<sub>3</sub> tectonic discrimination diagram. Categories are ocean island (OI); ocean-ridge and floor (ORF); continental (C); orogenic (O); and spreading-center island (SCI). Modified after Pearce and others (1977).

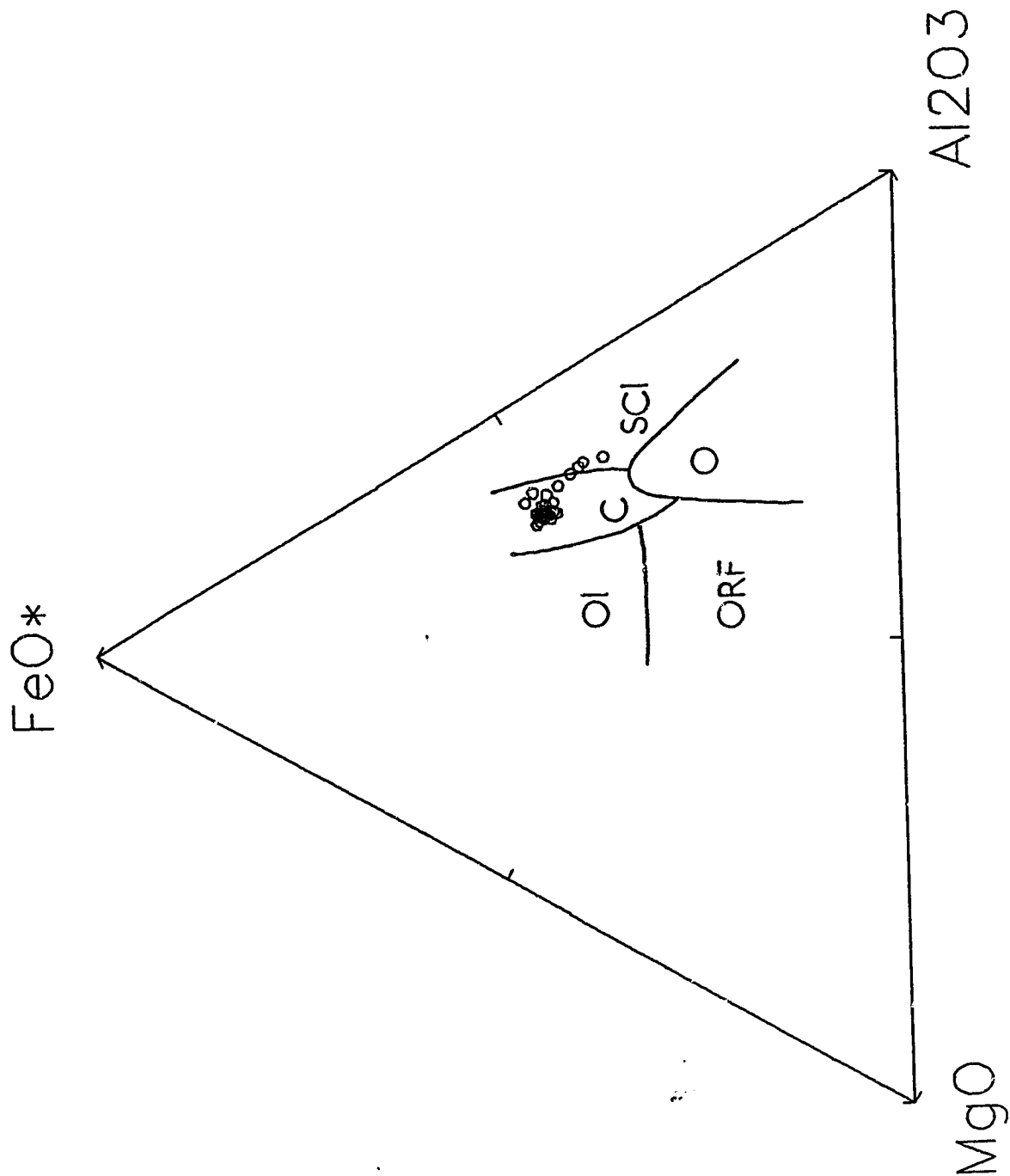
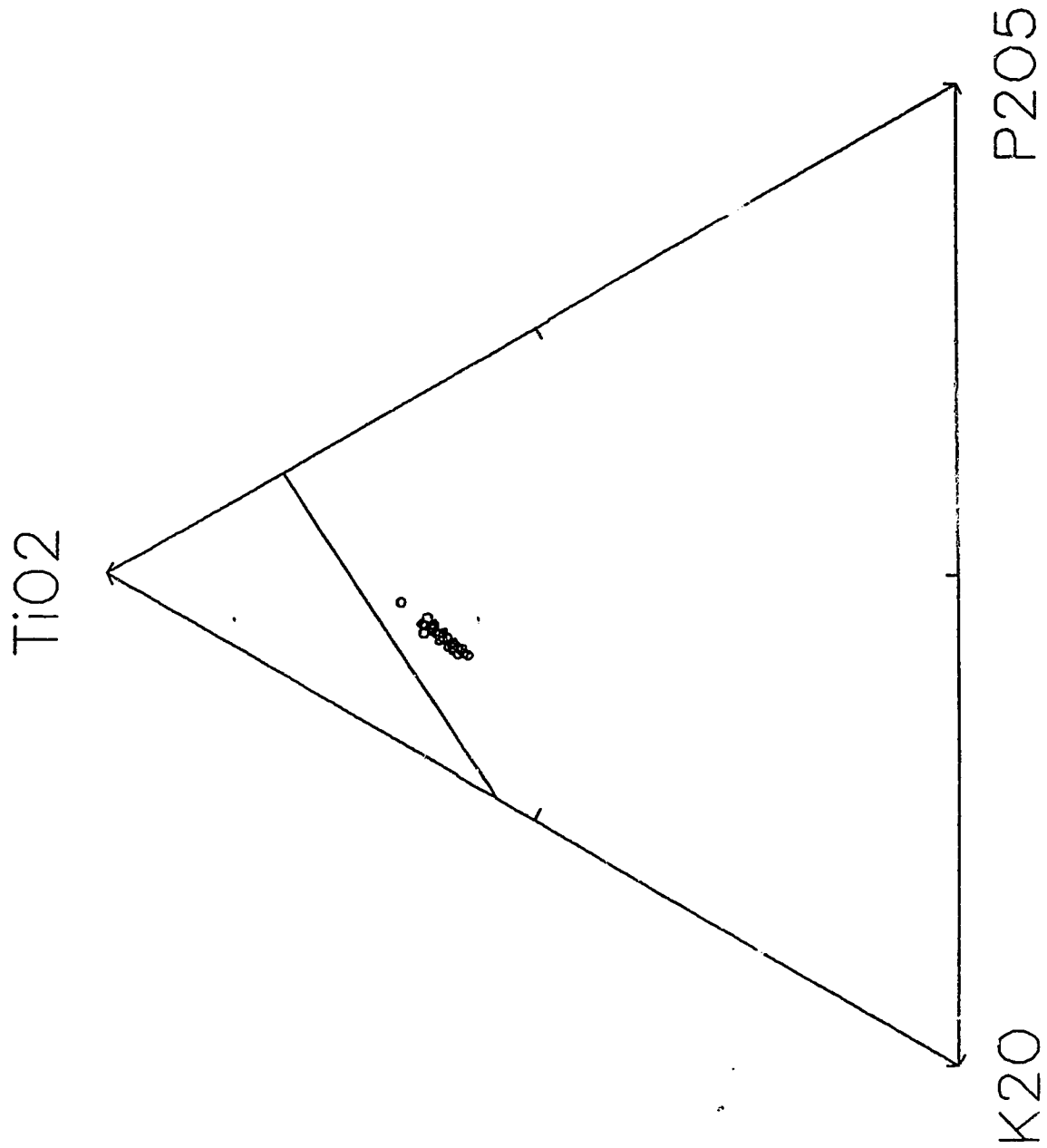


FIGURE 29.  $K_2O$ - $TiO_2$ - $P_2O_5$  plot of Roza flow and feeder system rocks, showing the position of the dividing line between the oceanic field (upper portion) and the non-oceanic field (lower portion). Modified after Pearce and others (1974).



**FIGURE 30.** N-type MORB normalized multi-element plot of averaged Roza subtypes and the Guaymas Basin, Gulf of California. Symbols as presented in Figure 5. Normalizing factors and figure modified from Saunders and Tarney (1984).

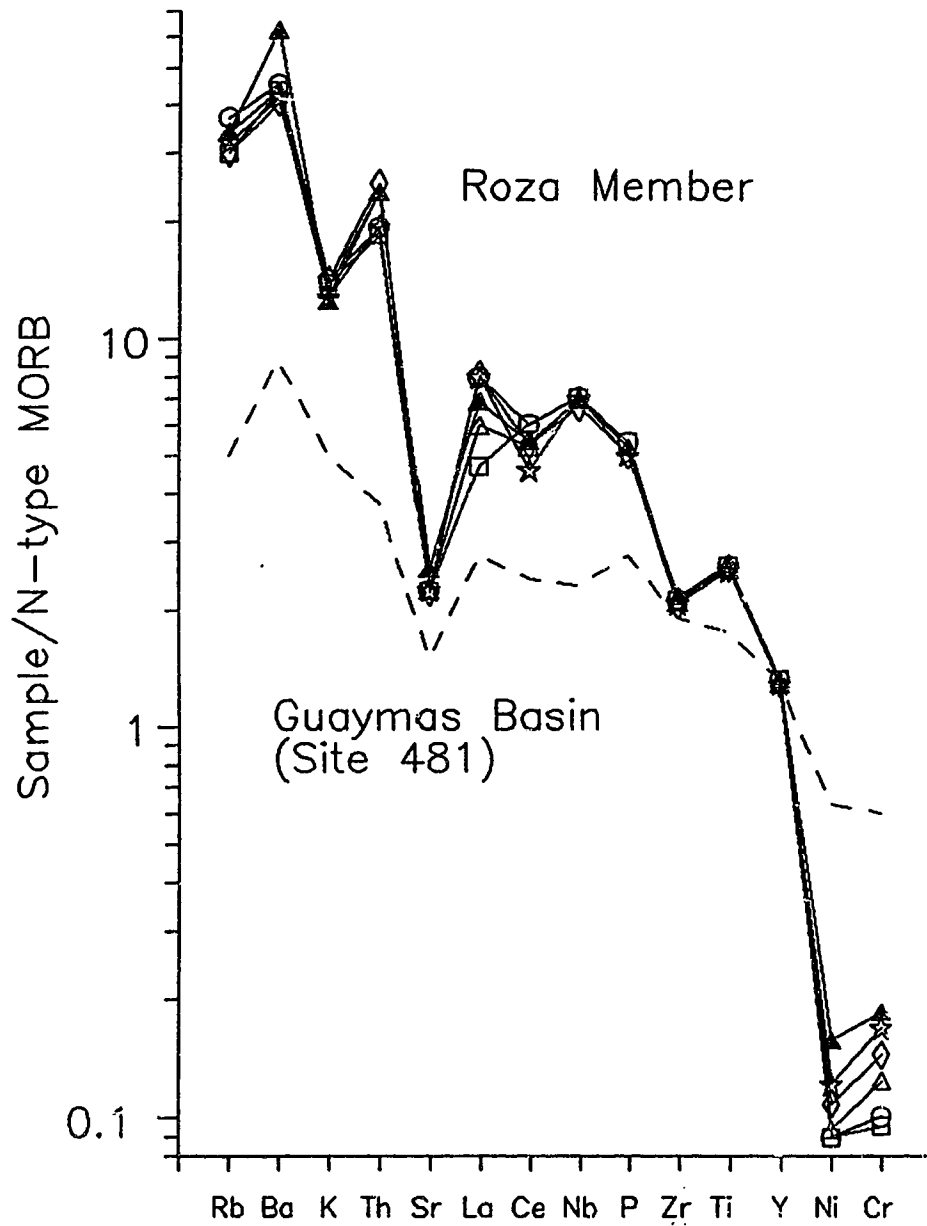


FIGURE 31.  $^{87}/^{86}$  Strontium versus strontium (ppm) plot of Roza samples. Filled circles indicate proposed CRBG contaminant compositions.

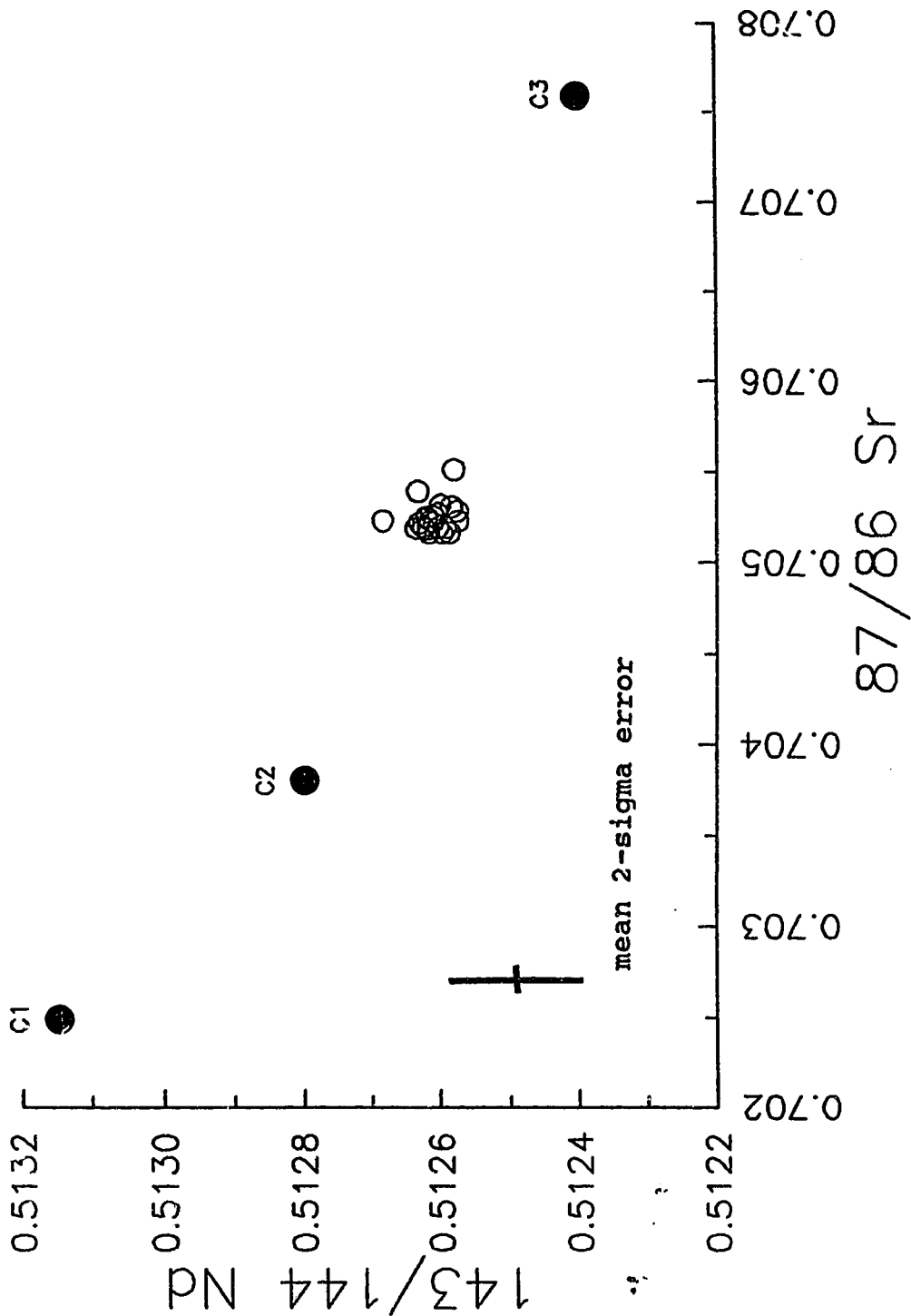


FIGURE 32.  $^{143}/^{144}$  neodymium versus  $^{87}/^{86}$  strontium plot of Roza samples. Filled circles indicate proposed CRBG contaminant compositions.

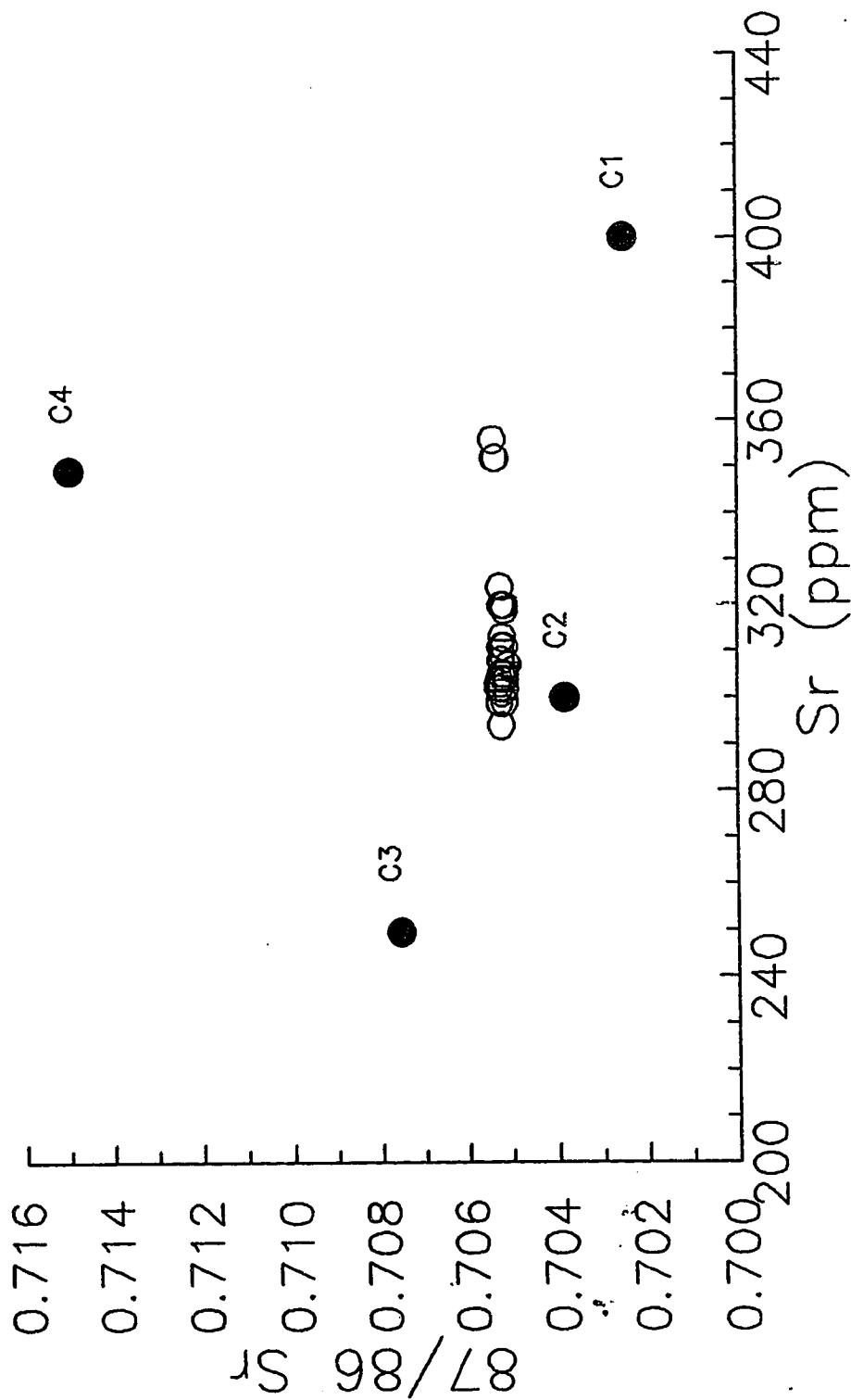


FIGURE 33. 207/204 lead versus 206/204 lead plot of Roza whole rock powders. Filled circles indicate proposed CRBG contaminant compositions.

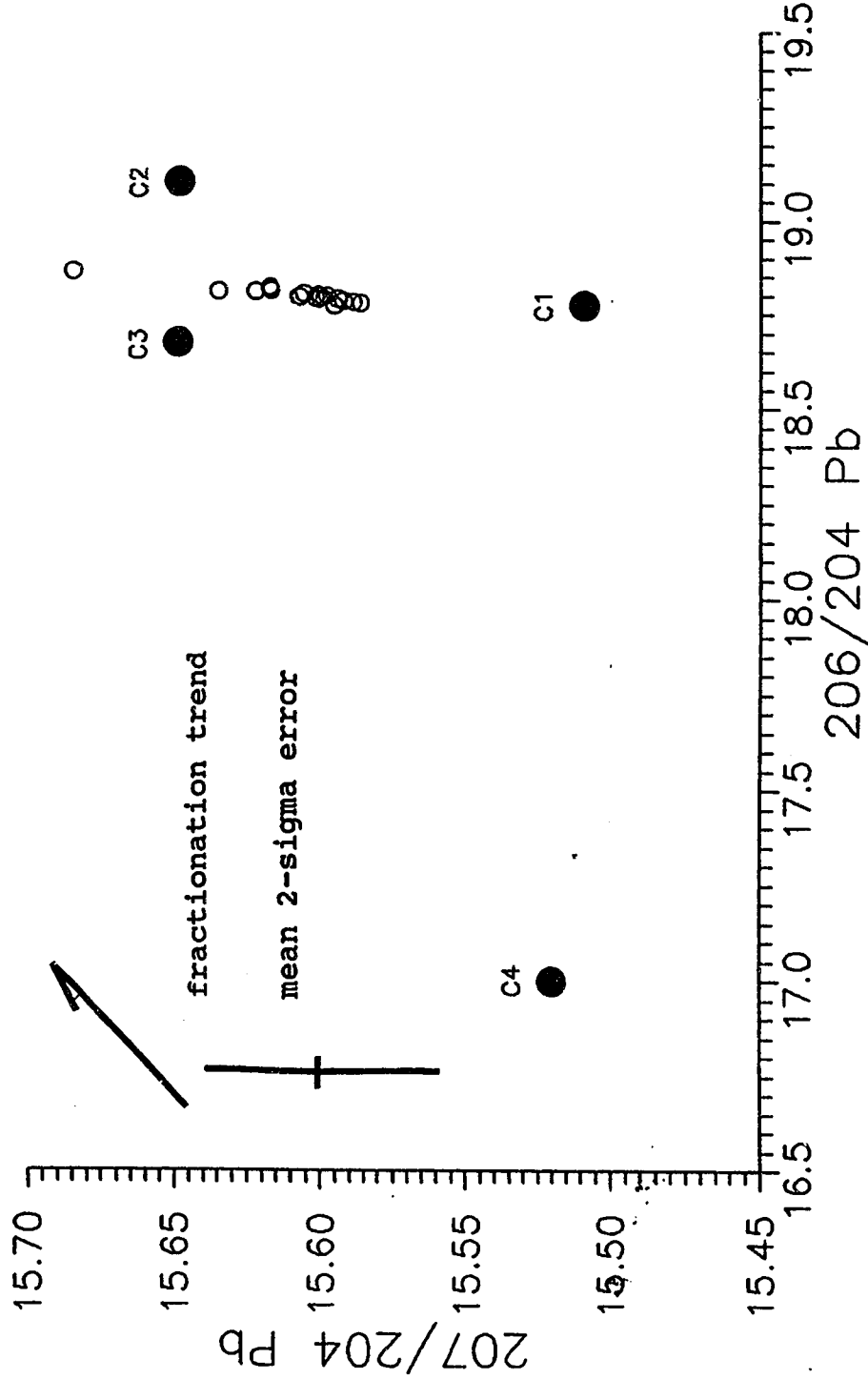




FIGURE 34. 208/204 lead versus 206/204 lead plot of Roza whole rock powders. Filled circles indicate proposed CRBG contaminant compositions.

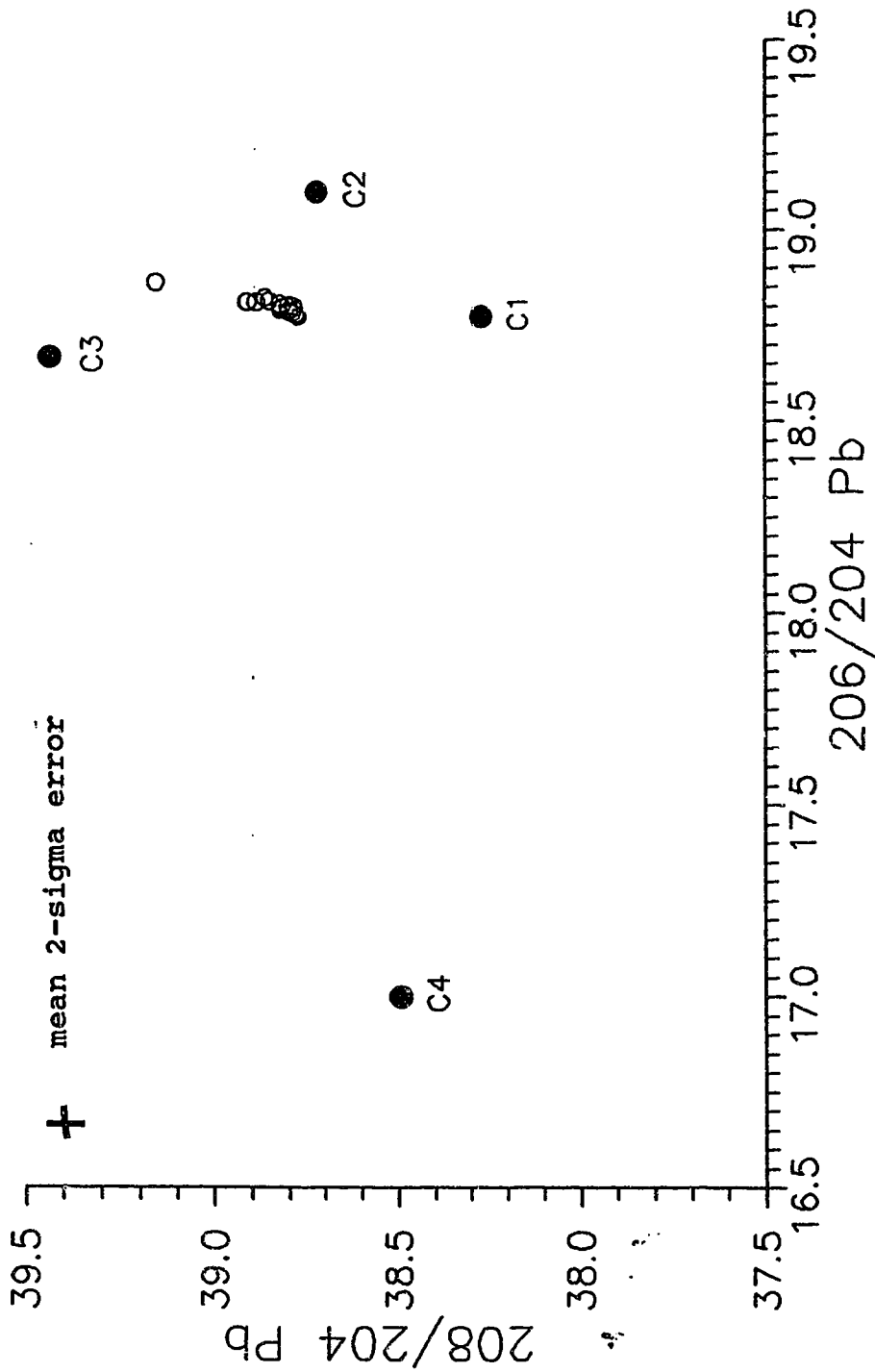


FIGURE 35. 206/204 lead versus 87/86 strontium plot of Roza samples. Filled circles indicate proposed CRBG contaminant compositions.

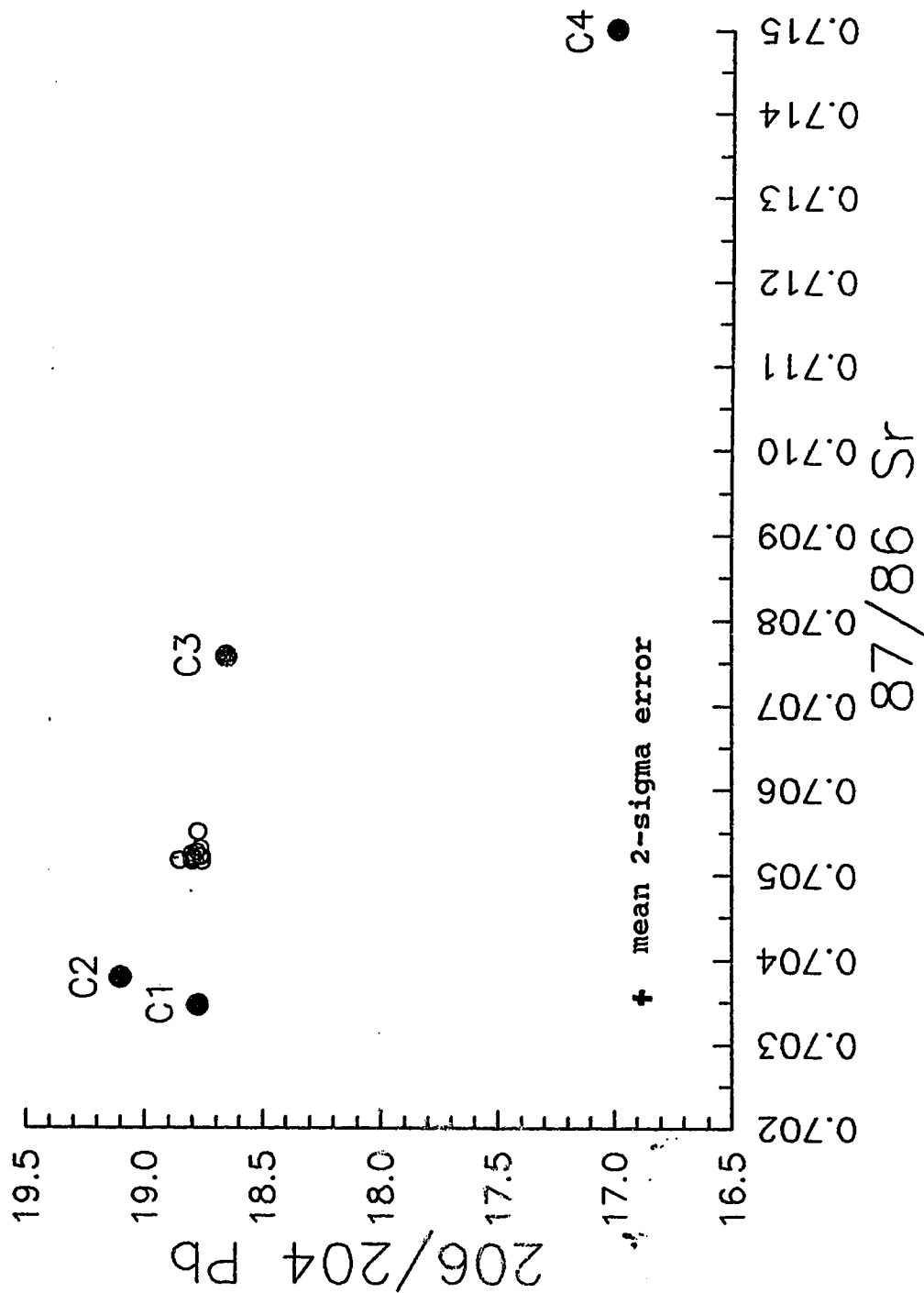


FIGURE 36.  $^{206}/^{204}$  lead versus  $^{143}/^{144}$  neodymium plot of Roza samples. Filled circles indicate proposed CRBG contaminant compositions.

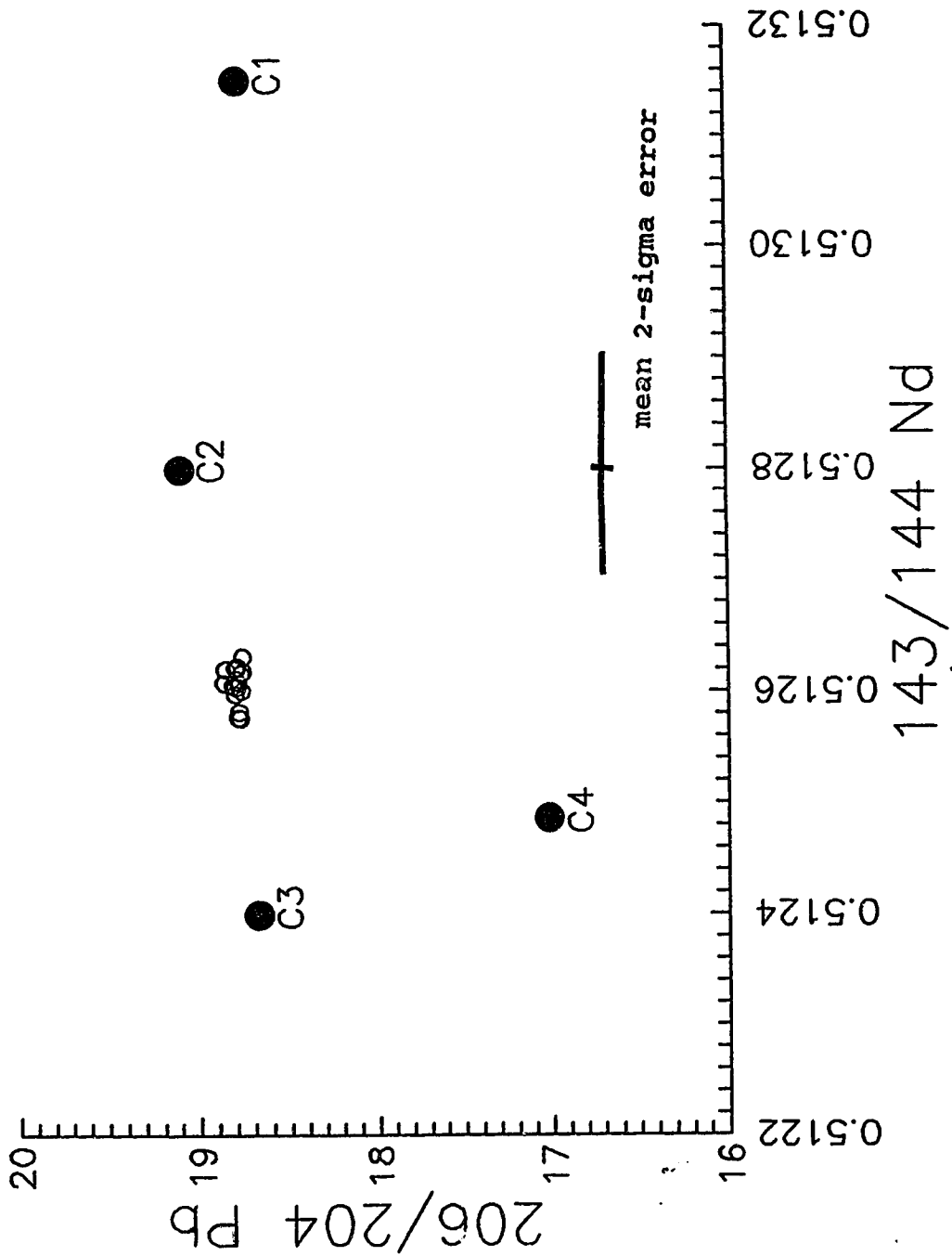
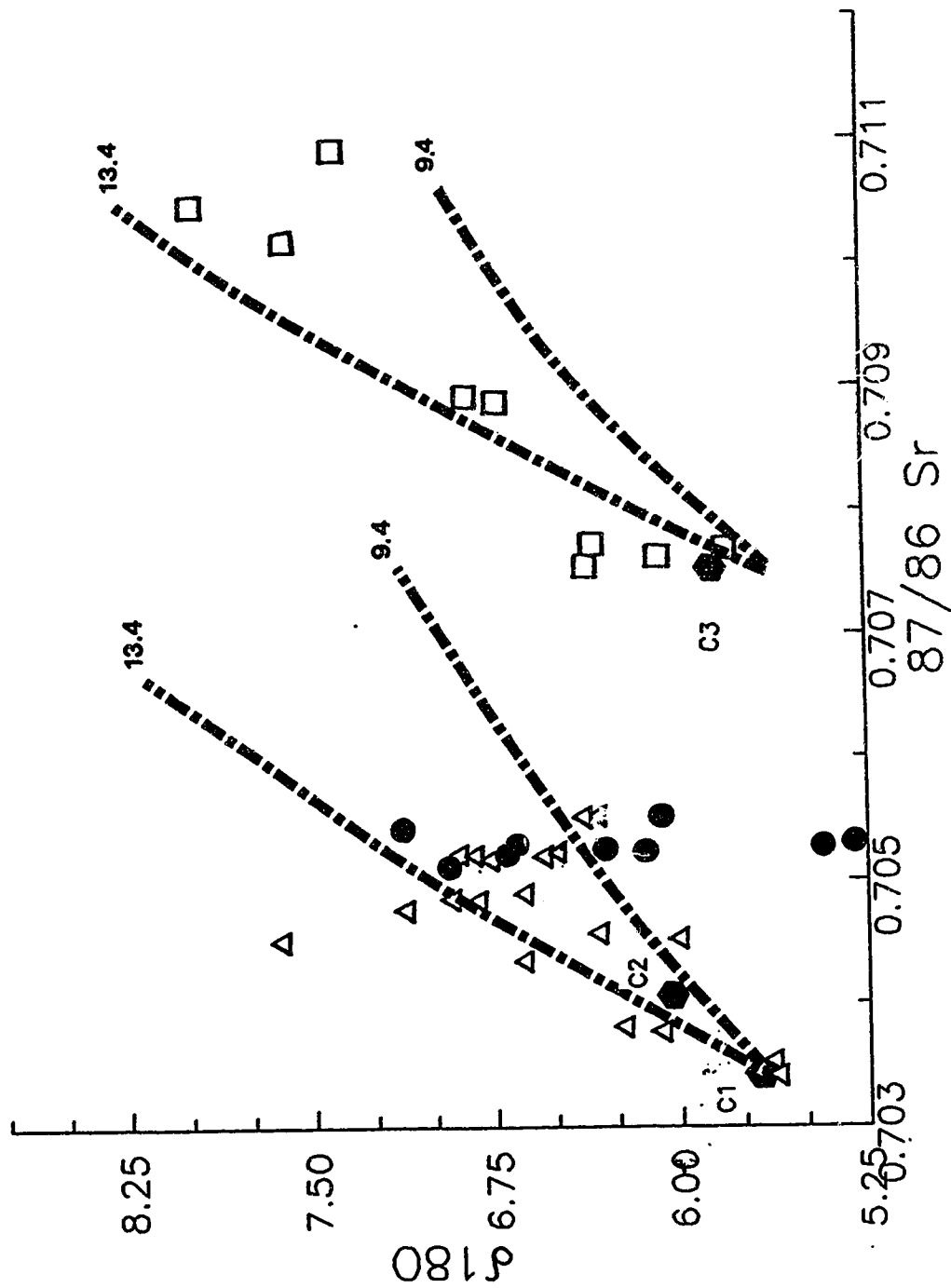


FIGURE 37.  $\delta^{18}\text{O}$  versus  $87/86$  strontium plot of Roza samples (circles), CRBG main series flows (triangles), Saddle Mountains Basalt (square) and proposed CRBG contaminants (hexagons). Curves calculated using combined fractional crystallization-assimilation model of Carlson and others (1981), show effects of assimilation of two distinct crustal endmembers, one with  $\delta^{18}\text{O}=9.4$  and another with  $\delta^{18}\text{O}=13.4$ . See text for further discussion.



## REFERENCES

- Anderson, J.L., Beeson, M.H., Bentley, R.D., Fecht, K.R., Hooper, P.R., Niem, A.R., Reidel, S.P., Swanson, D.A., Tolan, T.L., and Wright, T.L. 1987. Distribution maps of stratigraphic units of the Columbia River Basalt Group. In J.E. Schuster, (ed.), Selected papers on the geology of Washington. Wash. Div. of Geol. and Earth Resources Bull. v. 77. p. 183-195.
- Atkinson, S.S. and R. St J. Lambert, 1990. The Roza feeder dyke system, Columbia River Basalt Group: Compositional variation and emplacement, in A.J. Parker, P.R. Rickwood and D.H. Tucker, eds., Proceedings Volume of the Second International Dyke Conference, Adelaide: Rotterdam, Balkema. In Press.
- Baksi, A.K., and Watkins, N.D., 1973. Volcanic Production Rates: Comparison of oceanic ridges, islands, and the Columbia River Plateau basalts. Science, v. 180, p. 493-496.
- Beeson, M. H., Perttu, R., and Perttu, J., 1979, The origin of the Miocene basalts of coastal Oregon and Washington: an alternative hypothesis: Oregon Geology, v. 41, p. 159-166.
- Bingham, J.W., 1970. Several probable source vents for the Roza and Priest Rapids type basalts in Whitman and Adams counties, Washington, in Gilmour, E.H. and Stradling, D., eds., Proceedings of the Second Columbia River Basalt Symposium: Cheney, Eastern Washington State College Press, p. 171-172.
- Brandon, A.D. and Goles, G.G., 1988. A Miocene subcontinental plume in the Pacific Northwest: geochemical evidence. EPSL, v. 88, p. 273-283.
- Bruce, P.M. and Huppert, H.E. 1989. Thermal control of basaltic fissure eruptions. Nature. v. 342, p. 665-667.
- Camp, V.E., 1981. Geologic studies of the Columbia River Plateau: Part II. Upper Miocene basalt distribution, reflecting source locations, tectonism, and drainage history in the Clearwater embayment, Idaho. GSAB, Part 1, v. 92, p. 669-678.

- Camp, V. E., and Hooper, P. R., 1981. Geologic studies of the Columbia plateau: Part I. Late Cenozoic evolution of the south-east part of the Columbia River Basalt Province: Geological Society of America Bulletin, v. 92, p. 659-668.
- Campbell, N.P. 1989. Structural and stratigraphic interpretation of rocks under the Yakima fold belt, Columbia Basin, based on recent surface mapping and well data. In S.P. Reidel and P.R. Hooper, eds., Volcanism and tectonism in the Columbia River flood-basalt province, Special Paper 239. p. 209-222. Boulder, Colorado: Geol. Soc. of America.
- Carlson, R.W., 1983. Comment and Reply on "Implications of oxygen-isotope data and trace-element modeling for a large-scale mixing model for the Columbia River Basalt" Geology, p. 735.
- 1984, Isotopic constraints on Columbia River basalt genesis and the nature of the subcontinental mantle: Geochimica et Cosmochimica Acta, v. 48, p. 2357-2372.
- Carlson, R.W. and Hart, W.K. 1988. Flood basalt volcanism in the Northwestern United States. In J.D. MacDougall (ed.), Continental Flood Basalts, p. 35-61. Dordrecht: Kluwer Academic Publishers.
- Carlson, R.W., Lugmair, G.W., and MacDougall, J.D., 1981a. Crustal influence in the generation of continental flood basalts. Nature, v. 289, p. 160-162.
- 1981b. Columbia River volcanism: the question of mantle heterogeneity or crustal contamination: Geochimica et Cosmochimica Acta, v. 45, p. 2483-2499.
- 1983. "Columbia River Volcanism: the question of mantle heterogeneity or crustal contamination" (reply to a comment by D.J. DePaolo). Geochim. et Cosmo. Acta, v. 47, p. 845-846.
- Catchings, R.D. and Mooney, W.D., 1988. Crustal Structure of the Columbia Plateau: Evidence for Continental Rifting. Journal of Geophysical Research, v. 93, p. 459-474.
- Choiniere, S.R. and Swanson, D.A. 1979. Magnetostratigraphy and correlation of Miocene basalts of the northern Oregon coast and Columbia Plateau, southeast Washington. American Journal of Science. v. 279, p. 755-777.

- Church, S. E., 1985, Genetic interpretation of lead-isotopic data from the Columbia River Basalt Group, Oregon, Washington and Idaho: Geological Society of America Bulletin, v. 96, p. 676-690.
- Cox, K. G., 1980, A model for flood basalt volcanism: Journal of Petrology, v. 21, p. 629-650.
- Delaney, P.T. and Pollard, D.D., 1982. Solidification of basaltic magma during flow in a dike. American Journal of Science, v. 282, p. 856-885.
- Drury, C.M., 1976. Nine years with the Spokane Indians. The Diary, 1838-1848 of Elkanah Walker. The Arthur H. Clark Co., Glendale, California. p. 232.
- Farmer, G. Lang, 1989. The western limit of Precambrian basement in the northern Great Basin as defined by granite isotopic data-a review. Geological Society of America Abstracts with Programs, v. 21, p. 77.
- Fleck, R.J., Kistler, R.W. and Criss, R.E., 1989. Location and isotopic characteristics of the Mesozoic continental margin of North America in Idaho and Washington. Geological Society of America Abstracts with Programs, v. 21, p. 78.
- Fitton, J.G. and Dunlop, H.M., 1985. The Cameroon line, West Africa, and its bearing on the origin of oceanic and continental alkali basalt. EPSL, v. 72, p. 23-38.
- Godwin, C.I., Gabites, J.E. and Andrew, A., 1988. LeadTable: a galena lead isotope data base for the Canadian Cordillera. Geological Survey Branch of Mineral Resources Division of B.C. Paper 1988-4. pp. 188.
- Griggs, A.B., 1976, The Columbia River Basalt Group in the Spokane quadrangle, Washington, Idaho and Montana: U. S. Geological Survey Bulletin 1413, 39 p.
- Harris, C., 1989. Covariance of initial  $87\text{Sr}/86\text{Sr}$  ratios,  $\text{d}_{18}\text{O}$ , and  $\text{SiO}_2$  in continental flood basalt suites: The role of contamination and alteration. Geology, v. 17, p. 634-636.
- Harte, B. 1983. Mantle peridotites and processes- the kimberlite sample. In C.J. Hawkesworth and M.J. Norry (eds.), Continental basalts and mantle xenoliths, p. 46-91. Cheshire: Shiva.

- Hart, W. K., and Carlson, R. W., 1982, Chemical and isotopic characteristics of late Cenozoic volcanism in the north-western U.S.A.: Carnegie Institute of Washington Year Book 81, 1981-1982, p. 501-505.
- Hearn, P.P.Jr., Steinkampf, W.C., Horton, D.G., Solomon, G.C., White, L.D., and Evans, J.R., 1989. Oxygen-isotope composition of ground water and secondary minerals in the Columbia Plateau basalts: Implications for the paleohydrology of the Pasco Basin. *Geology*, v. 17, p. 606-610.
- Helz, R. T., 1978, The petrogenesis of the Ice Harbour Member, Columbia plateau, Washington - a chemical and experimental study: Unpublished Ph. D. thesis, Pennsylvania State University.
- Helz, R. T., Wright, T. L., and Swanson, D. A., 1975, Petrogenetic significance of chemical trends in the youngest unit of the Yakima Basalt on the Columbia Plateau, north-west USA: *Bulletin of Volcanology*, v. 38, p. 1-17.
- Helz, R.T, Wright, T.L., and Swanson, D.A., 1974. Petrogenetic significance of chemical trends in the youngest unit of Yakima Basalt on the Columbia Plateau, Northwest U.S.A., in Andean and Antarctic Volcanology Problems, International Association of Volcanology and Chemistry of the Earth's Interior. p.1-17.
- Hill, D. P., 1978, Seismic evidence for the structure and Cenozoic tectonics of the Pacific Coast states: In: Smith, R. B., and Eaton, G. P., (eds.), *Cenozoic Tectonics and Regional Geophysics of the Western Cordillera*, Geological Society of America Memoir, No. 152, p. 145-174.
- Hill, D. P., 1972. Crustal and upper mantle structure of the Columbia Plateau from long-range seismic-refraction measurements: *Geological Society of America Bulletin*, v. 84, p. 455-487.
- Hooper, P.R., 1980. The role of magnetic polarity and chemical analyses in establishing the stratigraphy, tectonic evolution and petrogenesis of the Columbia River Basalt, in Deccan volcanism and related basalt provinces in other parts of the world, *Memoir Geol. Soc. India*, v. 3, p. 362-376.



- 1982. The Columbia River Basalts. *Science*, v. 215, p. 1463-1468.
- 1984. Physical and chemical constraints on the evolution of the Columbia River Basalt. *Geology*, v. 12, p. 495-499.
- 1985. A case of simple magma mixing in the Columbia River Basalt Group: the Wilber Creek, Lapwai, and Asotin Flows, Saddle Mountains Formation. *Contributions to Mineralogy and Petrology*, v. 91, p. 66-73.
- 1988a. Crystal fractionation and recharge (RFC) in the American Bar Flows of the Imnaha Basalt, Columbia River Basalt Group. *Journal of Petrology*, v. 29, p. 1097-1118.
- 1988b. The Columbia River Basalt. In J.D. MacDougall (ed.), *Continental Flood Basalts*, p. 1-34. Dordrecht: Kluwer Academic Publishers.
- Hooper, P.R. and Camp, V.E., 1981. Deformation of the southeast part of the Columbia Plateau. *Geology*, v. 9, p. 323-328.
- Hooper, P.R. and Conrey, R.M., 1989. A model for the tectonic setting of the Columbia River Basalt eruptions. In S.P. Reidel and P.R. Hooper (eds.), *Volcanism and tectonism in the Columbia River flood-basalt province*, Special Paper 239. p. 293-306. Boulder, Colorado: Geol. Soc. of America.
- Hooper, P.R., Knowles, C.R., and Watkins, N.D., 1979. Magnetostratigraphy of the Imnaha and Grande Ronde Basalts in the southeast part of the Columbia Plateau. *American Journal of Science*, v. 279, p. 737-754.
- Hooper, P.R. and Swanson, D.A., 1987. Evolution of the eastern part of the Columbia Plateau. *Washington Division of Geology and Earth Resources Bulletin 77*, p. 197-217.
- Hooper, P.R. and Reidel, S.P., 1989. Dikes and vents feeding the Columbia River Basalts, in *Geologic guidebook for Washington and adjacent areas: Washington Division of Geology and Earth Resources Information Circular 86*, eds., Joseph, N.L. and others. p.257-273.
- Hooper, P. R., Kleck, W. D., Knowles, C. R., Reidel, S. P., and Theissen, R. L., 1984, Imnaha Basalt, Columbia River Basalt Group: *Journal of Petrology*, v. 25, p. 473-500.

- Huppert, H.E. and Sparks, R.S., 1985. Cooling and contamination of mafic and ultramafic magmas during ascent through continental crust. *EPSL*, v. 74, p. 371-386.
- Johnson, K.R., Thiessen, R.L., and Parodi, M.R., 1989. Geophysical constraints on the location of the cratonic margin beneath the Columbia Plateau. *Geological Society of America Abstracts with Programs*, v. 21, p. 98.
- Kistler, R.W., 1989. The location of and Mesozoic magmatic history near the western margin of the North American continent in Nevada. *Geological Society of America Abstracts with Programs*, v. 21, p. 102.
- Lambert, R. St J and Chamberlain, V.E., 1985. Columbia River Basalts: direct from the mantle or fractionated in layered intrusions in the mantle (abs.). *EOS*, v. 66, No. 16. p. 1112.
- Lefebvre, R.H., 1970. Columbia River Basalts of the Grand Coulee Area, in in Gilmour, E.H. and Stradling, D., eds., *Proceedings of the Second Columbia River Basalt Symposium*: Cheney, Eastern Washington State College Press, p. 1-38.
- Martin, B.S. 1989. The Roza Member, Columbia River Basalt Group; chemical stratigraphy and flow distribution. In S.P. Reidel and P.R. Hooper (eds.), *Volcanism and tectonism in the Columbia River flood-basalt province*, Special Paper 239. p. 85-104. Boulder, Colorado: Geol. Soc. of America.
- McKee, E.H., Swanson, D.A. and Wright, T.L., 1977. Duration and volume of Columbia River Basalt volcanism: Washington, Oregon and Idaho. *Geol. Soc. Am. Abstr. Programs*, v. 9, p. 463-464.
- Menzies, M. 1983. Mantle ultramafic xenoliths in alkaline magmas: evidence for mantle heterogeneity modified by magmatic activity. In C.J. Hawkesworth and M.J. Norry (eds.), *Continental basalts and mantle xenoliths*, p. 5-19. Cheshire: Shiva.
- Nelson, D. O., 1983, Interpretation of oxygen-isotope data and trace-element modeling for a large-scale mixing model for the Columbia River basalt: *Geology*, v. 11, p. 248-251.

- Norry, M.J. and Fitton, J.G. 1983. Compositional differences between oceanic and continental basic lavas and their significance. In C.J. Hawkesworth and M.J. Norry (eds.), *Continental basalts and mantle xenoliths*, p. 5-19. Cheshire: Shiva.
- Pearce, J.A., and Cann, J.R. 1973. Tectonic setting of basic volcanic rocks determined using trace-element analysis: *EPSL*. v. 19, p. 290-300.
- Pearce, J.A., Gorman, B.E., and Birkett, T.C., 1977. The relationship between major element chemistry and tectonic environment of basic and intermediate volcanic rocks: *EPSL*. v. 37, p. 121-132.
- Price and Vinson, 1989. Structural geometry and strain distribution within eastern Umtanum fold ridge, south-central Washington. In S.P. Reidel and P.R. Hooper (eds.), *Volcanism and tectonism in the Columbia River flood-basalt province*, Special Paper 239. p. 265-282. Boulder, Colorado: Geol. Soc. of America.
- Reidel, S. P., 1983, Stratigraphy and petrogenesis of the Grande Ronde basalt from the deep canyon country of Washington, Oregon and Idaho: *Geological Society of America Bulletin*, v. 94, p. 519-542.
- Reidel, S.P., Fecht, K.R., Anderson, J.L. 1989. The geologic evolution of the central Columbia Plateau. In S.P. Reidel and P.R. Hooper (eds.), *Volcanism and tectonism in the Columbia River flood-basalt province*, Special Paper 239. p. 247-264. Boulder, Colorado: Geol. Soc. of America.
- Reidel, S.P., Hooper, P.R. Hooper, and Price, S.M., 1987. Columbia River Basalt Group, Joseph and Grande Ronde Canyons, Washington, in *Geological Society of America Field Guide-Cordilleran Section*, p. 351-356.
- Shaffer, M.E. and West, M.W., 1989. Quaternary faulting in the Frenchman Hills Anticline, Yakima Foldbelt, Central Columbia Basin, Washington. *Geological Society of America Abstracts with Programs*, v. 21, p. 142.
- Shaw, H.R., and Swanson, D.A., 1970. Eruption and flow rates of flood basalts, in Gilmour, E.H. and Stradling, D., eds., *Proceedings of the Second Columbia River Basalt Symposium*: Cheney, Eastern Washington State College Press, p. 271-300.

- Snively, P. D. Jr., Macleod, N. S., and Wagner, H. C., 1973, Miocene tholeiitic basalts of coastal Oregon and Washington and their relations to coeval basalts of the Columbia plateau: Geological Society of America Bulletin, v. 84, p. 387-424.
- Shaw, H.R. and Swanson, D.A. 1970. Eruption and flow rates of flood basalts. In E.H. Gilmour and D. Stradling (eds.), Proceedings of the Second Columbia River Basalt Symposium, p. 271-300. Cheney: E. Wash. State College Press.
- Swanson, D. A., 1967, Yakima basalt of the Tieton River area, south-central Washington: Geological Society of America Bulletin, v. 78, p. 1077-1110.
- Swanson, D. A., Wright, T. L., and Helz, R. T., 1975, Linear vent systems and estimated rates of magma production and eruption for the Yakima basalt on the Columbia plateau: American Journal of Science, v. 275, p. 877-905.
- Swanson, D. A., Wright, T. L., Hooper, P. R., and Bentley, R. D., 1979, Revisions in stratigraphic nomenclature of the Columbia River basalt group: U. S. Geological Survey Bulletin 1457-G, 59 p.
- Swanson, D.A., 1978, Bedrock Geology of the Northern Columbia Plateau and adjacent areas, in The Channeled Scablands, eds. Baker, V.R. and Nummedal, D. NASA publication, p. 37-57.
- Swanson, D.A. and Wright, T.L., 1980. The regional approach to studying the Columbia River Basalt Group. Memoir Geol. Soc. India, v. 3, p. 58-80.
- Takahashi, E., 1988. High-pressure melting studies of Columbia River Basalts (abs.). EOS, v. 69, No. 16, April 19, 1988.
- Taubeneck, W.H., 1970. Dikes of Columbia River basalt in northeastern Oregon, western Idaho, and southeastern Washington, in Gilmour, E.H. and Stradling, D., eds., Proceedings of the Second Columbia River Basalt Symposium: Cheney, Eastern Washington State College Press, p. 73-96.
- Thompson, R. N., Morrison, M. A., Dickin, A. P., and Hendry, G. L., 1983, Continental flood basalts...arachnids rule OK?: In: Hawkesworth, C. J., and Norry, M. J., (eds.),

Continental basalts and mantle xenoliths, Shiva Publishing, p. 158-185.

- Thompson, D., 1911. The Publications of the Champlain Society. David Thompson's Narrative. 1784-1812. The Champlain Society, Toronto, p. 245.
- Tolan, T.L., Reidel, S.P., Beeson, M.H., Anderson, J.L., Fecht, K.R. and Swanson, D.A. 1989. Revisions to the estimates of the areal extent and volume of the Columbia River Basalt Group. In S.P. Reidel and P.R. Hooper (eds.), Volcanism and tectonism in the Columbia River flood-basalt province, Special Paper 239. p. 1-20. Boulder, Colorado: Geol. Soc. of America.
- Walker, G. W., 1973, Contrasting compositions of the youngest Columbia River basalt flows in Union and Wallowa counties, north-eastern Oregon: Geological Society of America Bulletin, v. 84, p. 425-430.
- Walker, G.P.L., 1970. Compound and simple flows and flood basalts. Bulletin Volcanologique, v.35, p. 579-590.
- Waters, A. C., 1961, Stratigraphic and lithologic variations in the Columbia River Basalt: American Journal of Science, v. 259, p. 583-611.
- Watters, Thomas R., 1989. Periodically spaced anticlines of the Columbia Plateau. In S.P. Reidel and P.R. Hooper (eds.), Volcanism and tectonism in the Columbia River flood-basalt province, Special Paper 239. p. 283-292. Boulder, Colorado: Geol. Soc. of America.
- West, M. W. and Shaffer, M.E., 1989. Late Quaternary tectonic deformation in the Smyrna Bench and Saddle Gap segments, Saddle Mountains Anticline, Yakima Fold Belt, central Columbia Basin, Washington. Geological Society of America Abstracts with Programs, v. 21, p. 157.
- Wilkinson, J. G., and Binns, R. A., 1977, Relatively iron-rich lherzolite xenoliths of the Cr-diopside suite: a guide to the primary nature of anorogenic tholeiitic andesite magmas: Contributions to Mineralogy and Petrology, v. 65, p. 199-212.
- Wright, T. L., Grolier, M. J., and Swanson, D. A., 1973, Chemical variation related to the stratigraphy of the Columbia River basalt: Geological Society of America Bulletin, v. 84, p. 371-386.

Wright, T.L., Mangan M., and Swanson, D.A., 1989. Chemical Data for flows and feeder dikes of the Yakima Basalt Subgroup, Columbia River Basalt Group, Washington, Oregon, and Idaho, and their bearing on a petrogenetic model, U.S. Geological Survey Bulletin 1821. p. 71.

APPENDIX A  
XRF ANALYSES

	SA-1	SA-2	SA-3	SA-4	SA-5	SA-6
<b>Normalized Results (weight %)</b>						
SiO <sub>2</sub>	51.49	51.21	51.3	51.15	51.15	50.95
Al <sub>2</sub> O <sub>3</sub>	13.33	13.31	13.26	13.56	13.63	13.35
TiO <sub>2</sub>	3.123	3.13	3.16	3.068	3.047	3.219
FeO*	14.43	14.3	14.11	13.91	14.16	14.53
MnO	0.236	0.227	0.226	0.223	0.244	0.227
CaO	8.19	8.43	8.52	8.61	8.54	8.49
MgO	4.22	4.47	4.57	4.57	4.37	4.43
K <sub>2</sub> O	1.31	1.49	1.43	1.34	1.22	1.38
Na <sub>2</sub> O	2.96	2.74	2.73	2.89	2.99	2.74
P <sub>2</sub> O <sub>5</sub>	0.701	0.696	0.682	0.678	0.65	0.693
Total	100.0	100.0	100.0	100.0	100.0	100.0

	<b>Trace Elements (ppm)</b>					
Ni	11	11	14	12	17	12
Cr	31	32	32	36	44	31
Sc	42	41	42	38	42	40
V	421	416	423	417	419	437
Ba	544	515	497	499	504	512
Rb	38	33	31	33	29	30
Sr	302	302	299	305	294	302
Zr	185	183	184	181	180	186
Y	45	44	44	45	44	47
Nb	17.7	17.3	17.8	16.5	18.1	16.3
Ga	18	22	20	18	19	23
Cu	25	19	22	27	30	26
Zn	136	134	134	131	136	136
Pb	6	9	9	9	8	6
La	17	23	17	29	24	13
Ce	42	72	58	61	44	67
Th	3	5	4	4	3	2

Total Fe is expressed as FeO;  
Major elements are normalized on a volatile-free basis.

SA-7    SA-8    SA-9    SA-10    SA-11    SA-12

Normalized Results (weight %)						
SiO <sub>2</sub>	51.22	51.42	51.62	51.31	51.15	52.14
Al <sub>2</sub> O <sub>3</sub>	13.73	13.39	13.85	13.36	13.55	14.49
TiO <sub>2</sub>	3.043	3.159	3.238	3.158	3.126	3.22
FeO*	13.62	14.05	14.45	14.3	13.96	12.34
MnO	0.218	0.221	0.149	0.223	0.221	0.671
CaO	8.78	8.4	8.47	8.37	8.62	9.22
MgO	4.62	4.38	3.42	4.31	4.55	3.39
K <sub>2</sub> O	1.29	1.24	1.26	1.23	1.41	0.98
Na <sub>2</sub> O	2.82	3.03	2.86	3.02	2.75	2.86
P <sub>2</sub> O <sub>5</sub>	0.659	0.7	0.64	0.713	0.654	0.698
Total	100.0	100.0	100.0	100.0	100.0	100.0

Trace Elements (ppm)						
Ni	19	12	15	10	15	22
Cr	53	26	55	37	42	52
Sc	38	42	42	40	40	39
V	434	426	458	422	428	437
Ba	515	521	487	530	485	1310
Rb	30	25	35	33	30	27
Sr	308	301	300	302	300	356
Zr	184	185	185	185	181	188
Y	45	45	46	45	45	48
Nb	18	18.9	19.1	16.5	16.5	16.5
Ga	17	22	20	23	18	23
Cu	34	26	37	26	26	33
Zn	136	135	135	139	133	141
Pb	3	6	6	6	7	6
La	26	0	14	0	24	14
Ce	50	54	46	47	53	53
Th	3	5	6	6	5	4

Total Fe is expressed as FeO;  
 Major elements are normalized on a volatile-free basis.



SA-14 SA-16 SA-19 SA-20C SA-20M SA-21C

Normalized Results (weight %)						
SiO <sub>2</sub>	52.92	51.84	51.46	53.18	52.73	51.76
Al <sub>2</sub> O <sub>3</sub>	14.71	13.71	13.66	14.95	14.53	13.30
TiO <sub>2</sub>	3.322	3.298	3.065	3.176	3.136	3.168
FeO*	11.51	15.18	13.66	10.56	11.73	13.76
MnO	0.177	0.204	0.211	0.180	0.197	0.223
CaO	9.33	8.01	8.91	9.65	9.40	8.50
MgO	3.18	3.71	4.47	3.34	3.24	4.35
K <sub>2</sub> O	1.24	1.22	1.31	1.32	1.47	1.54
Na <sub>2</sub> O	2.93	2.08	2.62	2.97	2.91	2.69
P <sub>2</sub> O <sub>5</sub>	0.700	0.755	0.635	0.678	0.658	0.713
Total	100.0	100.0	100.0	100.0	100.0	100.0

Trace Elements (ppm)						
Ni	12	14	19	27	26	13
Cr	53	28	54	54	57	26
Sc	40	43	40	39	44	42
V	444	421	414	434	423	413
Ba	566	521	459	582	537	530
Rb	35	29	30	35	37	36
Sr	342	304	310	352	332	308
Zr	195	191	178	189	188	187
Y	47	48	43	45	45	47
Nb	17.8	19.2	18.3	17.1	17.4	17.5
Ga	24	20	24	24	22	25
Cu	36	19	26	32	29	18
Zn	145	142	134	138	133	133
Pb	8	9	8	12	10	10
La	20	24	18	23	25	29
Ce	43	70	50	42	78	59
Th	6	5	5	5	4	4

Total Fe is expressed as FeO;  
Major elements are normalized on a volatile-free basis.

SA-24 SA-26 SA-27 SA-28 SA-29 SA-30A

Normalized Results (weight %)						
SiO <sub>2</sub>	51.58	51.54	51.57	51.61	51.55	51.65
Al <sub>2</sub> O <sub>3</sub>	13.21	13.37	13.25	13.27	13.31	13.23
TiO <sub>2</sub>	3.153	3.160	3.105	3.168	3.121	3.155
FeO*	14.13	14.06	14.26	13.99	13.86	13.87
MnO	0.229	0.229	0.230	0.230	0.229	0.238
CaO	8.41	8.51	8.39	8.52	8.49	8.47
MgO	4.36	4.25	4.41	4.41	4.48	4.44
K <sub>2</sub> O	1.49	1.24	1.57	1.56	1.42	1.46
Na <sub>2</sub> O	2.74	2.94	2.53	2.54	2.84	2.80
P <sub>2</sub> O <sub>5</sub>	0.700	0.705	0.690	0.698	0.698	0.695
Total	100.0	100.0	100.0	100.0	100.0	100.0

Trace Elements (ppm)						
Ni	12	11	11	16	12	14
Cr	28	29	30	30	33	29
Sc	39	40	38	38	38	43
V	413	410	402	410	404	422
Ba	530	535	527	533	536	528
Rb	36	33	46	43	36	34
Sr	302	304	303	302	299	302
Zr	186	186	186	184	183	187
Y	44	45	45	46	45	47
Nb	19.4	16.9	18.3	15.8	18.2	18.0
Ga	22	25	21	22	21	21
Cu	24	23	22	22	21	22
Zn	134	134	128	132	130	132
Pb	8	9	9	10	9	7
La	36	27	6	37	11	16
Ce	50	73	61	51	61	64
Th	3	4	5	3	5	4

Total Fe is expressed as FeO;  
 Major elements are normalized on a volatile-free basis.

SA-33 SA-35 SA-36 SA-37 SA-38C SA-38M

Normalized Results (weight %)						
SiO <sub>2</sub>	51.55	51.67	52.13	51.79	52.50	52.47
Al <sub>2</sub> O <sub>3</sub>	13.30	13.28	13.29	13.11	13.88	13.50
TiO <sub>2</sub>	3.177	3.187	3.171	3.145	3.233	3.274
FeO*	14.26	14.09	13.81	14.23	12.81	13.38
MnO	0.222	0.216	0.210	0.223	0.199	0.237
CaO	8.23	8.32	8.59	8.53	8.95	8.75
MgO	4.40	4.15	3.96	4.18	3.53	3.62
K <sub>2</sub> O	1.28	1.35	1.58	1.43	1.41	1.41
Na <sub>2</sub> O	2.90	3.03	2.56	2.67	2.77	2.63
P <sub>2</sub> O <sub>5</sub>	0.679	0.709	0.705	0.700	0.714	0.732
Total	100.0	100.0	100.0	100.0	100.0	100.0

Trace Elements (ppm)						
Ni	14	14	16	13	9	8
Cr	30	32	26	29	27	30
Sc	42	42	39	40	39	43
V	424	429	407	413	418	424
Ba	522	597	513	497	532	772
Rb	34	36	48	37	35	45
Sr	304	305	305	303	319	324
Zr	184	187	187	188	186	193
Y	45	52	46	46	46	49
Nb	17.5	15.8	16.8	16.8	17.5	17.5
Ga	23	23	24	23	25	23
Cu	23	20	27	25	22	19
Zn	131	138	140	137	138	141
Pb	10	10	10	9	9	12
La	33	30	30	20	18	13
Ce	58	70	61	71	41	72
Th	5	2	3	4	3	5

Total Fe is expressed as FeO;  
Major elements are normalized on a volatile-free basis.

SA-40 SA-40C SA-41C SA-43 SA-44 SA-49

Normalized Results (Weight %)						
SiO <sub>2</sub>	51.90	51.66	52.07	51.99	51.69	51.91
Al <sub>2</sub> O <sub>3</sub>	13.51	13.40	13.24	13.41	13.82	13.72
TiO <sub>2</sub>	3.153	3.175	3.168	3.057	3.026	3.072
FeO*	13.78	13.83	13.80	13.82	14.12	13.49
MnO	0.252	0.225	0.220	0.218	0.212	0.241
CaO	8.83	8.58	8.53	8.51	8.21	8.77
MgO	4.05	4.26	4.20	4.16	4.11	4.11
K <sub>2</sub> O	1.19	1.48	1.45	1.25	1.20	1.30
Na <sub>2</sub> O	2.66	2.69	2.62	2.94	2.96	2.71
P <sub>2</sub> O <sub>5</sub>	0.670	0.702	0.697	0.652	0.666	0.662
Total	100.0	100.0	100.0	100.0	100.0	100.0

Trace Elements (ppm)						
Ni	13	13	14	13	17	14
Cr	46	25	31	37	46	41
Sc	43	41	40	36	41	40
V	410	428	413	410	414	410
Ba	540	508	518	556	513	619
Rb	32	35	36	29	32	44
Sr	313	305	299	307	308	320
Zr	183	187	188	186	184	183
Y	46	46	46	46	47	44
Nb	17.1	17.0	17.9	16.7	15.4	18.0
Ga	19	25	23	22	23	22
Cu	23	24	28	28	30	23
Zn	129	133	130	133	134	130
Pb	8	11	12	8	8	9
La	26	21	26	25	34	13
Ce	47	52	65	29	43	37
Th	4	6	4	6	3	3

Total Fe is expressed as FeO;  
Major elements are normalized on a volatile-free basis.

SA-50 SA-51 SA-52 SA-53 SA-54 SA-75 SA-77 SA-78

Normalized Results (weight %)								
SiO <sub>2</sub>	51.39	51.49	50.88	51.42	51.53	51.32	51.48	51.31
Al <sub>2</sub> O <sub>3</sub>	13.32	13.27	13.16	13.38	13.58	13.15	13.39	13.13
TiO <sub>2</sub>	3.129	3.122	3.142	3.032	3.017	3.113	3.102	3.111
FeO*	14.15	14.23	14.67	14.10	13.76	14.36	13.78	14.29
MnO	0.226	0.221	0.233	0.219	0.241	0.228	0.225	0.229
CaO	8.68	8.54	8.52	8.61	8.80	8.48	8.60	8.51
MgO	4.50	4.47	4.70	4.52	4.36	4.54	4.67	4.57
K <sub>2</sub> O	1.42	1.44	1.25	1.46	1.46	1.42	1.21	1.28
Na <sub>2</sub> O	2.49	2.55	2.77	2.58	2.62	2.72	2.87	2.89
P <sub>2</sub> O <sub>5</sub>	0.683	0.672	0.685	0.667	0.632	0.682	0.674	0.682
Total	100.0	100.0	100.0	100.0	100.0	100.0	100.0	100.0

Trace Elements (ppm)								
Ni	13	9	12	12	16	13	12	17
Cr	33	29	31	38	47	35	39	35
Sc	41	40	40	38	40	44	41	40
V	402	415	413	409	408	413	414	400
Ba	510	529	509	477	488	508	502	506
Rb	41	45	27	35	38	34	29	31
Sr	311	305	305	304	305	301	301	298
Zr	184	185	185	183	180	185	182	183
Y	47	44	47	45	43	44	44	45
Nb	18.8	18.3	17.3	17.8	16.2	17.8	16.6	17.4
Ga	21	22	22	22	23	22	21	20
Cu	27	29	21	22	25	28	27	16
Zn	133	134	132	131	125	132	133	128
Pb	6	7	11	11	7	8	9	10
La	25	31	19	17	24	22	22	15
Ce	62	35	66	39	40	71	54	57
Th	3	4	1	5	3	6	5	5

Total Fe is expressed as FeO; Major elements are normalized on a volatile-free basis.

## APPENDIX B

### ROZA CHEMICAL SUBTYPE CLASSIFICATION METHOD

#### I. INTRODUCTION

The Roza has been subdivided into four major cooling units and at least six chemical subtypes. These divisions are based on lithologic and chemical variations. Cooling units (designated in stratigraphic order by roman numerals) may be composed of multiple flows and chemical subtypes, but are distinguished as one cooling event. Cooling units, I and II are each composed of two chemical subtypes, denoted by appending "A's" and "B'S" to their subtype designations. Both cooling units III and IV are single cooling units and chemical subtypes. Unlike cooling units I and II, III and IV consist of multiple flows. Chemical subtypes are designated by systematic variations in the abundance of compatible elements (Ca and Cr) and incompatible elements (P<sub>2</sub>O<sub>5</sub>, Nb, Zr, TiO<sub>2</sub>).

Systematic differences between analyses made for this study and those done by Martin (1989) necessitate normalization of those elements used to designate Roza chemical subtypes. Biases between Cr, P<sub>2</sub>O<sub>5</sub>, TiO<sub>2</sub>, CaO, Nb and Zr contents of twelve samples analyzed by both laboratories have been calculated. Correction factors have then been applied to the other Roza samples in this study for purposes of subtype classification. As shown in the following sections Cr, P<sub>2</sub>O<sub>5</sub>, TiO<sub>2</sub>, and CaO prove to be the most useful for making

subtype correlations.

## II. NORMALIZATION

The following diagrams (Figures 38, 39, 40, 41) have been constructed to determine the normalization or correction factors that has resulted from analytical biases between the XRF analyses furnished by B. Martin and those performed for this thesis at Washington State University. XRF analyses of twelve powders were made in both labs and compared for standard reference.

## III. CLASSIFICATION

Once the normalization factors were calculated, all the XRF analyses from Washington State University were "corrected" so that they could be classified into their chemical subtypes. Classification was based predominately on the rocks Cr, P2O5, TiO2, and CaO compositions, since these elements prove to be positively and closely correlated in the twelve reference samples.

FIGURE 38. Cr normalization diagram. Equation is that of the line.

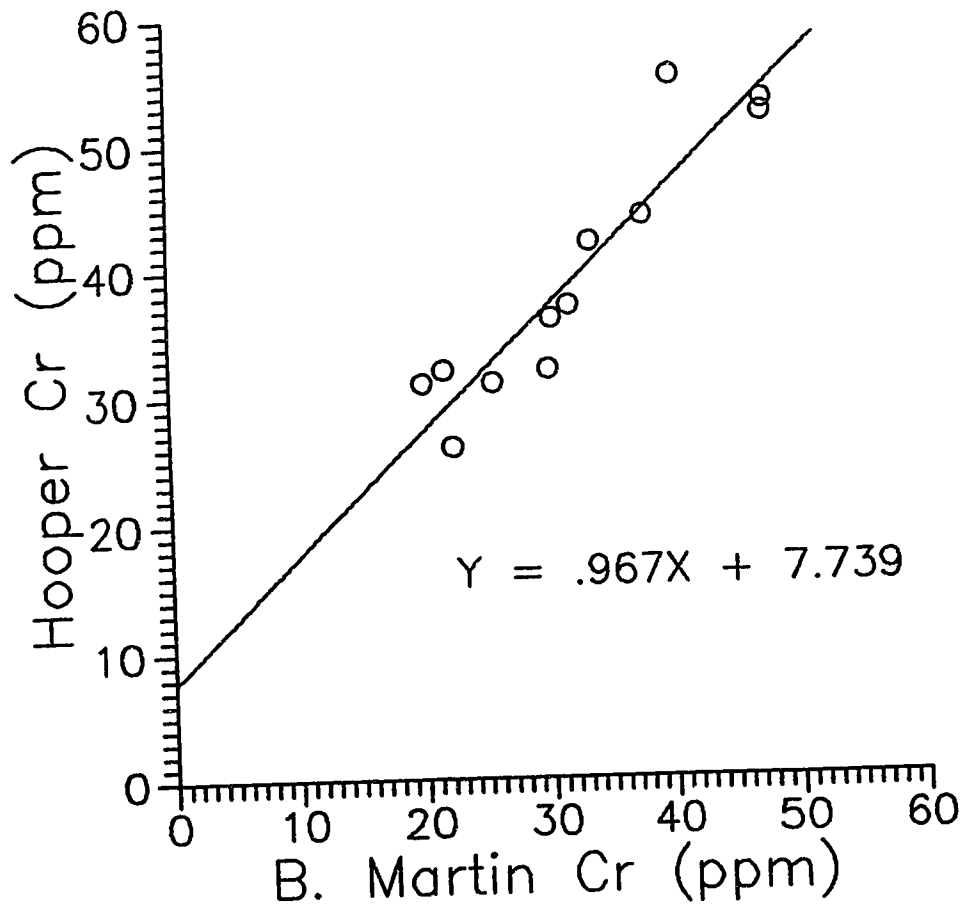




FIGURE 39. P205 normalization diagram. Equation is that of the line.

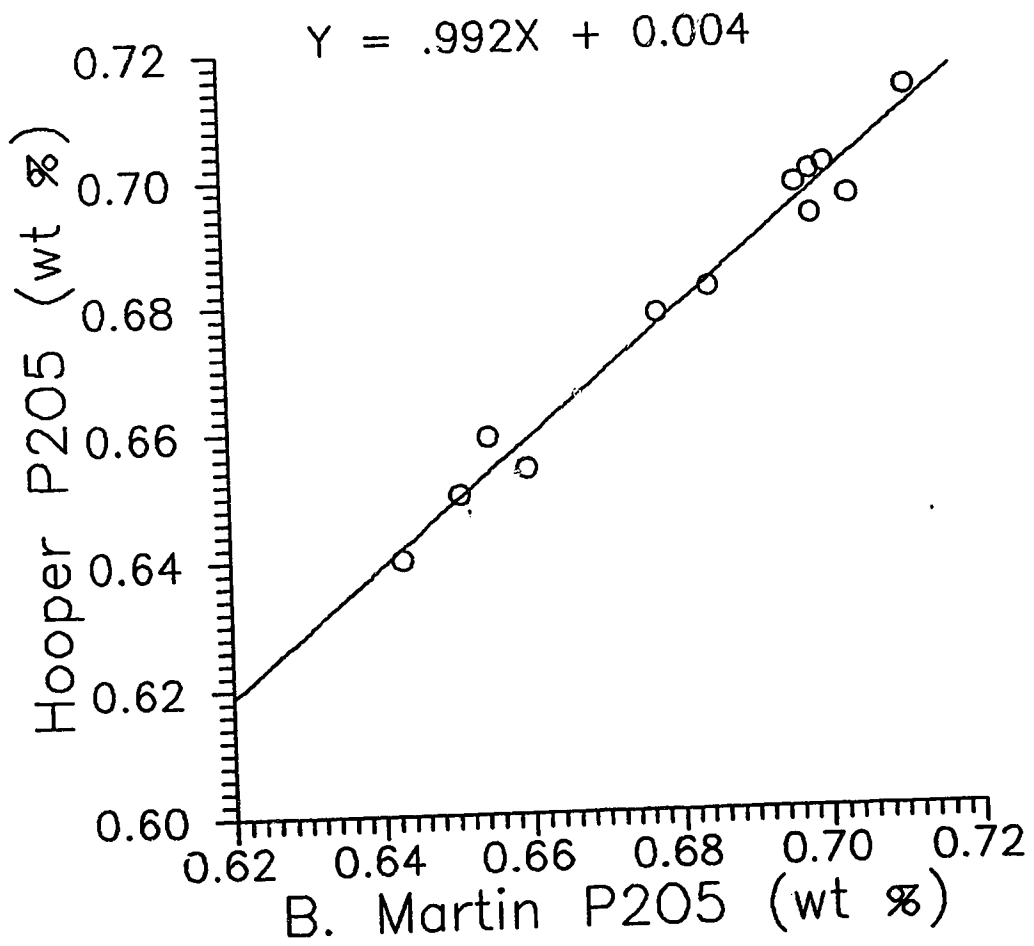
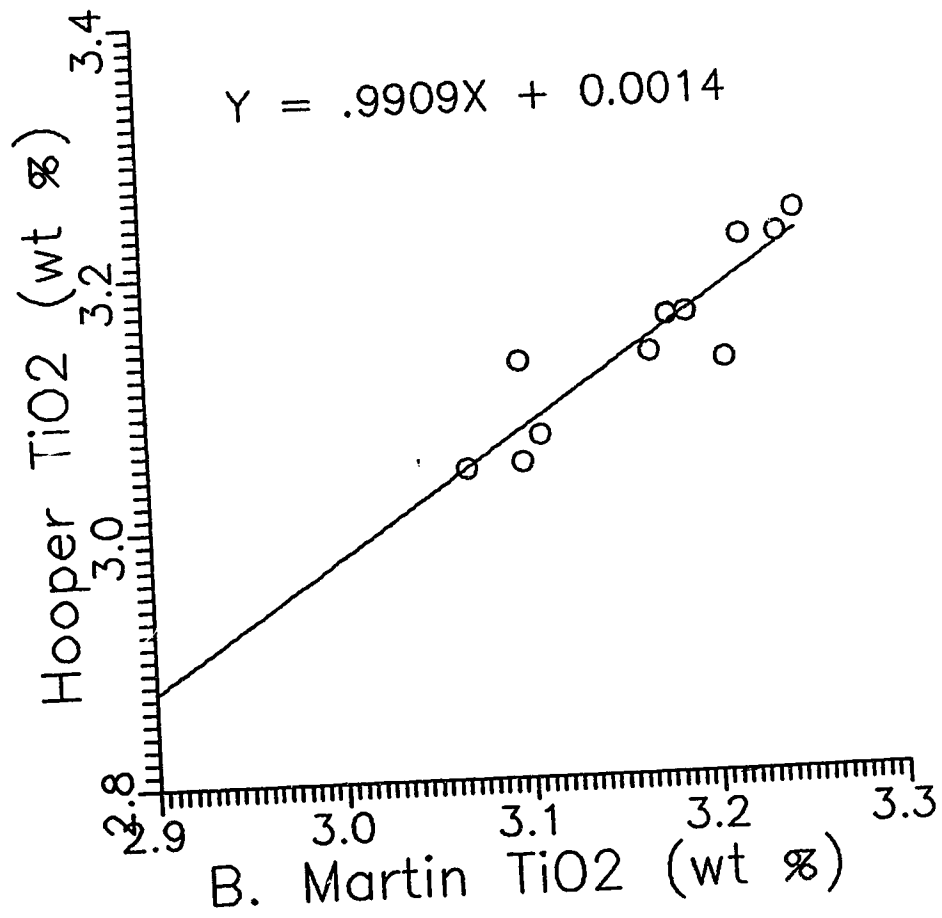
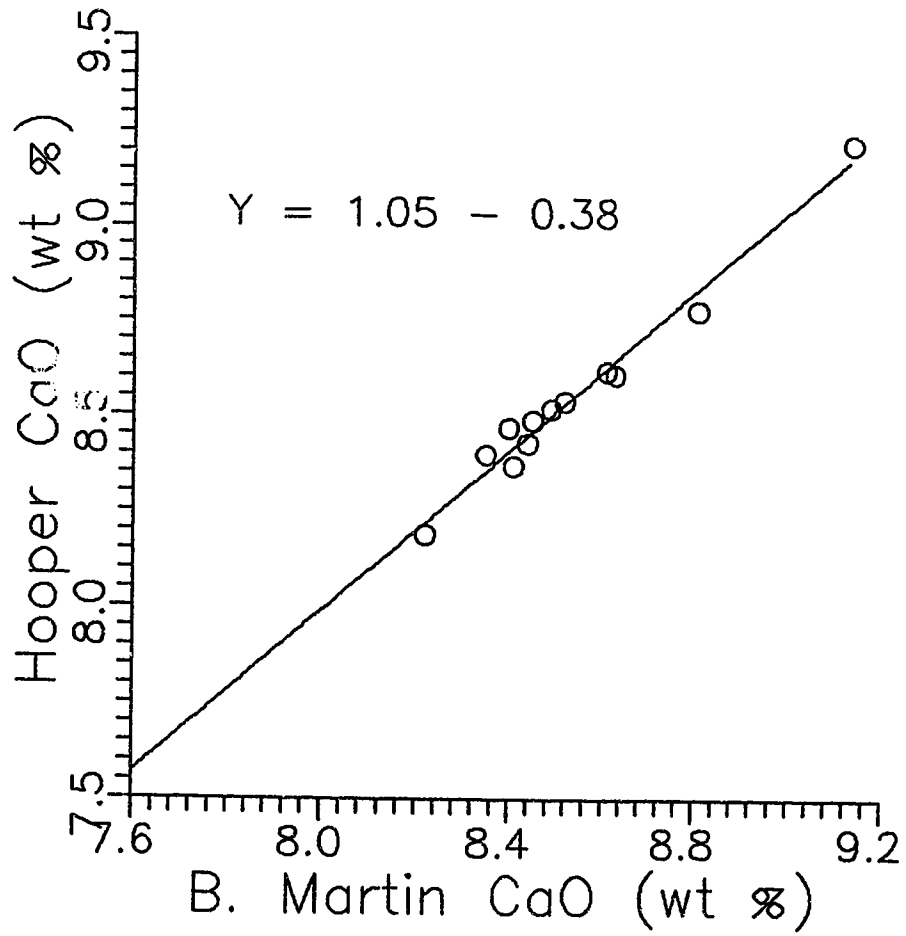


FIGURE 40. TiO2 normalization diagram. Equation is that of the line.



line.



## APPENDIX C

### ISOTOPIC CHEMICAL SEPARATION AND ANALYTICAL METHODS:

#### Strontium, Neodymium and Lead Separation Process for Isotope Ratio Analysis

- I. Decomposition of fine whole rock powders
  - A. decomposition (for every 2 grams do the following):
    1. weigh sample
    2. put in large teflon bombs (50 mm)
    3. moisten with millipore water
    4. add 14 ml of concentrated vapor distilled nitric acid
    5. add 14 ml of concentrated vapor distilled hydrofluoric acid
    6. heat for about 1 hour with lids loosely on at 150 C
    7. release vapors, tighten lids and allow to heat overnight
  - B. silica and fluoride release ( $\text{SiF}_4$  and  $\text{H}_2\text{SiF}_6$ )
    1. open vessels and allow to heat until evaporated
    2. moisten with millipore water
    3. add 4 ml of concentrated, V.D. nitric acid
    4. evaporate to dryness
    5. repeat steps 2 through 4 twice
  - C. final concentration
    1. add 10 ml of V.D. nitric
    2. add 10 ml of millipore water
    3. cover and heat until complete solution forms
    4. uncover and evaporate until at least half volume (10 ml) \*do not allow to go to dryness
    5. cool and centrifuge in teflon tubes
    6. discard gelatinous solid
    7. save supernate for barium coprecipitation (Sr, Nd and Pb in conc. nitric acid)
- II. Barium Coprecipitation
  - A. add 4 drops of saturated pure barium nitrate solution into 15 ml silica centrifuge tubes
  - B. pour supernate (C.7.) into centrifuge tubes
  - C. stir and rub sides of tubes with a teflon rod speed up precipitation (at least 3 minutes), or bubble solution using silica pipette.
  - D. wait at least 1 hour
  - E. centrifuge
  - F. pour off supernate containing REE's into large, 50 ml

- silica centrifuge tubes, and add water until all an equal, large volume. SAVE!!!!!!
- C. wash upper part of 15 ml tubes containing Sr-Pb precipitate with millipore water
  - H. take back up into solution with millipore water only if necessary, wash water should be sufficient
  - I. transfer into 3 ml silica centrifuge tubes, taking care to transfer as a unit
  - J. reprecipitate using conc. V.D. nitric acid \* do not overfill tubes, so teflon rod will go in
  - K. centrifuge 2 minutes
  - L. dump supernate, wash tube sides, dry sample upsidedown
  - M. mark twelve 10 ml teflon beakers for Pb and Sr aloquotes
  - N. clean Pb heat shrink columns

Dowex Ag-1-X8 chloride anion resin (1 ml)  
 100-200 mesh in teflon heat shrink tubing  
 5 mm diameter

- 1. remove resin and rinse with millipore water
- O. add new anion exchange resin
  - 1. wash twice with 6N HCl (about 2 ml each time)
  - 2. wash twice with millipore water
  - 3. wash twice with 1.5N HCl
  - 6. \*place Sr collection beakers in place
- P. load sample (II.L) in 1 ml of 1.5 N HCl using teflon eye dropper.
- Q. add 1 ml of 1.5N HCl four more times
- R. \* remove Sr collection beakers and replace with Pb collection beakers.
- S. add 2 ml of millipore water three times
- T. evaporate both Pb and Sr samples to dryness

### III. Neodymium separation

- A. R203 precipitation
  - 1. Take supernate of REE's (II.F.) and dilute with millipore water
  - 2. Preneutralize with pure NH<sub>3</sub> and add millipore water for volume
  - 3. Heat upper part of solution to create precipitate, \*hot solution is advised
  - 4. Stir with teflon rod to avoid "bumping" of the liquid
  - 5. Add more NH<sub>3</sub> until precipitate no longer goes into solution, then add just a squirt more to be sure all REE's are down in precipitate
  - 6. Top of with millipore water so that tubes are balanced in centrifuge
  - 7. Cover each tube with a square of kleenex and parafilm, then centrifuge for 2 minutes

8. Decant and rinse tube sides \*supernate is saved here only if spiking for Rb.

\*\* Steps 9 though 12 can be deleted if rocks are very low in Aluminum.

9. Add 5 pellets of Sodium Hydroxide (lye)  
\*we get rid of aluminum (AlO<sub>2</sub>) and bulkiness of sample here
10. Heat lightly to get rid of ammonia (smell factor)
11. Add best water for volume (Fe is still in precipitate)
12. Centrifuge 2 minutes
13. decant, wash sides and let drain upsidedown
14. add 6 N HCl to dissolve
15. dilute with millipore water and preneutralize with NH<sub>3</sub> and heat until boiling
16. add more NH<sub>3</sub> until just ammoniacal
17. Centrifuge, decant and wash sides again
18. add equal volume of 6N HCl to get sample down to 2.3N HCL

B. First R<sub>2</sub>O<sub>3</sub> Cation Columns

1. remove parafilm on column tips, allow to drain and wipe clean outside film
2. rinse inside of bulb with 2.3 N HCl - twist columns to wash completely
3. reequilibrate with 2.3 N HCl - resin height should be brought back to the black mark on column
4. clean 4 new silica pipettes by rinsing inside and out with 2.3 N HCl - 1 is for loading other 3 are for graduated cylynders.
5. fill grad. cyl. each with 2.3 N HCl so that sample plus HCl volume is = 80.0 ml
6. load in 1-3 ml of 2.3 N HCL
7. add 80 ml-sample volume gradually to columns (do at least 5 washes)
8. set out collection beakers
9. collect Nd in 55 ml of 2.3 N HCL, evaporate to dryness
10. wash columns to top of bulb with 6 N HCl
11. wash again with water and let drain
12. cap ends, and then add a touch more of water

C. MLA columns

1. uncap, drain and clean outside film
2. add MLA to top of bulb, to avoid bubbles use pipete to add initial drops
3. Add 33 ml of MLA to 2 graduated cylynders
4. Load samples in 2 drops or less of MLA from pipette

5. add 33 ml of MLA gradually to columns rinse at least 5 times
6. set out collection beakers
7. collect Nd in 14 ml of MLA
8. to clean columns, fill to top with 6 N HCl and drain
9. add water using capillary tube to top of bulb, necessary to avoid swelling and breakage
10. drain and then cap

D. second cation columns

1. allow storage water to drain
2. equilibrate in 0.1 N HCl
3. adjust MLA to pH 1 by adding 0.5 ml of 6.17 N HCl to about 15 ml Nd aliquote
4. add sample to column in small increments
5. rinse with 5 ml, 3 ml and 2 ml of 0.01 N HCl
6. elute with 8 ml of 2.3 N HCl
7. collect REE with 20 ml of 6.17 N HCl
8. evaporate to dryness
9. wash columns to top of bulb with 6 N HCl, add H<sub>2</sub>O, allow to drain and then cap

IV. Strontium Separation

A. First columns

1. Clean Sr heat-shrunk columns as follows:
  - 1 gram Dowex 50W-X8, 100 mesh cation exchange in 5 mm diameter heat shrink tubing
    - a. Flush four times with 6N HCl
    - b. Flush once with millipore water
    - c. Flush once with 1N HCl
    - d. Can either store or use now
  2. Load each Sr aliquote (III.N.6.) in .25 ml of 1N HCl
  3. Save and rinse teflon beaker for collection
  4. wash with 1.75 ml of 1N HCl (.25, .25, .25, 1.0ml)
  5. elute with 18 ml of 1N HCl (4,4,4,2 ml)
  6. elute with 2 ml of 2.3N HCl
  7. \*put collection beakers in place
  8. collect with 7 ml of 2.3 N HCl (4,3 ml)
  9. Heat overnight to dryness
  10. Clean and store columns as outlined above

B. Second columns

12 cm X 1 mm capillary columns for Sr final purification -  
Dowex 50W-X8 cation resin, 100-200 mesh

1. clear air out of columns with millipore water,

- blow through to dislodge any bubbles if present (i.e. visible).
2. add resin in a water medium. Allow to settle and use silica pipette to remove most of the excess just down to the capillary/bulb join.
  3. Fill columns to the top of the bulb with 1 N HCl and allow to drain about 1/2 way down bulb and then remove any excess resin again.
  4. add 0.05 ml of 1 N HCl to each sample using ependorf pipette
  5. load each using a rinsed silica pipette \* just touch side of pipette end to just above join and load one drop at a time
  6. wash 3 times with 0.05 ml of 1 N HCl
  7. elute once with 0.2 ml of 1 N HCl
  8. elute once with 0.25 ml of 2.3 N HCl
  9. put collection beakers in place
  10. collect next 0.25 ml of 2.3 N HCl
  11. evaporate to dryness